

Prediction and Evaluation of Annular Pressure in Horizontal Directional Drilling

by

Ali Rostami

A thesis submitted in partial fulfillment of the requirements for the degree of

Doctor of Philosophy

in

Construction Engineering and Management

Department of Civil and Environmental Engineering
University of Alberta

© Ali Rostami, 2017

Abstract

Horizontal directional drilling (HDD) is a crossing technique for the oil and gas, utilities, and infrastructure sectors for pipeline installations in different situations under natural or manmade obstacles. This technology was acquired from oil well drilling industry and was adopted in HDD. The environmental and social impacts caused by a lack of good practice in borehole drilling are major threats to the trenchless industry, especially to HDD. Although HDD technology has many advantages over open-cut methods, it sometimes carries the risk of loss of drilling fluid circulation, hydraulic fracture of the ground, and borehole collapse due to a lack of proper annular pressure management. Annular pressure (plan pressure) and maximum allowable pressure predictions are critical issues for annular pressure management. During HDD operation, annular pressure must not exceed the maximum allowable pressure to minimize the risk of hydraulic fracturing, which leads to loss of drilling fluid and increase in overall project risk.

This study aims to identify the shortcomings of common industrial methods in current HDD practices due to poor annular pressure management. Furthermore, this study intends to propose a scheme for better annular pressure management. To achieve this objective, the plan pressure and maximum allowable pressure during HDD operations must be estimated; however, the methods presently utilized by industry are not accurate. In the case of plan pressure estimation, the Bingham plastic model is commonly used in HDD operations to estimate the annular pressure. However, the Bingham plastic model overestimates the annular pressure, leading to incorrect bore path design and erroneous information from down-hole conditions. In the case of estimating the maximum allowable pressure of the drilling fluid, the Delft's cavity expansion method is commonly used. The Delft's method significantly overestimates the

maximum allowable pressure of the drilling fluid due to its simplified assumptions and can lead to hydraulic fracture of the ground during HDD operations.

This study introduces two methods extracted from the American Petroleum Institute (API) to estimate the plan pressure according to the power-law and Bingham plastic models, which are adjusted and modified for HDD operation during pilot boring. Prior to calculating the annular pressure, it is assumed that the borehole is under an ideal condition in which the borehole radius is not changed and the pressure loss and infiltration of drilling fluid are negligible. To understand the infiltration of drilling fluid into the adjacent soil, a series of experimental tests on the sandy soil have been conducted to show the formation of cake around the wellbore during HDD operation. The formation of the cake in high permeable soils such as sand prevents drilling fluid from infiltrating into the ground; however, the infiltration of the drilling fluid into the low permeable soil (e.g., clay) is negligible.

To estimate the maximum allowable pressure of the drilling fluid during HDD operation in non-cohesive soil, a new approach has been introduced to overcome the improper estimations based on Delft's method. This study has attempted to illustrate the lack of correlation between the allowable plastic radius and the failure pressure. This correlation has been applied in industry to the Delft's cavity expansion method and Yu and Houlsby's (1991) large strain cavity expansion method and has resulted in an overestimation of the failure pressure. The new approach is formulated based on the calculation of limit pressure using Yu and Houlsby's (1991) large-strain cavity expansion method. The suggested limit pressure approach has been advanced further to obtain a practical and useful solution to estimate the failure pressure in different geotechnical conditions by providing a coefficient of limit pressure following the Yu and Houlsby's (1991) method. To achieve this objective, the commercial finite element program

ABAQUS has been used to estimate the failure pressure based on the limit pressure approach and correlates it with Yu and Houlsbly's (1991) failure pressure. The coefficient of limit pressure is determined as a function of model and soil parameters (overburden depth, friction angle, and elastic modulus), and the significance of these parameters have been identified based on a parametric study.

To verify the developed methods for plan pressure estimation, two HDD case studies have been used. The proposed rheological models (Power Law, and modified Bingham models) have improved the accuracy of estimation of the annular pressure during pilot boring while the common industry methods (Bingham plastic model) significantly overestimate the annular pressure. Moreover, to verify the new approach for estimating the maximum allowable pressure of the drilling fluid, several experimental and field case studies from previous research have been used. In the current study, several graphs have been generated to calculate the coefficient of limit pressure to estimate the failure pressure properly. The new approach on annular pressure management enables engineers to better predict and monitor the annular pressure in the borehole during the HDD operation. This allows engineers to diagnose and prevent any upcoming issues during drilling and estimate the maximum allowable pressure of the drilling fluid to mitigate the risks associated with high annular pressure in the borehole during HDD operation.

Preface

This dissertation is an original work that I conducted and presented in paper format. For all of the papers, I am the first author and responsible for the numerical and analytical calculations, experiments, and manuscripts. Dr. Yi has reviewed the manuscripts and provided essential feedback to improve the manuscripts. My supervisor, Dr. Bayat, has set the objectives of the studies and monitored the research process. He is the corresponding author for all the manuscripts.

Chapter 3 of this dissertation has been accepted for publication as Rostami, A., Deng, S., Yi, Y., Kang, C., and Bayat, A., (2017). “Initial Experimental Study on Formation of Filter Cake in Sand during Horizontal Directional Drilling.” *NASTT No-Dig Show Conference*, Washington, D.C.

Chapter 4 of this dissertation has been published in: Rostami, A., Yi, Y., Osbak, M., and Bayat, A. (2016). “Annular Pressure Prediction in HDD using the Bingham Plastic Flow Model.” *International Journal of Petroleum Engineering*, 2(2), 79-90.

Chapter 5 of this dissertation has been published in: Rostami, A., Yi, Y., Bayat, A., and Osbak, M. (2015). “Predicting the Plan Annular Pressure Using the Power Law Flow Model in Horizontal Directional Drilling.” *Canadian Journal of Civil Engineering*, 43(3), 252-259.

Chapter 6 of this dissertation has been published in: Rostami, A., Yi, Y., and Bayat, A. (2016). “Estimation of Maximum Annular Pressure during HDD in Non cohesive Soils.” *International Journal of Geomechanics*, ASCE, 06016029.

Chapter 7 of this dissertation has been submitted to the *Geomechanics and Geoengineering: An International Journal* by Rostami, A., Kang, C., Yi, Y., and Bayat, A. “Numerical Modeling of the Failure Pressure during Horizontal Directional Drilling in Non-Cohesive Soil.”

The co-authors of the aforementioned manuscripts actively assisted the first author in writing and revising the manuscripts.

Dedicated

To

My Parents,

who taught me the lesson of resistance and patience

&

My Wife,

who taught me the lesson of love

Acknowledgment

I would like to express my gratitude to my supervisor, Dr. Alireza Bayat, for giving me this great opportunity to work on such a challenging topic. His valuable guidance, patience, encouragement, and financial support will always be acknowledged.

I would like to express my gratitude to my final exam committee members Dr. Erez Allouche, Dr. Dave Chan, Dr. Roger Cheng, Dr. Huazhou (Andy) Li, Dr. Vivek Bindiganavile, and Dr. Alireza Bayat for their insightful suggestions and comments to improve my dissertation. I would also like to sincerely appreciate the contributions of my supervisor committee members, Dr. Dave Chan and Dr. Roger Cheng, to my dissertation before my PhD defence exam. I would also like to thank Dr. Yaolin Yi and Dr. Chao Kang, the postdoctoral fellows in our research group at the University of Alberta, for their peer review of my manuscripts and constructive comments on my research study. I would also like to thank our professional editors at CETT, Tejay Gardiner, Lauren Wozny, Tatiana Boryshchuk, and Sheena Moore, for their great editorial comments.

Finally, I would like to express my deep gratitude to The Crossing Company for their technical and financial contribution, as well as the Natural Sciences and Engineering Research Council of Canada, the Faculty of Graduate Studies and Research (FGSR), and Graduate Students' Association (GSA) for providing financial support.

Table of Content

Abstract	ii
Preface	v
Dedicated.....	vii
Acknowledgment	viii
Table of Content	ix
List of Tables	xiii
List of Figures	xiv
1- Introduction.....	1
1-1- Introduction to HDD Technology.....	1
1-2- Objective and Scope	6
1-3- Methodology.....	7
1-4- Outline.....	9
Reference.....	12
2- Literature Review.....	1
2-1- Estimation of Annular Pressure	1
2-2- Prediction of Maximum Allowable Pressure	7
2-2-1- Theoretical Approach	7
2-2-2- Numerical Analysis	11
2-2-3- Experimental Research	15
2-3- Summary	17
Reference.....	18
3- Initial Experimental Study on Formation of Filter Cake in Sand during Horizontal Directional Drilling.....	23

3-1-	Introduction.....	23
3-2-	Experimental Study.....	25
3-2-1-	Material Properties	25
3-2-2-	Simulating Cake Formation.....	27
3-2-3-	Experiment Procedure	28
3-3-	Shear Strength.....	34
3-4-	Conclusion	36
	Reference.....	37
4-	Annular Pressure Prediction in HDD using the Bingham Plastic Flow Model	39
4-1-	Introduction.....	39
4-2-	Methodology.....	42
4-2-1-	Justification of Viscometer Data	43
4-2-2-	Determination of Bingham Rheological Parameters.....	44
4-2-3-	Calculation of Annular Pressure.....	45
4-3-	Case Study	46
4-3-1-	Project Overview and Measurements.....	46
4-3-2-	Comparison of Predicted and Field-Measured Annular Pressures.....	50
4-4-	Conclusion	52
	Reference.....	53
5-	Predicting the Plan Annular Pressure using the Power Law Flow Model in Horizontal Directional Drilling.....	56
5-1-	Introduction.....	56
5-2-	Objective.....	58
5-3-	Methodology.....	58

5-3-1-	Mechanical Behaviour of Drilling Fluid	58
5-3-2-	Concentric Annular Flow	61
5-3-3-	Annular Pressure.....	61
5-3-4-	Predicting Annular Pressure	62
5-3-4-1-	Power Law model	62
5-3-4-2-	Calculating frictional mud loss pressure	64
5-3-4-3-	Annular shear rate of drilling fluid.....	65
5-3-4-4-	Assumptions in using Power Law model.....	66
5-4-	Comparison of Prediction with Measurement	67
5-4-1-	Case Study 1	67
5-4-2-	Case Study 2	71
5-4-3-	Discussion.....	74
5-5-	Conclusion	76
	Reference.....	77
6-	Estimation of Maximum Annular Pressure during HDD in Non-Cohesive Soils	80
6-1-	Introduction.....	80
6-2-	Methodology	82
6-2-1-	Delft's method	82
6-2-2-	Yu and Houlsby's (1991) method	85
6-2-3-	Experimental Tests Used for Calculation.....	88
6-2-3-1-	Small-scale laboratory test (Elwood, 2008).....	88
6-2-3-2-	Large-scale laboratory test (Xia, 2009).....	89
6-2-3-3-	Full-scale field test (Keulen, 2001).....	90
6-3-	Estimation of Maximum Allowable Pressure	90

6-3-1-	Maximum Plastic Radius-Based Method	90
6-3-2-	Maximum Hoop Strain-Based Method.....	93
6-3-3-	Limit Pressure-Based Method	95
6-4-	Conclusion	96
	Reference.....	97
7-	Numerical Modeling of the Failure Pressure during Horizontal Directional Drilling in Non-Cohesive Soil	102
7-1-	Introduction.....	102
7-2-	Numerical Model Development.....	106
7-3-	Validation of Limit Pressure Method	111
7-4-	Parametric Study	113
7-5-	Coefficient of Limit Pressure.....	116
7-6-	Conclusion	121
	Reference.....	122
8-	Conclusion and Recommendation	127
8-1-	Conclusion	127
8-2-	Recommendation	130
	Reference.....	132

List of Tables

Table 3-1 Calculated permeability of sand specimens with cake	34
Table 4-1 Viscometer data of the fluids.....	48
Table 4-2 Shear stresses on the spindle and cup of viscometer	49
Table 4-3 Bingham rheological parameters.....	50
Table 5-1 Rheological properties: six-speed viscometer data of Case 1	69
Table 5-2 Power law parameters of Case 1	70
Table 5-3 Rheological properties: six speed viscometer data of Case 2.....	73
Table 5-4 Power Law parameters of Case 2	73
Table 6-1 Soil properties for laboratory and field tests	88
Table 6-2 Failure pressure measurements for laboratory and field tests	89
Table 6-3 Back-calculated normalized plastic radius with respect to the overburden depth.....	92
Table 6-4 Back-calculated hoop strain for cavity expansion methods	94
Table 7-1 Geotechnical properties of the soil for laboratory and field tests.....	112
Table 7-2 Measured and calculated failure pressure for laboratory and field tests	112
Table 7-3 Variation of independent parameters for parametric study	114

List of Figures

Figure 1-1 Horizontal directional drilling process: a) pilot hole drilling, b) reaming the pilot hole, c) product pipe pull back (Canadian Association of Petroleum Producers, 2004)	4
Figure 2-1 API dial reading for shear rates of 300 and 600 RPM	3
Figure 2-2 Logarithmic plot of Power Law fluid.....	5
Figure 2-3 Fann viscometer device.....	6
Figure 2-4 Internal pressure (pressure of the drilling fluid) within the borehole versus borehole radius (line A) and radial stresses versus radial distance outside the borehole (line B) (reproduced from Keulen, 2001).....	10
Figure 3-1 Particle size distribution curve for sand 20-40.....	26
Figure 3-2 Rheogram of drilling fluids following viscometer test	27
Figure 3-3 Schematic of cake formation simulation test set-up	28
Figure 3-4 a) Schematic of mounted specimen in the triaxial cell, b) filling up the triaxial cell with water.....	29
Figure 3-5 Measured flow rate for sand specimens using drilling fluid as a permeant fluid	31
Figure 3-6 Formation of thin layer of cake after injection of the drilling fluid	32
Figure 3-7 Undrained shear strength of the sand specimens with and without cake.....	36
Figure 4-1 Illustration of Bingham plastic flow model (Drilling fluids processing handbook modified).....	43
Figure 4-2 Drill path profile of Case A.....	47
Figure 4-3 Drill path profile of Case B.....	47
Figure 4-4 Comparison of predicted and measured annular pressure for Case A	51
Figure 4-5 Comparison of predicted and measured annular pressure for Case B	52
Figure 5-1 Distribution of velocity and shear stress in a flow channel	59
Figure 5-2 Schematic of laminar flow between two plates.....	60

Figure 5-3 Concentric annular flow through the borehole.....	62
Figure 5-4 Longitudinal profile of HDD crossing of Case 1	68
Figure 5-5 Comparison of the predicted and measured annular pressures of Case 1	71
Figure 5-6 Longitudinal cross-section of HDD crossing of Case 2.....	72
Figure 5-7 Comparison of the predicted and measured annular pressures of Case 2	74
Figure 5-8 Annular pressure measurement during drilling and after cleaning the borehole	76
Figure 6-1 Schematic of pressure-expansion relation in a borehole.....	83
Figure 6-2 Comparison of calculated maximum allowable pressure ($R_{p,max}=2/3H$) with measured failure pressure.....	91
Figure 6-3 Comparison of predicted maximum allowable pressure ($\varepsilon_{\theta,max}=2\%$) with measured failure pressure.....	93
Figure 6-4 Comparison of calculated limit pressure with measured failure pressure.....	96
Figure 7-1 The mesh discretization and boundary condition in ABAQUS numerical modeling	108
Figure 7-2 Typical deformation contour in ABAQUS numerical modeling	110
Figure 7-3 Effect of variation of each parameter on the limit pressure based on ABAQUS numerical modeling	115
Figure 7-4 The coefficient of limit pressure used for Yu and Houlsby's (1991) method: a) Elastic modulus of 20 MPa, b) Elastic modulus of 30 MPa, c) Elastic modulus of 40 MPa, d) Elastic modulus of 50 MPa, e) Elastic modulus of 60 MPa	119

1- Introduction

1-1- Introduction to HDD Technology

An early method of pipeline installation was performed by excavating a trench in the ground, placing and stabilizing the pipeline in the trench, and backfilling it. This method is time-consuming and costly, and it is often not practical for a river crossing and other sensitive environmental areas, such as below an embankment or levees and steep slopes (Staheli et al., 1998).

In the early 1970s, a new method called horizontal directional drilling (HDD) has been developed to install pipelines and utilities underground without using a trench. This new method is designed to be an alternative to open-cut methods, especially in sensitive environmental areas and congested urban areas, such as below rivers and watercourses, railroads, highways, embankments, steep slopes, and any other manmade or natural obstacles (Staheli et al., 1998). The HDD industry has experienced huge improvement since its inaugural 1971 crossing across the Pajaro River in Watsonville, California, and it has become a worldwide trenchless solution with 32,135 HDD rigs manufactured in 2011 (Sarireh et al., 2012).

The accelerated growth of the industry has also made significant improvement in HDD capabilities to accommodate borehole diameters up to 1,524 mm (60 inches), lengths exceeding 2,000 m, and installations in challenging geological environments (Najafi, 2005). This has placed significant demands upon acquiring suitable drilling equipment, special tools, experienced operators, and different engineering design requirements. These demands are affected by environmental and social risks caused by the migration of drilling fluid to the ground surface due

to a buildup of annular pressure in the borehole (hydraulic fracturing or frac-out), and they require accurate prediction and management of annular pressure. HDD technology is a safe, affordable, and time-effective method for pipeline installation compared to the other trenchless methods (Staheli et al., 1998). However, good HDD practices are required to secure a successful HDD installation while a lack of good industrial practices elevates the risk of failure in HDD projects.

Prior to starting the pipe installation process, pre-site planning is mandatory. The investigation of the geological condition and topography of the field is required to determine if the HDD crossing is feasible and if there is any potential risk to the project (Hashash et al., 2011). Afterward, the drill path and its entry and exit locations are determined. The HDD rig and other supplements are set up at the entry pit location during the pre-site planning phase.

HDD pipe installation comprises three steps (Figure 1-1). The first step involves the use of a steerable mechanical cutting head to excavate a guided bore with a diameter of 73 to 114.3 mm. The probe located near the drill bit sends the coordinates of the drill bit periodically; also, a surface tracking system can be used to track the location of the drill bit by taking measurements from surface points. The drill bit is powered by a mud motor located behind the drill bit. The drilling fluid is injected from the nozzle at the drill bit under high pressure and is an essential parameter in HDD. It is comprised of 2 to 5 percent bentonite mixed with water, and sometimes polymers are added to improve the specific functions of drilling fluids. The primary function of the drilling fluid is to power the cutting tools. The secondary function of drilling fluid is to lubricate the pipeline during pullback, carry the cuttings soil and clean the bottom hole, cool down the drill bit, stabilize the borehole, and form a filter cake inside the borehole.

The second step of HDD is to ream the borehole size in one or more steps (depending on the geotechnical condition of the ground and product pipe size) 25 to 50 percent larger than the final product pipe size by using a reamer replaced with the down-hole assembly. Then the product pipe is pulled back through the slurry path while the drilling fluid is still injected ahead of the reamer nozzle to lubricate the bore path (Canadian Association of Petroleum Producers, 2004).

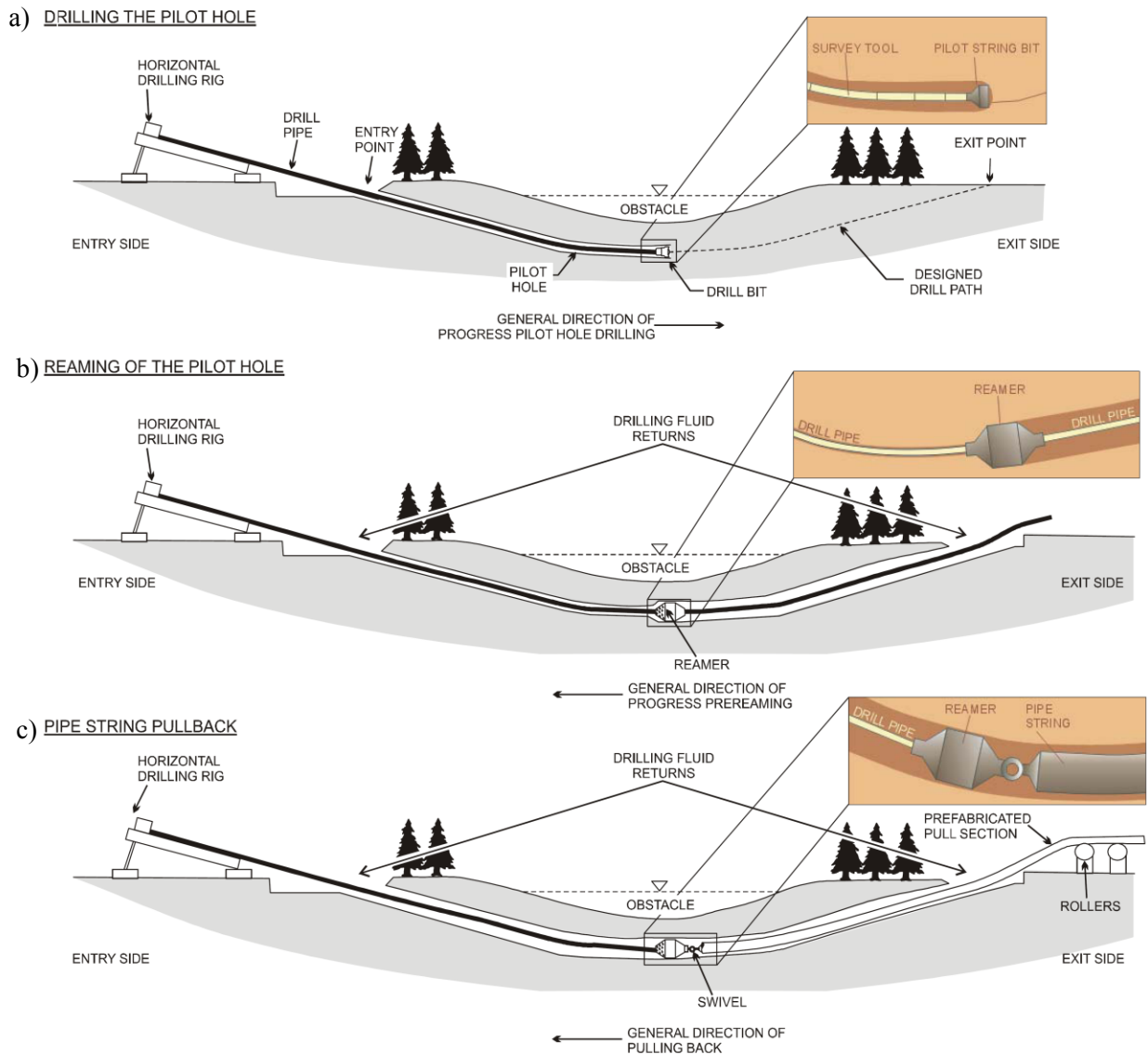


Figure 1-1 Horizontal directional drilling process: a) pilot hole drilling, b) reaming the pilot hole, c) product pipe pull back (Canadian Association of Petroleum Producers, 2004)

The circulation of the drilling fluid through the borehole develops annular pressure inside the borehole, and mud column weight exerts pressure on the borehole. Annular pressure is comprised of friction loss and hydrostatic pressure, and during borehole excavation, it is determined based on the total pump output rate, annular area within the borehole, and drilling

fluid rheological properties (Ariaratnam et al., 2007). The common method that predicts the friction loss pressure during pilot boring is the Bingham plastic model, suggested by the American Petroleum Institute (API) (Baroid, 1997; Staheli et al., 1998; Ariaratnam et al., 2003; Stauber et al., 2003; Baumert et al., 2005; Ariaratnam et al., 2007; Duyvestyn, 2009; Bennett, 2012). The Bingham plastic model overestimates the shear stress for lower shear rates (Baroid, 1997; Growcock and Harvey, 2005); this in turn overestimates the annular pressure that causes deeper and longer drill path designs and increases construction costs (Baumert et al., 2005). The plan pressure should be estimated properly to be able to diagnose the down-hole issues (cutting bed development, clogging, borehole collapse, hydraulic fracture, etc.) during HDD. On the other hand, drilling fluid pressure must not exceed the allowable pressures of the ground to minimize the risk of hydraulic fracture; otherwise, it leads to the loss of circulation, delay in project completion, and increase in the overall costs of the project. The common method to predict the maximum allowable pressure of the drilling fluid is Delft's method (Yanagisawa and Panah, 1994; Delft Geotechnics, 1997; Staheli et al., 1998; Conroy, 2002; Stauber et al., 2003; Kennedy et al., 2004; Baumert et al., 2005; Elwood et al., 2007; Xia and Moore, 2007; Staheli, 2010). However, the previous research studies showed that Delft's method overestimates the hydraulic fracture pressure significantly and leads to a non-conservative borehole design (Elwood, 2008; Xia, 2009).

In order to prevent the destructive deviation of annular pressure due to upcoming down-hole issues and risk of hydraulic fracturing during drilling, annular pressure management can be used to maintain the drilling fluid pressure in a safe range. Annular pressure management is critical to controlling construction schedules and minimizing environmental impacts. However, there is a lack of proper annular pressure management in the HDD industry due to the adoption

of oil well drilling industry practices without properly adjusting them to the HDD industry's requirements. As a result, issues can arise in regards to the specific range of operations, such as drilling horizontally in shallow-depth soils with low shear rates of the drilling fluid through the annulus and considering the laminar flow of the drilling fluid.

1-2- Objective and Scope

The main goal of this study is to propose proper methods of improving the current HDD good practices used in annular pressure management during HDD in non-cohesive soils, especially during pilot boring. This study aims to identify the shortcomings of the current practices, modify the existing methods, and develop new methods of estimating the plan annular pressure and maximum allowable pressure of drilling fluid during HDD. To achieve the objective of this dissertation, the following tasks are carried out:

1- Conducting an initial experimental study to assess the impact of infiltrating 2%, 3%, and 4% bentonite in drilling fluid on both the formation of the cake in a poorly graded sand medium and the shear strength parameters of the sand with and without cake

2- Modifying the Bingham plastic model by using proper shear rate ranges through a six-speed viscometer device and verifying the model by using two case studies

3- Addressing the shortcomings of a common industry method (Bingham plastic model considering a shear rate of 300–600 RPM) that is used to estimate the annular pressure during HDD, proposing a method to estimate the plan annular pressure through the Power Law flow model, and verifying the suggested model by using two case studies

4- Investigating the effectiveness of estimating the maximum allowable annular pressure during HDD in non-cohesive soils by using two theoretical cavity expansion solutions (small-

strain and large-strain), addressing the shortcomings of a common industry method (Delft's method) used to estimate the maximum allowable pressure during HDD, and suggesting a new approach to estimating the failure pressure independent of the plastic radius and dependent on the limit pressure of the borehole

5- Applying a numerical modeling using the commercial finite element program ABAQUS software to estimate the maximum allowable pressure of the drilling fluid in several case studies following limit pressure approach, and proposing specific coefficients of limit pressure to estimate the maximum allowable pressure in different geotechnical conditions

1-3- Methodology

To achieve the objective of this study, a comprehensive literature review was conducted to investigate the annular pressure management technique that has been used in the HDD industry and address the shortcomings of the previous research studies in this area. The literature review includes two parts. The first part includes the study of the estimation of the annular pressure during pilot boring following HDD good practice methods, which is adopted from the oil well drilling industry as suggested by API.

Prior to investigating the rheological models to estimate the annular pressure, the borehole's physical and geotechnical conditions during the circulation of drilling fluid are assessed. It is assumed that the seepage of drilling fluid is negligible during drilling in cohesive frictional soils which are low permeable medium while it is considerable in frictional soils such as sand. Thus, an initial experimental study is conducted to assess the impact of drilling fluid on sandy soils during drilling to observe if the filter cake is formed. To perform this experimental study, a new test set-up is designed to inject the drilling fluid in a constant pressure head into the

small sandy soil sample while applying the confining stress. Also, a constant flow rate injection test is carried out to measure the permeability of the pure sand samples. Further, an unconsolidated, undrained triaxial shear test is conducted to measure the changes in shear strength parameters of the sandy soil sample before the drilling fluid injection and after that, when the cake is formed.

As the ideal borehole has a negligible seepage of drilling fluid into the surrounding soil, it is possible to use rheological models to estimate the annular pressure during the pilot bore. In this section, two rheological models, the Bingham plastic and the Power Law models are used to estimate the rheological properties of drilling fluid and the annular pressure. In this case, new shear rate ranges that are compatible with the shear rates of drilling fluid in the borehole annulus are defined to calculate the rheological properties of drilling fluid. The calculated annular pressures based on the Bingham plastic and the Power Law models are verified with two HDD case studies. The estimated annular pressure can be used as a plan pressure for HDD engineers to monitor down-hole pressure properly to reduce the risks of upcoming issues such as the clogging of drill bit, loss of circulation, hydraulic fracture, and borehole collapse.

The second part of this study is concerned with the estimation of the maximum allowable pressure of the drilling fluid during pilot boring in non-cohesive soils to prevent hydraulic fracture (frac-out, or failure). The current HDD good practice for estimating the maximum allowable pressure of the drilling fluid is assessed to determine if it can provide an accurate estimation. Experimental and real field case studies are used to verify the current method.

A back-calculation technique is applied to the previous experimental and field case studies on hydraulic fracturing phenomenon for assessing the correlation of plastic radius and

plastic strain around the borehole with the failure pressure to estimate the maximum allowable pressure of the drilling fluid. Afterward, a new approach called limit pressure solution following Yu and Houlsby's (1991) method is introduced to better estimate the maximum allowable pressure (failure pressure) of the drilling fluid; this approach overcomes the shortcomings of the previous current HDD good practice methods.

Finally, a numerical modeling using the commercial finite element program ABAQUS software is employed to estimate the failure pressure in several case studies following the limit pressure approach. The large-strain cavity expansion solution suggested by Yu and Houlsby (1991) is used to estimate the failure pressure, which is then compared to those estimations based on numerical modeling following the limit pressure approach. A parametric study using numerical modeling is conducted to examine the influence of geotechnical parameters of soil medium on the limit pressure. The ratio of limit pressure following analytical and numerical methods resulted in coefficients of limit pressure in different geotechnical conditions and can be used to estimate the failure pressure in non-cohesive soils using the suggested limit pressure approach.

1-4- Outline

This dissertation is compiled of five articles and integrated in a paper-based format. The dissertation's chapters are presented as follow:

Chapter 1: An introduction to HDD as a trenchless construction method and its critical engineering issues in the field of annular pressure management is presented. Also, the objectives, methodology, and structure of the dissertation are discussed.

Chapter 2: A comprehensive literature review of annular pressure management that has been used in HDD as a good practice by the industry is presented. This chapter has two parts: the first part is about the prediction of annular pressure during HDD in pilot boring stage, and the next part is about estimating the maximum allowable pressure of drilling fluid during HDD in cohesive and frictional soils.

Chapter 3: An initial experimental study on the formation of filter cake in sand during HDD is conducted. This chapter presents the impact of bentonite-based drilling fluid on the formation of filter cake in sandy soils. Three different concentrations of bentonite-based drilling fluid are used as a permeant fluid to inject into the sand sample. Meanwhile, the permeability of sand samples is measured. Also, the undrained triaxial shear test is used to investigate the impact of drilling fluid penetrating into the sand samples on the shear strength parameter of them.

Chapter 4: The annular pressure prediction in HDD using the Bingham plastic flow model is discussed. This chapter provides the shortcomings of the Bingham plastic flow model suggested by API for estimating the rheological properties of drilling fluid and calculating the annular pressure. Then, this study presents a method to better estimate the annular pressure following the Bingham plastic model by obtaining the yield stress and viscosity of drilling fluid based on a lower shear rate of 100–200 RPM. Two case studies are used to verify the suggested model.

Chapter 5: A method for predicting the plan annular pressure using the Power Law flow model during pilot boring in HDD is introduced. This chapter discusses the shortcomings of the previous model for estimating the annular pressure in HDD and suggests the Power Law model,

which can estimate the annular pressure sufficiently. Two case studies are used to verify the suggested model.

Chapter 6: A new approach to estimating the maximum annular pressure during HDD in non-cohesive soils is presented. This chapter addresses the shortcomings of the common close-form and analytical methods of predicting the maximum allowable pressure of the drilling fluid during HDD, such as Delft's method and Yu and Houlsby' (1991) method, which are based on maximum allowable plastic radius and Verruijt's (1993) method, which is based on maximum allowable plastic strain. This study introduces a new approach to estimating the maximum allowable pressure based on the coefficient of limit pressure following Yu and Houlsby's (1991) large-strain cavity expansion method. Several experimental and field case studies are used to verify the suggested new approach.

Chapter 7: A finite element numerical modeling of the maximum annular pressure during HDD in non-cohesive soils is presented. This chapter completes the study in the previous chapter by providing different coefficients of the limit pressure for different geotechnical conditions to estimate the maximum allowable pressure of the drilling fluid during HDD. To verify the estimation of maximum allowable pressure of the drilling fluid following limit pressure method, the commercial finite element program ABAQUS software is used. Accordingly, sensitivity analyses are conducted to investigate the essential parameters that affect the limit pressure. Thereafter, several graphs are generated to provide the coefficient of the limit pressure for a rational range of overburden depth, friction angle, and elastic modulus.

Chapter 8: The achievements of this study are summarized and reviewed, and recommendations for future follow-up studies are proposed.

Reference

- Ariaratnam, S.T., Harbin, B.C., and Stauber, R.L. 2007. Modeling of annular fluid pressures in horizontal boring, *Tunnelling and Underground Space Technology*, 22, 610–619.
- Ariaratnam, S.T., Stauber, R.M., Bell, J., Harbin, B., and Canon, F. 2003. Predicting and controlling hydraulic fracturing during horizontal directional drilling, Proceedings of the International Conference on Pipeline Engineering and Construction, Baltimore, Maryland, 1334-1345.
- Baroid. 1997. Fluids Handbook. Baroid Fluid Services, Chapter 9, Rheology and Hydraulics, Haliburton, Houston, TX.
- Baumert, M.E., Allouche, E.N., and Moore, I.D. 2005. Drilling fluid considerations in design of engineered horizontal directional drilling installations, *International Journal of Geomechanics*, 5(4), 339–349.
- Bennett, R.D., Osbak, M., and Wallin, M. 2012. Improving the standard of mud management, In Proceedings of 2012 No-Dig Conference, Nashville, Tennessee.
- Canadian Association of Petroleum Producers, 2004. Planning for Horizontal Directional Drilling for pipeline construction, CAPP publication 2004-0022
- Conroy, P.J., Latorre, C.A., and Wakeley, L.D. 2002. Guidelines for installation of utilities beneath Corps of Engineers levees using horizontal directional drilling, *ERDC/GSL TR-02-9, Geotechnical Structures Laboratory*, Vicksburg, Mississippi.
- Delft Geotechnics. 1997. A report by Department of Foundations and Underground Engineering prepared for O'Donnell Associates, Inc., Sugarland, Texas.
- Duyvestyn, G. 2009. Comparison of predicted and observed HDD installation loads for various calculation methods, In Proceedings of 2009 International No-Dig Conference, Toronto, Ontario, Canada.

- Elwood, D, Xia, H., and Moore, I.D. 2007. Hydraulic fracture experiments in a frictional material and approximations for maximum allowable mud pressure, In Proceedings of 60th Canadian Geotechnical Society Annual Conference, Ottawa, Ontario, Canada, 1681-1688.
- Elwood, D. 2008. Hydraulic fracture experiments in a frictional material and approximations for maximum allowable mud pressure, Master thesis, Queen's University, Kingston, Ontario, Canada.
- Growcock, F., and Harvey, T. 2005. Drilling fluids. Drilling Fluids Processing Handbook, UK: Elsevier Ink, 15-66.
- Hashash, Y., Javier, J., Petersen, T., and Osborne, E. 2011. Evaluation of horizontal directional drilling (HDD), *FHWA-ICT-11-095*.
- Kennedy, M.J., Skinner, G.D., and Moore, I.D. 2004. Elastic calculations of limiting mud pressures to control hydro fracturing during HDD, In Proceedings of No-Dig Conference 2004, New Orleans, Louisiana.
- Najafi, M. 2005. Trenchless technology: pipeline and utility design, construction, and renewal, McGraw-Hill, New York.
- Sarireh, M., Najafi, M., and Slavin, L. 2012. Usage and applications of horizontal directional drilling, In Proceedings of ICPTT 2012: Better pipeline infrastructure for a better life, Wuhan, China.
- Staheli, K., Bennett, R.D., O'Donnell, H.W., and Hurley, T.J. 1998. Installation of pipelines beneath levees using horizontal directional drilling, Technical Report CPARGL-98-1, U.S. Army Engineer Waterways Experiment Station, Vicksburg, Mississippi.
- Staheli, K., Christopher, G. P. and Wetter, L. 2010. Effectiveness of hydrofracture prediction for HDD design, In Proceedings of No-Dig 2012 Conference, Chicago, Illinois.

- Stauber, R.M., Bell, J., and Bennett, R.D. 2003. A rational method for evaluating the risk of hydraulic fracturing in soil during horizontal directional drilling (HDD), In Proceedings of 2003 No-Dig Conference, Las Vegas, Nevada.
- Verruijt, A. 1993. *Grondmechanica*, Delftse Uitgevers Maatschappij, Delft, Netherlands.
- Xia, A. 2009. Investigation of maximum mud pressure within sand and clay during horizontal directional drilling, PhD thesis, Queen's University, Kingston, Ontario.
- Xia, H. and Moore, I.D. 2006. Estimation of maximum mud pressure in purely cohesive material during Directional Drilling, *International Journal Geomechanics and Geoengineering*, 1(1), 3-11.
- Yanagisawa, E. and Panah, A. K. 1994. Two dimensional study of hydraulic fracturing criteria in cohesive clays, *Soils and Foundations*, 34(1), 1-9.
- Yu, H.S., and Houlsby, G.T. 1991. Finite cavity expansion in dilatant soil: loading analysis, *Geotechnique*, 41(2), 173-183.

2- Literature Review

It has long been recognized that annular pressure plays a critical role in HDD. This chapter presents the research studies conducted in the field of annular pressure management during HDD in two parts. The first part discusses the common industry method to estimate the plan pressure (annular pressure) during pilot boring, and the second part reviews the common industry methods to estimate the maximum allowable pressure (failure pressure) of the drilling fluid during pilot boring based on theoretical, numerical, and experimental approaches.

2-1- Estimation of Annular Pressure

The first step of HDD (pilot boring) has the greatest construction concern due to the high risk of hydraulic fracture and loss of drilling fluid circulation. The probability of a sudden increase in annular pressure is much higher in this step than in others, primarily due to the small area of the annulus and cutting bed development at the bottom of the borehole, which increases the risk of hydraulic fracture. In this stage, drilling fluid pressure should be maintained within an appropriate range to provide borehole stability, and adequate circulating pressure must be preserved to transport cuttings out of the borehole and prevent risk of hydraulic fracture.

Circulation of the drilling fluid through the annulus leads to pressure developing inside the borehole. Increase in the annular pressure arises from a clogged borehole annulus or a change in material properties of the drilling fluid. When the annular pressure is excessively high, it can cause shear or tensile failure of the surrounding soil, loss of drilling fluid circulation, and the inadvertent return of mud to the ground surface. The inadvertent return of drilling fluid to the ground surface is considered a critical risk to HDD projects due to the negative environmental

and operational impacts (Staheli et al., 2010; Christopher et al., 2003; Harris, 2004; Duyvestyn, 2006; Xia, 2009; Bennett et al., 2001; Osbak, 2011). HDD contractors should apply proper annular pressure management systems to achieve a targeted drilling fluid rheology and to predict the mechanical behaviour of drilling fluid (Stauber et al., 2003; Osbak, 2011). An effective annular pressure management system provides essential information about the mechanical behaviour of the drilling fluid and surrounding soil to monitor and control risk events resulting from elevated annular pressures. To create a successful management system, the annular pressure must be accurately estimated and the boundary of maximum allowable pressure of the drilling fluid must be determined prior to project execution.

The most common approach the HDD industry uses to predict annular pressure inside the borehole is the Bingham plastic model (Baroid, 1997; Staheli et al, 1998; Ariaratnam et al, 2003; Stauber et al, 2003; Baumert et al, 2005, Bennett and Wallin, 2008; Duyvestyn, 2009). The Bingham plastic model accounts for the yield stress of laminar drilling fluids but overestimates the shear stress for lower shear rates due to calculation of yield stress based on shear rate ranges of 300-600 RPM (Hemphill et al., 1993; Baroid, 1997; Harris, 2004). Therefore, the circulating pressure predicted via this model is too conservative, which increases design costs of HDD projects (Baumert et al., 2005). This model has been adopted by the American Petroleum Institute (API, 2009) to determine the circulating pressure in oil well drilling, but it can also be applied to HDD. The Bingham model equation is as follows (Baroid, 1997; API, 2009):

$$\tau = YP + PV \cdot \dot{\gamma} \text{ (Pa)} \quad (2-1)$$

where τ is the shear stress (Pa), YP is the yield point or yield stress (Pa), PV is the plastic viscosity (Pa.s), and $\dot{\gamma}$ (1/s) is the shear rate of the drilling fluid. The shear stress is the force per

unit area required to maintain a particular rate of flow (API, 2009). The YP and PV are calculated using a two-speed viscometer, which can provide shear stress at shear rates of 300 and 600 RPM; the yield point (YP) can be determined by the Y intersection of the shear stress-shear rate line, and plastic viscosity (PV) can be expressed as a slope of the shear stress-shear rate line (Figure 2-1). The shear rate is the slope of the velocity profile at any point on the radius between two adjacent flow layers, which is maximum at the annulus wall and zero at the central axis.

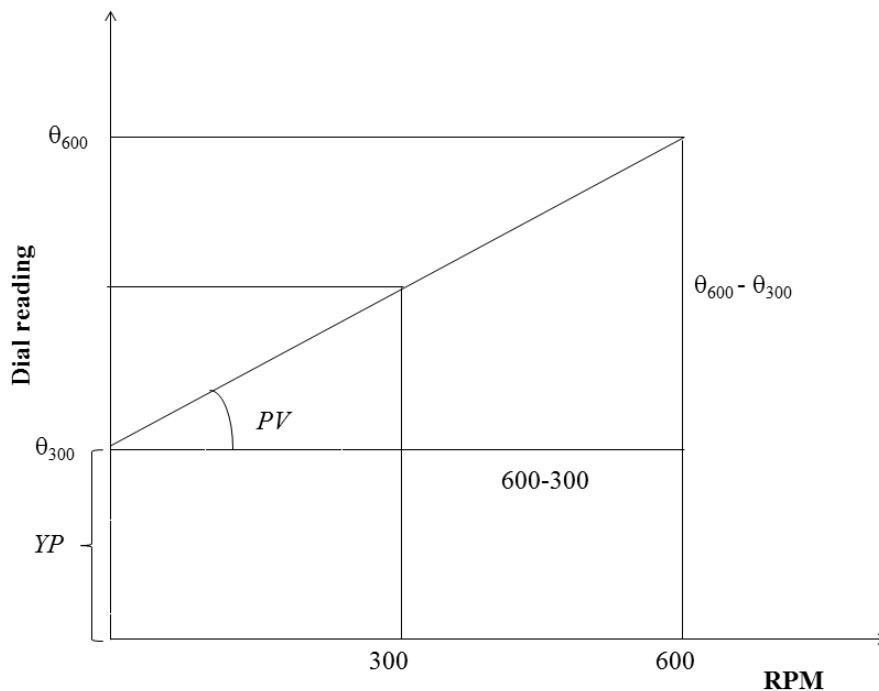


Figure 2-1 API dial reading for shear rates of 300 and 600 RPM

The Power Law model is the second prediction method that is considered by standard in determining drilling fluid pressure within the borehole (API, 2009), but it is not a common model in HDD while it needs a six-speed viscometer device instead of two-speed viscometer device to calculate the rheological parameters of the drilling fluid. This method is more accurate in predicting circulating pressure since it accounts for the nonlinear relationship of the shear

stress and shear rate (shear thinning behaviour) (Harris, 2004), and it also considers lower shear rates compatible with those of the fluid inside the borehole. A non-linear relationship exists between the shear stress and the shear rate of the fluid; the constitutive equation is as follows:

$$\tau = k \cdot \dot{\gamma}^n \quad (2-2)$$

where τ is the shear stress, k is the consistency index, n is the Power Law index, and $\dot{\gamma}$ is the shear rate. Power Law parameters can be calculated by applying a logarithm to both sides of the Equation (2-2) using two sets of data from the viscometer test as follows (Baroid, 1997; API, 2009):

$$n = \frac{\log \frac{\tau_2}{\tau_1}}{\log \frac{\dot{\gamma}_2}{\dot{\gamma}_1}} \quad (2-3)$$

$$k = \frac{\tau_2}{\dot{\gamma}_2^n} \quad (2-4)$$

The slope of this line is n , the Power Law exponent that indicates the fluid's degree of non-Newtonian behaviour over a range in shear rate. When $n = 1$, the fluid is Newtonian and the viscosity is constant. The intercept of the log-log plot is denoted as k , the Power Law consistency index, and it approximately corresponds to the yield point (Figure 2-2).

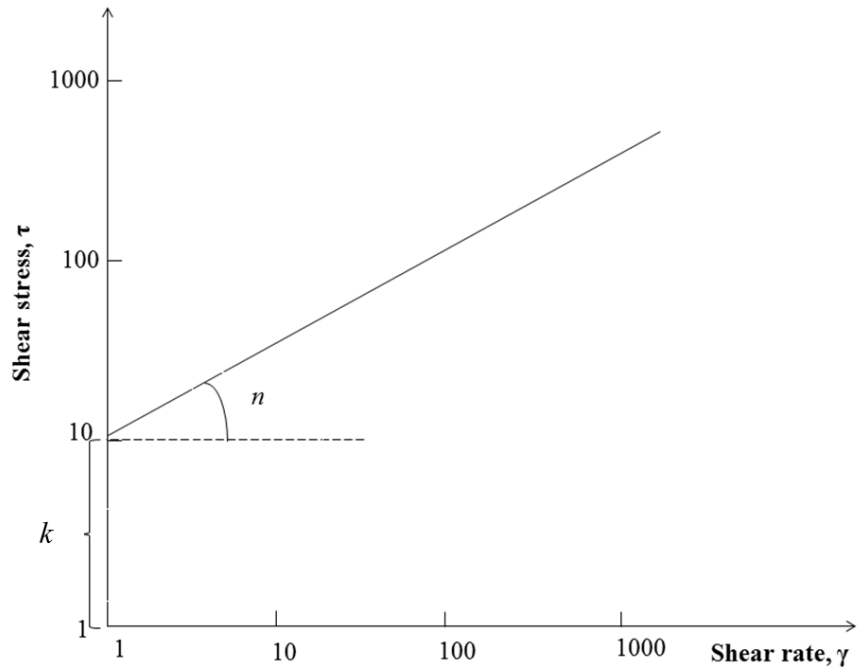


Figure 2-2 Logarithmic plot of Power Law fluid

To employ rheological models for predicting circulating pressure, rheological parameters of the drilling fluid should be identified. A viscometer can be used to obtain the viscosity and yield point of the fluids based on shear stress (torque) and shear rate (RPM) (Figure 2-3). A two-speed viscometer ($\theta_{600} - \theta_{300}$) is the most common device for measuring the viscosity and yield point of the drilling fluid when using the Bingham plastic model (API, 2009). However, a six-speed viscometer is required to extract the rheological parameters of the Power Law fluids. The six-speed viscometer is rarely used in the HDD industry because it takes much longer to measure the rheological parameters.

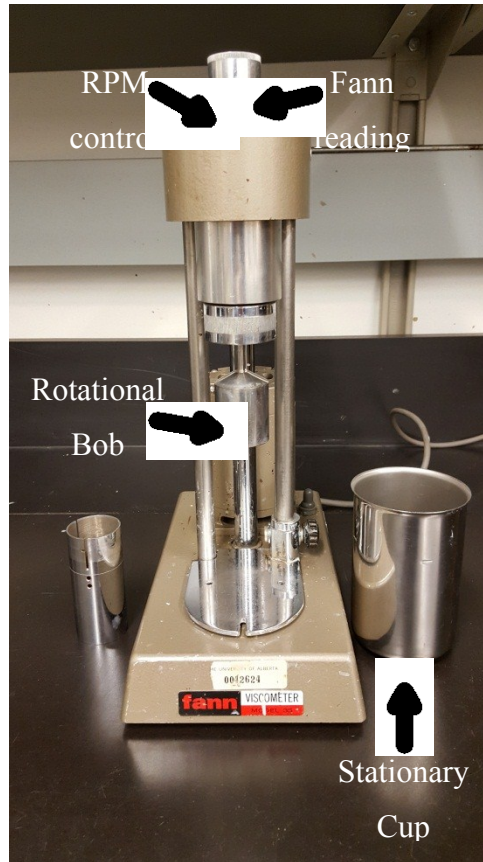


Figure 2-3 Fann viscometer device

However, HDD operations occur at a low shear rate (much lower than 300 RPM), resulting in the Bingham model overestimating the shear stress since the Bingham plastic model is based on the shear rate range of 300–600 RPM (Hemphill et al., 1993; Baroid, 1997). Baroid (1997) indicated that over-prediction ranged from 40 to 90 percent when using a high shear rate range for viscosity; hence, low shear rates are suggested when determining a low shear rate yield point to overcome this deficiency. Baumert et al. (2005) evaluated the current state of practice to determine annular pressures in HDD, particularly relating to pipeline installation. They reported that the approximate solution assuming laminar flow within a concentric annulus using the Bingham plastic flow model is overly conservative. Overestimation of the friction loss pressure component results from the concentric configuration of the drill stem in the annulus, which

oversimplifies flow velocity. Further overestimation results from the application of rheology parameters relating to high shear rate flows (300–600 RPM).

The literature has recognized the significance of annular pressure prediction and modelling in HDD. An attempt to maintain a simple method of practice coupled with a conservative result prompted the researchers to apply the Bingham plastic flow model for friction loss pressure calculations. Therefore, a proper comparison and calibration of predicted annular pressure and field measurements cannot be made. Due to the widespread use of two-speed (300–600 RPM) viscometers in the HDD industry, lower shear rate ranges are not accommodated. Also, the plan pressure is not properly established, leading to poor annular pressure management that inhibits success in HDD projects.

2-2- Prediction of Maximum Allowable Pressure

2-2-1- Theoretical Approach

In order to mitigate risk of hydraulic fracture, a demand-capacity solution should be used. In this method, circulating pressure is determined by using rheological models and the calculated pressure is compared with the soil capacity, which is related to the shear or tensile strength of the surrounding soil (Stauber, 2003). Thus, the measured or calculated annular pressure should be in a safe pressure range and lower than the determined maximum allowable pressure of the drilling fluid to prevent hydraulic fracture phenomenon during HDD.

According to the current HDD good practice methods, closed-form and analytical methods have been applied to investigate the limiting pressure of the drilling fluid when performing HDD in different soil types. There are two common mechanisms of failure around the borehole (cavity) according to the shear strength of soil, and initial stresses in the soil

medium. Tensile failure is a common type of fracture in cohesive soil at greater depths, and shear failure occurs in low-cohesive and frictional soils at shallow depths. All presented closed-form solutions for shear failure arise from the expansion of the cavity in an infinite medium with consideration to the Mohr-Coulomb constitutive model (Lugar and Hergarden, 1988; Van Brussel and Hergarden, 1997; Keulen, 2001; Arends, 2003; Wang and Sterling, 2007; Moore, 2005; Xia and Moore, 2007).

Luger and Hergarden (1988) proposed the first model applied to predict the maximum allowable pressure of the drilling fluid following shear failure assumption, which is known as Delft's method. This method is widely accepted by the standard for determining hydraulic fracture pressure in HDD (Yanagisawa and Panah, 1994; Delft Geotechnics, 1997; Staheli et al. 1998; Conroy, 2002; Stauber et al., 2003; Kennedy et al, 2004; Baumert et al., 2005, Elwood et al., 2007; Xia et al., 2007; Bennett, 2008; Staheli et al, 2010). This method can determine the maximum allowable pressure of the borehole in both cohesive and frictional soils at a shallow depth by using a cavity expansion theory formulated based on the Mohr-Coulomb small-strain elastic-perfectly plastic constitutive model. The assumptions in this method are as follows:

- 1- The borehole is axially symmetric and the soil medium is isotropic, homogenous with an unbounded boundary.
- 2- The geostatic stress is independent of the gravity, and the stress gradient is neglected.
- 3- The state of stress obeys Hook's law until the onset of yield, which is determined by the Mohr-Coulomb failure criterion.
- 4- Elastic strain is neglected in the plastic zone.

5- There is no volume change in the plastic zone.

6- Tension positive is adopted, and it is assumed that the radial stress σ_r is the major principal stress and the tangential stress σ_θ is the minor principal stress.

The effective maximum allowable pressure of the drilling fluid p'_{\max} which is the intersection point of lines A and B (Figure 2-4), can be used to correlate the maximum plastic radius $R_{p, \max}$ and the maximum allowable pressure p'_{\max} . The p'_{\max} is the maximum allowable pressure of the drilling fluid called the “Delft’s method,” which is the current “state-of-the-art” equation, to determine maximum allowable drilling fluid pressure in HDD (Equation [2-5]). Currently, this equation is considered the only method to estimate the maximum allowable pressure of the drilling fluid during HDD, and it is used as a threshold for the annular pressure along the bore path to mitigate the risk of hydraulic fracture.

$$P'_{\max} = (\sigma'_0(1 + \sin\varphi) + c\cos\varphi + ccot\varphi) \times \left\{ \left(\frac{R_0}{R_{p,\max}} \right) + \frac{(\sigma'_0\sin\varphi + c\cos\varphi)}{G} \right\}^{\frac{-\sin\varphi}{1+\sin\varphi}} - ccot\varphi \quad (2-5)$$

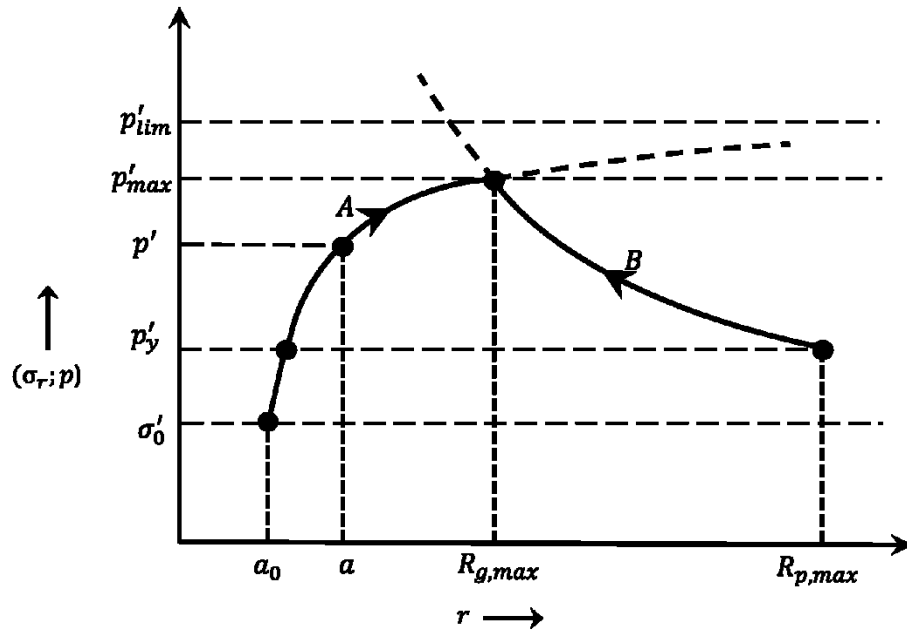


Figure 2-4 Internal pressure (pressure of the drilling fluid) within the borehole versus borehole radius (line A) and radial stresses versus radial distance outside the borehole (line B) (reproduced from Keulen, 2001)

Van Brussel and Hergarden (1997) suggested that the maximum allowable pressure of the soil is limited to the extension of the plastic radius to halfway to the ground surface in purely cohesive soils and to two thirds of the way in frictional soils. However, for deep excavation, the maximum allowable pressure is independent to the plastic radius, while the failure pressure reaches the limit pressure if the plastic radius tends to half or two thirds of the overburden depth. Also, the small-strain theory cannot be a good estimator of the failure when the large-strain or displacement is occurring through the surrounding soil. These issues are one of the major shortcomings of the Delft's method based on the small-strain theory with specific plastic radius.

There are some other close-form and analytical methods that are rarely used in HDD and are formulated based on a cavity expansion method, such as the Verruijt (1993) method, in

which to estimate the maximum allowable pressure of the drilling fluid, the maximum allowable strain following Delft's method is adopted instead of the maximum plastic radius, and Yu and Houlsby's (1991) large-strain analytical method, which considers dilative behaviour of soil during cavity expansion. Yu and Houlsby's (1991) method was formulated based on the direct integration of logarithmic strain to consider large-strain behaviour of soil during borehole expansion, and the Mohr–Coulomb failure criterion was adopted considering the non-associated plastic flow rule. Further details of Verruijt's (1993) method and Yu and Houlsby's (1991) analytical method are discussed in chapter 5.

2-2-2- Numerical Analysis

Kennedy et al. (2004) examined the effect of tensile failure in an undrained condition to determine the maximum allowable pressure of drilling fluid. Numerical modeling was also conducted with consideration to elastic plate theory for the prediction of the tensile strength of the surrounding soil. Kennedy showed that as a conservative assumption, when the tangential stress around the cavity decreases to zero, tensile failure occurs. According to the elastic plate theory, an increase in the annular pressure decreases the tangential stress. Equation (2-6) shows the relationship between tangential stress and the principal stresses at the crown of the borehole.

$$\sigma_{\theta}=3\sigma_x-\sigma_y-P_i \quad (2-6)$$

where σ_{θ} is the tangential stress at the crown of the borehole, σ_x is the minor principal stress in X direction, σ_y is the major principal stress in Y direction, and P_i is the internal or annular pressure. Tensile failure occurs around crown or springlines depending on the value of coefficient of lateral earth pressure (K_0). It is shown that the initiation of a tensile fracture occurs at the crown of the borehole where $K_0 < 1$, and at the springline where $K_0 > 1$ (Kennedy et al, 2004). This

mechanism is denoted “hydrofracture” here. Maximum allowable pressure in cohesive soils is calculated according to the elastic continuum theory as follows:

for $K_0 < 1$:

$$P_{max} = P_0 \times (3K_0 - 1) \quad (2-7)$$

for $K_0 > 1$:

$$P_{max} = P_{sp} \times (3 - K_0) \quad (2-8)$$

Kennedy et al. (2006) conducted a series of numerical analyses to investigate the effect of drilling fluid pressure on the tangential stress around the borehole in a sand medium. Their analysis considered the anisotropic geostatic stress and effects of the filter cake around the cavity. The investigation assumed that the filter cake parameters were the same as those of the host soil in an undrained state, and numerical results were compared to the theory of elasticity and plasticity for pure cohesive soil (filter cake) and pure frictional soil (host soil). Equation (2-9) shows the calculation of the undrained shear strength of the filter cake based on the host soil parameters:

$$S_{u(FC)} = 1/2 \sigma_v (1 + K_0) \sin \varphi \quad (2-9)$$

where $S_{u(FC)}$ is the undrained shear strength of the filter cake, σ_v is the major principal stress at the crown of the borehole, K_0 is the coefficient of lateral earth pressure, and φ is the friction angle of the host sand. Following the drained and undrained failure criterion of the soil, the tensile failure criterion in pure sand and sand with filter cake are formulated as follows:

when the filter cake is not formed:

$$\sigma_{\theta} = \sigma_r N_{\phi} \quad \text{For } \sigma_r < \sigma_{\theta} \quad (2-10)$$

$$\sigma_{\theta} = \frac{\sigma_r}{N_{\phi}} \quad \text{For } \sigma_r > \sigma_{\theta} \quad (2-11)$$

when the filter cake is formed:

$$\sigma_{\theta} = \sigma_r + 2C_u \quad \text{For } \sigma_r < \sigma_{\theta} \quad (2-12)$$

$$\sigma_{\theta} = \sigma_r - 2C_u \quad \text{For } \sigma_r > \sigma_{\theta} \quad (2-13)$$

The principal stresses around the borehole follow the plastic theory equations (Equations [2-10] and [2-11]) when the filter cake is not formed. In this condition, at the initial step of increasing the annular pressure, the squeezing occurs in the borehole in which the tangential stresses at the crown of the borehole increase. Then a gradual increase in the annular pressure decreases the squeezing deformation until the onset of stable conditions in the borehole, when the state of stresses around the borehole is elastic. In this condition, the state of stresses around the borehole follows the elastic theory equation (Equation [2-6]). With a gradual increase in the annular pressure, the state of stresses around the borehole intersects with the plastic failure criterion and follows the plastic theory equations (Equations [2-10] and [2-11]). The same changes in the state of stresses occur when the filter cake is formed around the borehole, while the plastic theory equations are defined based on Equations (2-12) and (2-13). According to this theory, the formation of the filter cake increases the risk of hydraulic fracture with an increase in the annular pressure while the tangential stress tends to a negative value in the elastic state. The theories are compatible in predicting the hoop stress of the lower filter cake thickness with the numerical modeling.

Conversely, Elwood's (2008) assumption concerning the filter cake parameters varies drastically from Kennedy's (Equation 2-9). Elwood reported that the physical properties of the filter cake are the same as native sand, with the exception that the moisture content increases from 2 to 6 percent in native sand, while the permeability decreases from 3.2×10^{-3} cm/s in sand to 7×10^{-6} cm/s in the filter cake. Elwood (2008) illustrated that the filter cake does not have a significant impact on the maximum allowable pressure of the drilling fluid or the size of the plastic zone around the cavity during HDD operations, which is in contrast to the results obtained by Wang and Sterling (2007) and Rostami et al. (2016). However, there is no common agreement on the impact of the filter cake on stability, failure pressure of the borehole, and geotechnical parameters of the formed filter cake.

Wang and Sterling (2007) furthered investigation of the effects of drilling fluid seeping into sandy soils by solving a coupled diffusion-displacement finite element model. The soil-drilling fluid interaction showed that the effective stress in high permeable soils drops to zero at a low drilling fluid pressure due to the rapid drainage of the flow and the lack of an efficient filter cake. The effect of the filter cake on borehole stability was also investigated, and it was determined that the formation of a filter cake can reduce the risk of shear failure at lower internal pressure by considering cohesion for filter cake and ultimately preventing the development of excess pore water pressure around the cavity (Kennedy et al., 2006; Wang and Sterling, 2007, Elwood, 2008). Also, the stiffness and shear strength parameters of filter cake positively impact the plastic radius. Wang and Sterling (2007) believe that the thickness of filter cake can play an important role on stability of the borehole as well. However, more research studies were required to investigate the impact of the thickness and geotechnical parameters of the filter cake on the stability of the borehole.

One of the major issues cited by some researchers is the effect of lateral earth pressure on the stress-strain behaviour around the borehole. Kennedy et al. (2004) as well as Xia and Moore (2006) examined the effect of lateral earth pressure in both frictional and cohesive soils. It was shown that the lateral earth pressure influenced the growth of the maximum allowable pressure and the orientation of the plastic zone and tensile fracture around the borehole. For k_0 values greater than one, critical condition occurs on the springlines of the borehole, while values below one find critical conditions occurring at the crown and invert. According to the theory of elastic in an infinite plane with a circular hole, the relationships between tangential and radial stresses are formulated as follows (Obert and Duvall, 1967):

Tangential stress at the springline:

$$\sigma_{\theta} = 3\sigma_y - \sigma_x - P_i \quad (2-14)$$

Tangential stress at the crown is defined in Equation (2-6). As the K_0 is defined as $\frac{\sigma_x}{\sigma_y}$ for a K_0 value below and above one, the initiation of tensile failure can represent the critical point at the borehole in which tensile failure tends to have negative value prior to the tangential stress at the crown or the springline.

2-2-3- Experimental Research

All analytical and close-form methods are based on the simplified assumptions that require a little practical assessment to be verified. The only way to assess the approximation of each model is by conducting an experimental test or field investigation on hydraulic fracture during HDD. There are limited experimental studies to simulate hydraulic fracture during HDD

in sandy soil. This section reports the procedures and results of experimental studies by a number of researchers.

Xia (2009) conducted a series of large- and small-scale laboratory tests employing finite element methods on sand to evaluate the effectiveness of the Delft's method and to quantify the maximum allowable pressure of drilling fluid during HDD. The small-scale tests were conducted in a designed set-up system with 0.78 m height, 0.80 m length, and 0.32 m width. Poorly graded medium sand was used as a host soil and was compacted with a hand tamper in 20 cm layers. Overburden pressure was applied using an MTS servo-controlled test system applying pressure on a metal plate located over three hardwood planks. The borehole was excavated using a Shelby tube with a diameter of 0.045 m and length of 0.6 m. The excavated borehole was sealed with an expandable packer, and the annular pressure was applied using a displacement pump. The annular pressure was measured using an ATS pressure transducer, and annular pressure was increased until a pressure drop occurred or the slurry was exposed at the ground surface. The large-scale tests were conducted using a box with 1.5 m height, 2.0 m length, and 2.0 m width. The borehole was excavated using a Shelby tube with a diameter of 0.055 m and length of 1.5 m. The other materials and procedures were the same as the small-scale test.

Xia (2009) showed that the Delft cavity expansion method overestimated the measured failure pressure by 2.5 times. According to the Xia (2009) numerical analysis, the conducted three-dimensional finite element modeling showed that the maximum allowable pressure overestimated the measured failure pressure, while the two-dimensional numerical modeling underestimated the maximum allowable pressure.

Elwood (2008) investigated the maximum allowable pressure of drilling fluid in cohesionless and multilayered soils by conducting large- and small-scale experimental tests and numerical modeling. The experimental test procedure and the set-up were the same as Xia's (2009) experimental study. The results obtained through numerical modeling were compatible with experimental measurements. However, other cavity expansion methods overestimated the measured failure pressure significantly. Elwood also investigated the effect of filter cakes around the borehole on the strength of the borehole during HDD operations. Elwood reported that the filter cake does not change the maximum allowable pressure of the borehole significantly. According to his experimental observation, the filter cake formed around the borehole in a uniform shape two to four times greater than the borehole diameter, which varies from Kennedy's assumption of a 2 to 3 cm formation around the borehole.

All in all, the experimental studies that researchers conducted prove that the suggested close-form methods, such as cavity expansion methods formulated based on the plastic radius by the HDD industry, cannot estimate the failure pressure properly and overestimate this pressure significantly, which leads to a non-conservative design of the borehole and an increase in the risk of failure in the HDD projects. Also, there are no common agreements on the size and properties of the formed filter cake around the borehole.

2-3- Summary

This chapter discussed the previous research studies in the field of annular pressure management. The current HDD good practice provided methods to estimate the annular pressure during pilot boring via the Bingham plastic model and the maximum allowable pressure of drilling fluid via Delft's method. By developing proper annular pressure management strategies

and monitoring annular pressures while drilling, the risk impacts resulting from the elevated annular pressures, such as hydraulic fracture, will be diminished.

According to the literature, the conventional Bingham plastic flow model at high shear rates (300–600 RPM) that is used as a current HDD good practice method to estimate the annular pressure is not accurate enough. Thus, the Bingham plastic model requires modification since the shear rate ranges of the drilling fluid during HDD are lower than 300 RPM. Also, the Delft close-form method overestimates the maximum allowable pressure of the drilling fluid significantly due to its simplified assumptions. Thus, further investigation is required to better understand the mechanical behaviour of the borehole during expansion to provide an accurate estimation of the maximum allowable pressure of the drilling fluid during HDD.

Reference

- American Petroleum Institute (API). 2009. Recommended practice on the rheology and hydraulics of oil-well drilling fluids, API RP 13D. Washington, D.C.
- Arends, G. 2003. Need and possibilities for a quality push within the technique of horizontal directional drilling (HDD), In Proceedings of 2003 No-Dig Conference, Las Vegas.
- Ariaratnam, S.T., Stauber, R.M., Bell, J., Harbin, B., and Canon, F. 2003. Predicting and controlling hydraulic fracturing during horizontal directional drilling, Proceedings of the International Conference on Pipeline Engineering and Construction, Baltimore, Maryland, 1334-1345.
- Baroid. 1997. Fluids Handbook. Baroid Fluid Services, Chapter 9, Rheology and Hydraulics, Haliburton, Houston, TX.

- Baumert, M.E., Allouche, E.N., and Moore, I.D. 2005. Drilling fluid considerations in design of engineered horizontal directional drilling installations, *International Journal of Geomechanics*, 5(4), 339–349.
- Bennett, D., and Wallin, K. 2008. Step-by-step evaluation of hydrofracture risks for HDD projects, In Proceeding of No-Dig Conference, North American Society for Trenchless Technology (NASTT), Cleveland.
- Bennett, D., Ariaratnam, S. and Como, C. 2001. Horizontal directional drilling good practice guidelines, HDD Consortium, Washington.
- Christopher, J.S., and Michael, M. 2003. Drilling fluid loss events in the Denver basin aquifers, H2GEO: *Geotechnical Engineering for Water Resources*, ASCE, 220-227.
- Conroy, P.J., Latorre, C.A., and Wakeley, L.D. 2002. Guidelines for installation of utilities beneath Corps of Engineers levees using horizontal directional drilling, *ERDC/GSL TR-02-9, Geotechnical Structures Laboratory*, Vicksburg, Mississippi.
- Delft Geotechnics. 1997. A report by Department of Foundations and Underground Engineering prepared for O'Donnell Associates, Inc., Sugarland, Texas.
- Duyvestyn, G. 2009. Comparison of predicted and observed HDD installation loads for various calculation methods, In Proceedings of 2009 International No-Dig Conference, Toronto, Ontario, Canada.
- Duyvestyn, G. M. 2006. Challenging ground conditions and site constraints, not a problem for HDD, In Proceedings of 2006 North American No-Dig Conference, Nashville, Tennessee.
- Elwood, D, Xia, H., and Moore, I.D. 2007. Hydraulic fracture experiments in a frictional material and approximations for maximum allowable mud pressure, In Proceedings of 60th Canadian Geotechnical Society Annual Conference, Ottawa, Ontario, Canada, 1681-1688.

- Elwood, D. 2008. Hydraulic fracture experiments in a frictional material and approximations for maximum allowable mud pressure, Master thesis, Queen's University, Kingston, Ontario, Canada.
- Harris, O. 2004. Evaluation of equivalent circulating density of drilling fluids under high pressure-high temperature conditions. M.Sc. thesis, University of Oklahoma, Norman, OK.
- Hemphill, T., Campos, W., and Pilehvari, A. 1993. Yield-power law model more accurately predicts drilling fluid rheology, *Oil and Gas Journal*, 91(34): 45-50.
- Kennedy, M.J., Moore, I.D., and Skinner, G.D. 2006. Development of tensile hoop stress during horizontal directional drilling through sand, *International Journal of Geomechanic*, 6(5), 367-373.
- Kennedy, M.J., Skinner, G.D., and Moore, I.D. 2004. Elastic calculations of limiting mud pressures to control hydro fracturing during HDD, In Proceedings of No-Dig Conference 2004, New Orleans, Louisiana.
- Keulen, B. 2001. Maximum allowable pressures during horizontal directional drillings focused on sand, PhD thesis, Delft University of Technology, Delft, Netherlands.
- Luger, H.J., and Hergarden, H.J.A.M. 1988. Directional drilling in soft soil: influence of mud pressures, In Proceedings of No-Dig Conference on Trenchless Technology, Washington, D.C.
- Moore, I.D. 2005. Analysis of ground fracture due to excessive mud pressure, Proceedings of 2005 No-Dig Conference, Orlando, Florida.
- Obert, L., and Duvall, W. I. 2013. Rock Mechanics and the Design of Structures in Rock.
- Osbak, M. 2011. Theory and application of annular pressure management, In Proceedings of No-Dig 2011 Conference, Washington, D.C.

- Rostami, A., Yi, Y., and Bayat, A. 2016. Investigating filter-cake formation on borehole stability during horizontal directional drilling in non-cohesive soil, NASTT No-Dig Show Conference, Dallas, Texas
- Staheli, K., Bennett, R.D., O'Donnell, H.W., and Hurley, T.J. 1998. Installation of pipelines beneath levees using horizontal directional drilling, Technical Report CPARGL-98-1, U.S. Army Engineer Waterways Experiment Station, Vicksburg, Mississippi.
- Staheli, K., Christopher, G. P., and Wetter, L. 2010. Effectiveness of hydrofracture prediction for HDD design, In Proceedings of No-Dig 2012 Conference, Chicago, Illinois.
- Stauber, R.M., Bell, J., and Bennett, R.D. 2003. A rational method for evaluating the risk of hydraulic fracturing in soil during horizontal directional drilling (HDD), In Proceedings of 2003 No-Dig Conference, Las Vegas, Nevada.
- Van Brussel, G.G., and Hergarden, H.J.A.M. 1997. Research (CPAR) program: Installation of pipeline beneath levees using horizontal directional drilling, Department of Foundation and Underground Engineering, Delft Geotechnics, 1-16.
- Verruijt, A. 1993. *Grondmechanica*, Delftse Uitgevers Maatschappij, Delft, Netherlands.
- Wang, X., and Sterling, R.L. 2007. Stability analysis of a borehole wall during horizontal directional drilling, *Tunneling and Underground Space Technology*, 22, 620–632.
- Xia, A. 2009. Investigation of maximum mud pressure within sand and clay during horizontal directional drilling, PhD thesis, Queen's University, Kingston, Ontario.
- Xia, H. and Moore, I.D. 2006. Estimation of maximum mud pressure in purely cohesive material during Directional Drilling, *International Journal Geomechanics and Geoengineering*, 1(1), 3-11.
- Xia, H. and Moore, I.D. 2007. Discussion of limiting mud pressure during directional drilling in clays, *Geo2007*, Ottawa, Canada.

Yanagisawa, E. and Panah, A. K. 1994. Two dimensional study of hydraulic fracturing criteria in cohesive clays, *Soils and Foundations*, 34(1), 1-9.

Yu, H.S., and Houlsby, G.T. 1991. Finite cavity expansion in dilatant soil: loading analysis, *Geotechnique*, 41(2), 173-183.

3- Initial Experimental Study on Formation of Filter Cake in Sand during Horizontal Directional Drilling¹

3-1- Introduction

Horizontal directional drilling (HDD) is a successful trenchless construction technique to install pipelines and underground utilities (Ariaratnam et al., 1999). In general, HDD operations consist of three steps: drilling a pilot bore, reaming the pilot bore 25–50% larger than the product pipe’s diameter, and installing the pipe. Drilling fluid, which generally comprises fresh water mixed with bentonite and/or additives, is a circulating fluid injected from the bottom hole assembly (BHA) into the borehole during HDD operations. Bentonite is classified as a material composed of the montmorillonite group of minerals, which enriches the properties of bentonite (Grim and Guven, 1978). Montmorillonite minerals have specific characteristics, such as a large cation exchange capacity, large specific surface area, high swelling potential, and low hydraulic conductivity to water (Gleason et al., 1997). Bentonite-based drilling fluid assists in cooling and lubricating the BHA and drill string, transporting cuttings to the surface, suspending cuttings when circulation stops, and reducing shear stresses during product pipe pull-back operations. Additionally, drilling fluid provides stability to the bore through static pressure and forms a thin, low permeable cake that seals the annulus from pores and opens fractures for cohesionless soils such as sand and gravel (Bennett and Ariaratnam, 2008). Formation of thin, low permeable cake in the borehole during HDD, especially in sandy soil, is essential to prevent distribution of

¹ A version of this chapter has been accepted for publication in the proceeding of the NASTT No-Dig Show Conference 2017, Washington, D.C.

excess pore water pressure around the cavity, which may result in hydraulic fracture (Elwood, 2008; Kennedy et al., 2006; Rostami et al., 2016; Wang and Sterling, 2007).

Limited research studies are available on the formation of filter cake in sand during HDD and its influence on the geotechnical parameters of initial soil, such as shear strength and permeability. Kennedy et al. (2006) used the Mohr-Coulomb model in an undrained condition to predict the shear strength of the filter cake. Conversely, Elwood's (2008) experimental study on the geotechnical parameters of filter cake implied inconsistent results with Kennedy et al. (2006). Elwood (2008) conducted small- and large-scale laboratory tests to simulate hydraulic fracture in HDD. These findings showed that according to the triaxial test results on soil samples around the borehole, the physical properties of the filter cake were similar to the native sand, while the moisture content increased from 2% to 6% and the permeability decreased from 3.2×10^{-5} m/s in the sand to 7×10^{-8} m/s in the filter cake. Thus, there is no common agreement on the geotechnical parameters of formed filter cake.

According to previous experimental studies (Kim and Tonon, 2010; Min et al., 2010, 2013), several factors influence the formation of filter cake, such as permeability of soil, slurry pressure, and slurry properties (density, viscosity, slurry particle size, etc.). Min et al. (2013) conducted a series of pressure filtration tests on nine different slurries and five different non-cohesive soils to investigate the formation of cake during shield tunnel boring machine (TBM) tunneling projects in high-permeable zones. The tests resulted in three different types of infiltration of slurry: a formed cake, a formed cake with an infiltrated zone, and an infiltrated zone without cake. This study showed that the formation of cake could be defined by the ratio of slurry particle size to pore size of the soil. However, experimental studies of formation of cake at the borehole wall during HDD in sandy soil while considering overburden pressure are rare.

The key objective of this study is to simulate the formation of cake in sandy soil in a small-scale test, and then to assess the geotechnical parameters. To achieve this objective, an experimental setup was designed to apply confining pressure on a sand specimen and inject bentonite-based drilling fluid as a permeant fluid into a sand specimen; this method is similar to the flexible wall permeability test but follows a different test procedure. Thereafter, unconsolidated and undrained triaxial shear tests were carried out on the sand specimens with and without cake in the same confining stress. This study presents the permeability and shear strength of the specimens.

3-2- Experimental Study

3-2-1- Material Properties

A fine-graded silica sand with a grain size distribution of mesh number 20-40 was used as a soil medium for infiltrating drilling fluid to form a cake at the surface of the sand specimen. A gradation of 20-40 means that the soil passes through mesh number 20 and retains on mesh number 40. The result of a sieve analysis for the sand is plotted as the percentage passing versus the sand particle size (Figure 3-1). The sand was compacted following a standard proctor compaction test (ASTM D698). The optimum water content is around 13.5%, and the dry density is $1,727 \text{ kg/m}^3$. Accordingly, the bulk density of the sand is $1,960 \text{ kg/m}^3$, the saturated density of the sand is $2,075 \text{ kg/m}^3$, and the initial void ratio is 0.53.

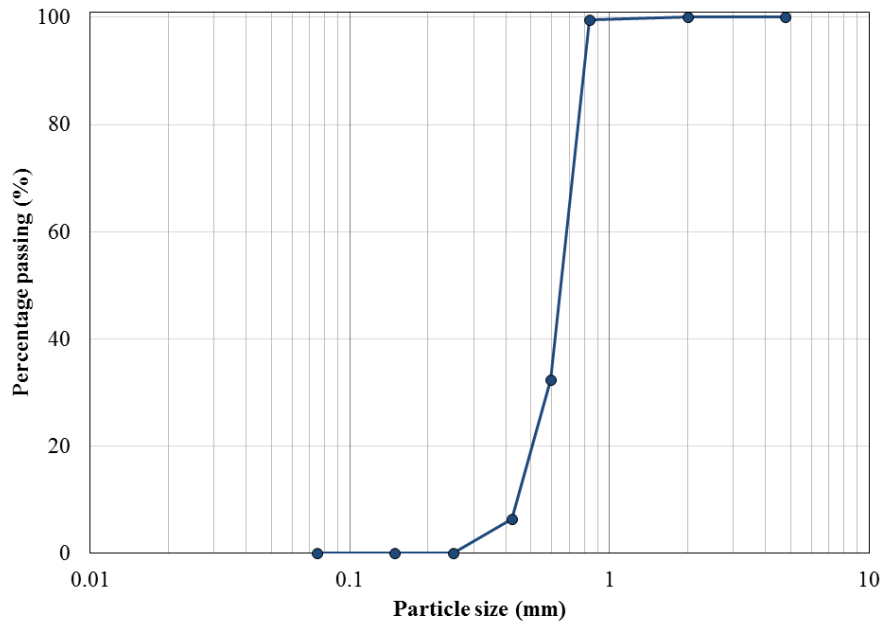


Figure 3-1 Particle size distribution curve for sand 20-40

The drilling fluid was prepared by using three concentrations of 2%, 3%, and 4% sodium bentonite mixed with tap water at room temperature. Figure 3-2 shows the rheogram of the drilling fluids using Fann viscometer. In the oil industry, API (2010) suggests that yield point and plastic viscosity parameters of the Bingham plastic model are calculated based on the 300 and 600 RPM shear stress viscometer readings (θ_{300} and θ_{600}); as a result, the yield stress is 5.74 Pa and the plastic viscosity is 0.006 Pa.s for the bentonite concentration of 2%, the yield stress is 12.92 Pa and the plastic viscosity is 0.006 Pa.s for the bentonite concentration of 3%, and the yield stress is 22.02 Pa and the plastic viscosity is 0.006 Pa.s for the bentonite concentration of 4%.

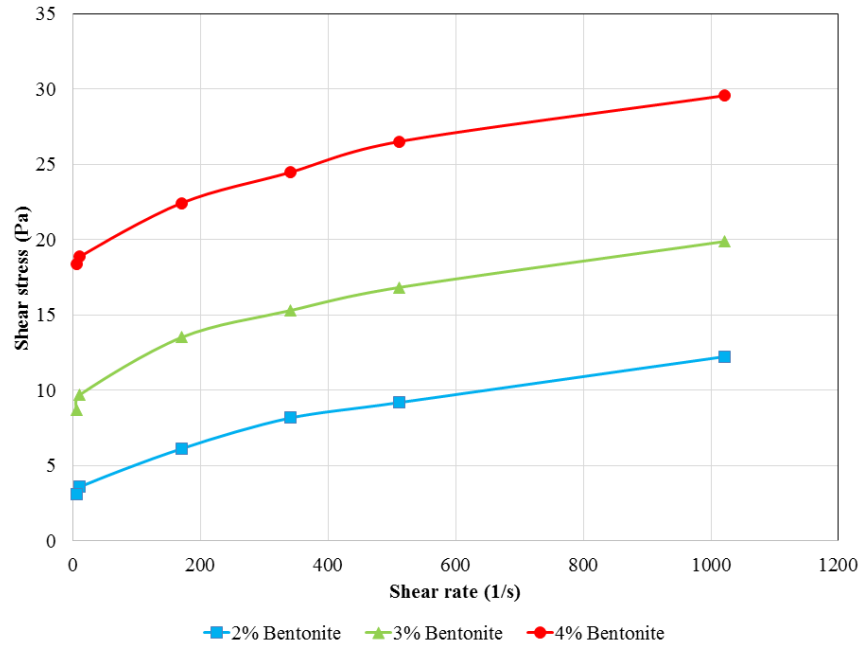


Figure 3-2 Rheogram of drilling fluids following viscometer test

3-2-2- Simulating Cake Formation

To simulate the formation of the cake in the sand, a setup was designed to inject the drilling fluid with a specific pressure or flow rate while applying confining stress on compacted sand. This test setup is similar to the flexible wall permeability test in which the constant head or constant flow rate method was conducted while using the drilling fluid as a permeant fluid. The triaxial cell used has double drainage lines at the top and bottom of the test specimen. In this study, the top drainage line opened to the atmospheric pressure for the drilling fluid outflow, and the two bottom drainages were used for the drilling fluid inflow and the pressure head transducer. The drilling fluid passed through the compacted sand with a constant head or flow rate using a 500 D syringe pump. The pump has a capacity of 500 mL and can pump a wide range of chemical materials requiring flow rates up to 200 mL/min at pressures up to 25 MPa. To adjust the confining pressure inside the triaxial cell, a control panel with an adjustable air

pressure gauge was used. A data logger was connected to the control panel, pressure gauges, and strain gauge to better monitor the data. Figure 3-3 shows a schematic of the test setup.

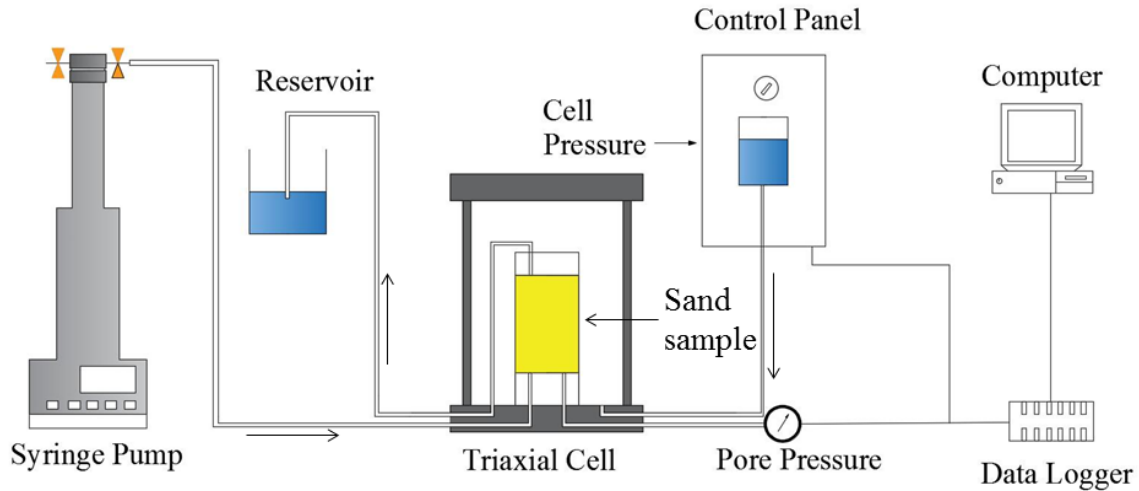


Figure 3-3 Schematic of cake formation simulation test set-up

3-2-3- Experiment Procedure

The designed setup was used to form a cake at the surface of the sand specimen. In this study, the drilling fluid (which is the mixture of water with 2%, 3%, and 4% bentonite) was used separately as a permeant fluid during injection to simulate the formation of cake in different sand specimens. First, the sand specimen was compacted to the optimum water content of 13.5% in a small mold with a diameter of 38 mm and height of 76 mm. In this test, two rigid screens with a mesh number of 40 (0.430 mm), equal to the minimum sand particle size, were located at the bottom and top of the specimens to prevent the sand particles from intruding into the flow lines. The specimen was mounted on the triaxial pedestal, and a top cap was located over the specimen at the top of the screen. The pedestal screens, specimen, and top cap were enclosed by a flexible membrane, and then the triaxial cell was filled with de-aired tap water (Figure 3-4).

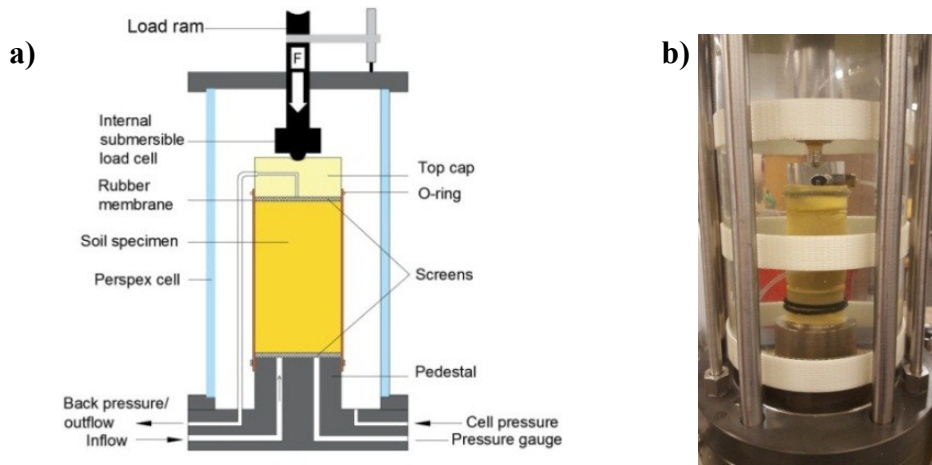


Figure 3-4 a) Schematic of mounted specimen in the triaxial cell, b) filling up the triaxial cell with water

The system was then de-aired using a flushing and vacuum technique. Afterward, the specimen was saturated based on a back pressure technique similar to the method used before initiating the normal triaxial shear test. Following the back pressure saturation, the confining pressure was increased to generate the confining stress of 100 kPa to consolidate the specimen simulating the overburden stress of about 5 meters' depth. Prior to pumping the drilling fluid into the sample, the constant flow rate permeability test was conducted on the sand using water as a permeant fluid. Using a constant head test on a high permeable sand specimen is not desirable; this is due to the permeant fluid increasing its flow rate and exceeding the flow rate limit of the syringe pump which is 200 mL/min. During the constant flow rate test, the drainage valve was open to atmospheric pressure to gather the outflow, and the flow rate was constant at 60 mL/min while a pressure gauge monitored the pressure head at the bottom of the specimen. The flow rate should not be low to decrease the impact of pressure gauge error, nor should it be high to prevent disturbing the specimen. The constant flow rate test was carried out on 12 different sand specimens.

In the next step, the syringe pump was filled with the drilling fluid with a specific concentration of bentonite, and the drilling fluid was pumped into the bottoms of the same specimens with a pressure head of 70 kPa. During the injection of the fluid, the syringe pump flow gauge monitored the flow rate. To simulate the formation of the cake, a constant flow rate test is not desirable because during the formation of the cake, the syringe pump requires the pressure head to increase to keep the flow rate constant at the defined flow rate, which can rise to 25 MPa based on the capacity of the syringe pump. Thus, it is not safe if the pressure head exceeds the defined confining stress or the capacity of the used triaxial cell, which is 3 MPa. It should be noted that during HDD, the annular pressure may reach or exceed the overburden pressure. In the experimental test, on the other hand, if the pressure head exceeds the confining stress, it may lead to the movement of soil particles, expansion of membrane, and leakage of water into the specimen. Three tests were conducted on three different specimens using 2%, 3%, and 4% bentonite concentrations mixed with water as a permeant fluid to simulate formation of the cake. The sand specimens with cake denoted the concentrations of bentonite used as a drilling fluid. Figure 3-5 shows the flow rate generated by the syringe pump to keep the head constant at 70 kPa for sand specimens with cake.

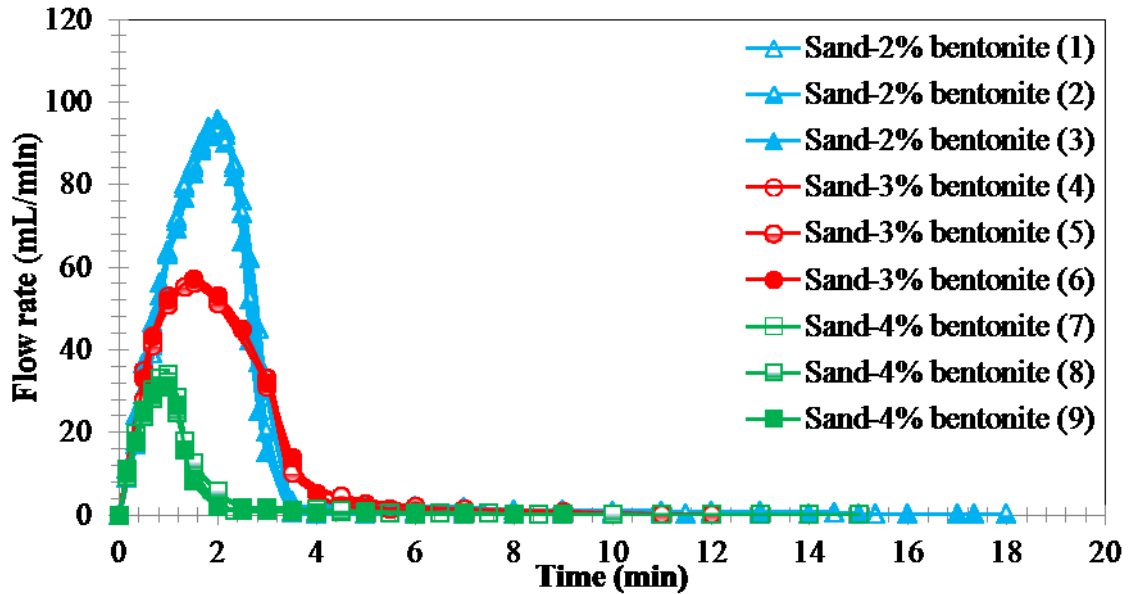


Figure 3-5 Measured flow rate for sand specimens using drilling fluid as a permeant fluid

Figure 3-5 shows the flow rate increases from zero to 32 mL/min for 2% bentonite, 57 mL/min for 3% bentonite, and 95 mL/min for 4% bentonite. The flow rate then drops rapidly to around 0.1 mL/min which indicates the quick formation of the cake and a decrease in the specimen's permeability over time. During infiltration of the drilling fluid from the bottom of the specimen, the bentonite particles rapidly filled the pores of the sand and accumulated at the bottom of the specimen. During the permeability test, it was observed that the fluid that came out of the effluent valve was almost pure water during the first two minutes; this implies that the sand medium works as a filter. Once a thicker fluid came out, the flow rate started to drop. Figure 3-6 illustrates the formation of the cake on the mesh screen; the cake is covered with sand particles and blocks the seepage path of the drilling fluid. Also, prior to the permeability test on the sand sample, it was observed that the cake was not formed on the screen when the sand is not mounted on the screen. It should be noted that the mesh screen does not hinder the drilling fluid seeping into the sample. The mesh size is equal to the minimum pore size of the sand specimen,

and the screen functions to prevent washout of the sand particles. The bentonite particles from the bottom of the specimen filled the pores of the sand specimen while the drilling fluid was injected from the bottom of the sample. Therefore, the bentonite particles actually hindered the seepage of the drilling fluid.

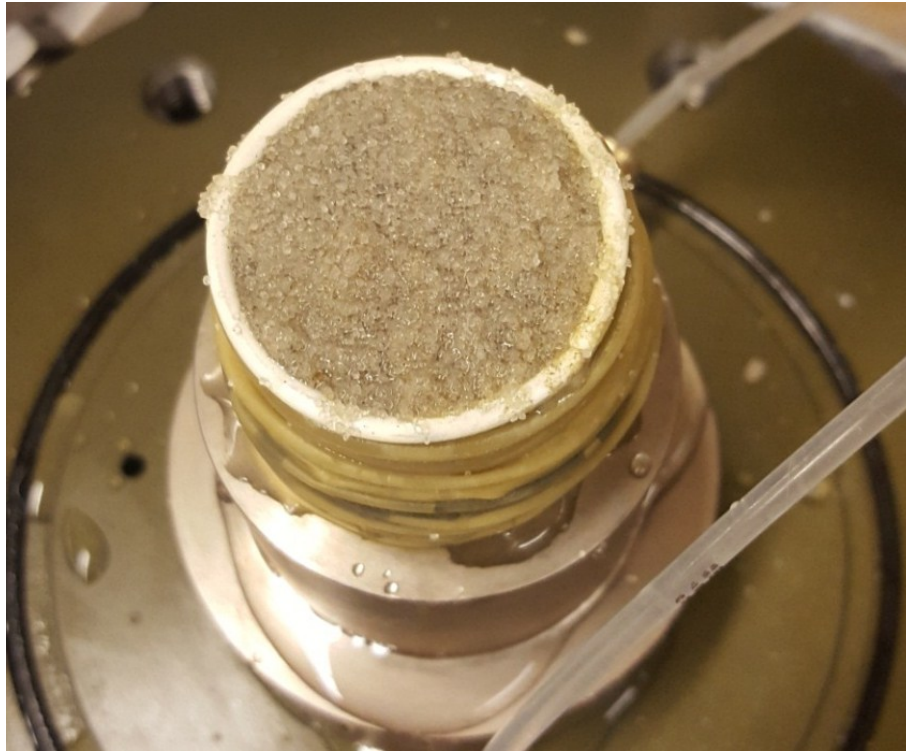


Figure 3-6 Formation of thin layer of cake after injection of the drilling fluid

According to the test procedure conducted to simulate the cake formation which was similar to the flexible wall permeability test, it is possible to calculate the permeability of the sand specimen. To calculate the coefficient of permeability of the specimen, the flow rate must be measured in a steady state condition in which the inflow and outflow rates are stable and equal. In this case, the drilling fluid injection continued for a longer period of time (about 24 hours). In the case of a constant flow rate test on the pure sand specimens, the steady state condition occurred in a minute while at the beginning of the test, some air bubbles came out of

the drainage valves and the pressure head at the bottom of the sample became stable and constant. According to ASTM D5084, the coefficient of permeability for both constant flow rate and constant head tests was calculated as follows:

$$k = \frac{\Delta Q \cdot L}{A \cdot \Delta h \cdot \Delta t} \quad (3-1)$$

where:

k = coefficient of permeability (m/s)

ΔQ = flow rate for given time interval Δt (m³/s)

L = length of specimen (m)

A = cross-sectional area of specimen (m²)

Δt = interval of time (s) over which the flow ΔQ occurs

Δh = average head loss across the permeameter/specimen (m)

Using Equation 3-1, the coefficient of permeability of the sand specimen without cake is around 8×10^{-5} m/s, which is in the rational ranges of 10^{-5} m/s to 10^{-3} m/s for fine and coarse sand (Das, 2013). During simulation of the cake formation in sand specimens with different bentonite concentrations, the coefficient of permeability of the specimen decreases dramatically (Table 3-1). After formation of the cake, the value of the permeability is low enough (10^{-5} times that of pure sand) to prevent the drilling fluid from further infiltrating the specimen and can be considered an impermeable layer at the surface of the HDD borehole wall. The bentonite concentration in the drilling fluid impacts the coefficient of permeability. By increasing the

bentonite concentration, the coefficient of permeability decreases, e.g., it drops to zero for concentrations above 3% (Table 3-1). Additionally, the cake forms faster compared to lower bentonite concentrations (Figure 3-5).

Table 3-1 Calculated permeability of sand specimens with cake

Test No.	Bentonite concentration (%)	Flow rate (m ³ /s)	Pressure head (kPa)	Permeability (m/s)	Average (m/s)
1	2	0.004	70	5.8×10 ⁻¹⁰	
2	2	0.005	70	7.2×10 ⁻¹⁰	7.3×10 ⁻¹⁰
3	2	0.006	70	8.8×10 ⁻¹⁰	
4	3	0.002	70	2.7×10 ⁻¹⁰	
5	3	0.001	70	1.4×10 ⁻¹⁰	2.3×10 ⁻¹⁰
6	3	0.002	70	2.8×10 ⁻¹⁰	
7	4	0	70	0	
8	4	0	70	0	0
9	4	0	70	0	

3-3- Shear Strength

In order to investigate the shear strength of the specimen after infiltrating the drilling fluid when the cake was formed, an unconsolidated and undrained triaxial shear test (UU) following ASTM D2850 with a confining stress of 100 kPa and axial strain of 0.474 mm/min was carried out over the previously tested specimens. As well, the UU triaxial shear test was conducted over three different sand specimens without cake in similar conditions so as to compare the impact of the drilling fluid infiltration on the shear strength parameters of the specimens. In this case, the outflow valve at the top of the sample was closed and no seepage was allowed into the sample. The undrained shear strength of the sand specimens with cake and

the pure sand specimens without cake are shown in Figure 3-7. Figure 3-7 clarifies that the undrained shear strength of the sand filter cake specimens are close to the pure sand specimens. This means that a negligible amount of bentonite particles are trapped in the soil specimen while the formation of the cake prevents further migration of the bentonite particles into the soil specimen. Thus, using drilling fluids with 2%, 3%, and 4% bentonite does not change the undrained shear strength of sand. Accordingly, using bentonite concentrations higher than 4% is expected to provide the same results compared to 4% bentonite because of even faster formation of the cake and a negligible amount of infiltrated bentonite particles in the sand.

However, the drilling fluid may penetrate into the coarse-grained and highly permeable soils and the cake may not form. In this case, it is expected that the shear strength of the soil decreases due to the decrease in the friction angle of the soil and increase in the plastic behaviour of the soil. The penetration of the bentonite particles into the sand medium disturbs the intergranular interaction of the sand particles and decreases the internal friction angle of the sand; this is due to the bentonite swelling when soaked in water and then breaking up the sand particles' contacts. Thus, a decrease in the shear strength of the surrounding soil due to infiltration of the drilling fluid may disrupt the stability of the borehole in a short-term period. Also, a lack of formation of a proper cake at the borehole wall can increase the risk of hydraulic fracturing due to the generation of excess pore water pressure during drilling and decrease the effective shear stress of the surrounding soil medium. A critical issue facing HDD Engineers is how to form an impermeable cake at the borehole wall during HDD in non-cohesive soil (sand or gravel). More studies are required to investigate the relationship between the drilling fluid properties (viscosity, particle size, density, etc.) and pore size of the sand on the formation of cake on the surface of

the sand. The gradation and porosity of the soil medium can be useful in designing a proper drilling fluid with specific rheological properties and particle size distribution.

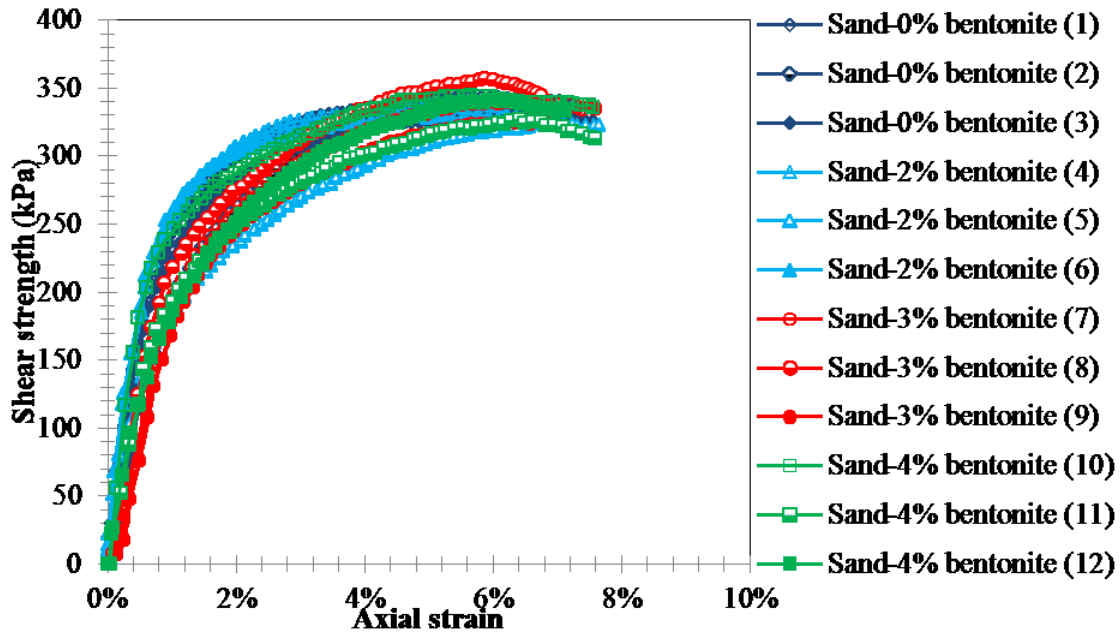


Figure 3-7 Undrained shear strength of the sand specimens with and without cake

3-4- Conclusion

To simulate the formation of the cake on the surface of the sand during HDD, an experimental test setup was designed. Accordingly, following the formation of the cake at the bottom of the specimen due to injecting the drilling fluid with different concentrations, it was possible to measure the permeability of the sand specimens. The results of the permeability test showed that the coefficient of permeability drops rapidly when using 2%, 3%, and 4% bentonite drilling fluid. During pumping, the flow rate of the drilling fluid with a constant head starts to increase at the initial stage when the drilling fluid fills the voids of the sand specimen; the flow rate then drops rapidly when the cake forms, thus preventing further penetration of the drilling fluid. In order to investigate the impact that infiltrating the drilling fluid has on shear strength

parameters of the sand medium, a UU triaxial shear test was carried out on specimens with cake and on pure sand specimens without cake. The UU triaxial shear tests showed that the shear strength parameter of the specimen was hardly changed. The results implied that the formation of the cake prevented the drilling fluid from further infiltrating the sand specimen; thus, negligible amounts of bentonite particles were trapped in the sand specimen, which did not impact the shear strength parameter of the soil much. More studies are required to investigate the relationship between the drilling fluid properties (viscosity, particle size, density, etc.) and sand pore size on the formation of the cake at the surface of the sand.

Reference

- American Petroleum Institute (API). 2010. Recommended practice on the rheology and hydraulics of oil-well drilling fluids API RP 13D, Washington, D.C., USA.
- Ariaratnam, S.T., Lueke, J.S., and Allouche, E.N. 1999. Utilization of trenchless construction methods by Canadian municipalities, *Journal of Construction Engineering and Management*, 125(2), 76-86.
- ASTM D2850-15. 2015. Standard test method for unconsolidated-undrained triaxial compression test on cohesive soils, ASTM International, West Conshohocken, PA, USA.
- ASTM D5084. 2003. Standard test methods for measurement of hydraulic conductivity of saturated porous materials using a flexible wall permeameter, American Society for Testing and Materials, Philadelphia, PA, USA.
- ASTM D698. 2012. Test Methods for Moisture-Density Relations of Soils and Soil-Aggregate Mixtures. Method A (Standard Proctor).
- Bennett, R.D., and Ariaratnam, S.T. 2008. Horizontal directional drilling good practices guidelines. Third Edition, HDD Consortium.

- Das, B. M. 2013. Advanced soil mechanics. CRC Press.
- Elwood, D. 2008. Hydraulic fracture experiments in a frictional material and approximations for maximum allowable mud pressure, Master thesis, Queen's University, Kingston, Ontario, Canada.
- Gleason, M.H., Daniel, D.E., and Eykholt, G.R. 1997. Calcium and Sodium Bentonite for Hydraulic Containment Applications, *Journal of Geotechnical and Geoenvironmental Engineering*, ASCE, 123(5), 438-445.
- Grim, R., and Guven, N. 1978. Bentonite: Geology, Mineralogy, Properties, and Uses, Elsevier Science Publishing, New York.
- Kennedy, M.J., Moore, I.D., and Skinner, G.D. 2006. Development of tensile hoop stress during horizontal directional drilling through sand, *International Journal of Geomechanic*, 6(5), 367-373.
- Kim, S.H., and Tonon, F. 2010, Face stability and required support pressure for TBM driven tunnels with ideal face membrane drained case, *Tunneling and Underground Space Technology*, 25(5), 526–542.
- Min, F., Zhu, W., and Han, X. 2013. Filter cake formation for slurry shield tunneling in highly permeable sand. *Tunnelling and Underground Space Technology*, 38, 423–430.
- Min, F.L., Zhu, W., Han, X.R., and Zhong, X.C. 2010. The effect of clay content on filter cake formation in highly permeable gravel, *Geotechnical Special Publication*, 204 GSP, 210–215.
- Rostami, A., Yi, Y., and Bayat, A. 2016. Investigating filter-cake formation on borehole stability during horizontal directional drilling in non-cohesive soil, NASTT No-Dig Show Conference, Dallas, Texas
- Wang, X., and Sterling, R.L. 2007. Stability analysis of a borehole wall during horizontal directional drilling, *Tunneling and Underground Space Technology*, 22, 620–632.

4- Annular Pressure Prediction in HDD using the Bingham Plastic Flow Model²

4-1- Introduction

Horizontal directional drilling (HDD) is a steerable trenchless construction technique used for the installation of pipelines and other underground utilities with minimal surface disruption (Ariaratnam et al., 1999). Since its inaugural crossing of the Pajaro River in Watsonville, California in 1971, the HDD industry has experienced accelerated growth and is now a worldwide multibillion dollar construction solution, manufacturing over 32,000 HDD rigs in 2011 (Sarireh et al., 2012). Generally, HDD operations consist of three steps: drilling a pilot bore with a drill bit, pre-reaming and reaming the pilot bore 25-50 percent larger than the product pipe's diameter, and pipe installation. Drilling fluid, which generally comprises of fresh water mixed with bentonite and/or addition of polymer or other additives, is critical for a successful pipe installation (Bennett and Ariaratnam, 2008). It assists in cooling and lubricating the bottom hole assembly and drill string, transporting cuttings to the surface, suspending cuttings when circulation stops, and reducing shear stresses during product pipe pull-back operations. Additionally, drilling fluid provides stability to the bore through static pressure and forms a thin, low permeable filter cake that seals the annulus from pores and open fractures for cohesionless soils (Bennett and Ariaratnam, 2008).

Circulation of the fluid through the bore develops an annular pressure inside the bore. When the annular pressure exceeds the hydraulic fracture pressure of surrounding soil, a loss of

² A version of this chapter was published in the International Journal of Petroleum Engineering in 2016.

fluid circulation and inadvertent release of mud at the ground surface occurs (Christopher et al., 2003; Bennett and Ariaratnam, 2008; Duyvestyn, 2009; Staheli et al, 2010; Osbak, 2011). These critical conditions are most likely to occur within the first step of drilling operations (pilot boring) as the annular space is relatively small and the annular fluid pressure is relatively high during this phase (Baumert et al., 2005), also the risk of inadvertent return of drilling fluid is high near the entry and exit locations due to the shallow depth (Conroy et al., 2002). The release of drilling fluid to the ground surface or within water can lead to environmental and social impacts. Additionally, risk impacts resulting from elevated annular pressure also play considerable roles in evaluating HDD construction risk. Osbak et al. (2012) identified HDD construction risk events experienced in 100 HDD projects within Alberta and Northern British Columbia, Canada, and quantified the average schedule impact for each event. Risks associated with annular pressure have the following average schedule impacts (Osbak et al., 2012): loss of circulation (8 percent), hydraulic fracturing (7 percent), collapsing bore (13 percent), elevated annular pressure (6 percent), and drill cutting buildup in the annulus (11 percent). In order to minimize the construction and environmental impacts associated with annular pressure during HDD, a technique called annular pressure management can be employed (Stauber et al., 2003; Osbak et al., 2012), which uses a predicted plan pressure as a target. The plan pressure can be predicted using an appropriate flow model, such as Bingham plastic model, Power Law model, and Herschel Bulkley model, among which the Bingham plastic model is the most widely used in HDD industry due to its simplicity.

Annular pressure is comprised of friction loss and hydrostatic pressure of fluid in the bore. During bore excavation in HDD operations, the annular pressure is determined by the pump output rate, annulus geometry, and annular fluid properties (Ariaratnam et al., 2007).

Hydrostatic pressure is equal to fluid column weight through the bore, and friction loss pressure can be calculated through rheological models such as the Bingham plastic flow model, which accounts for the yield stress of laminar fluids and is the most widely used flow model in HDD industry (Baroid, 1997; Staheli et al., 1998; Ariaratnam et al., 2003; Stauber et al., 2003; Baumert et al., 2005; Ariaratnam et al., 2007, Duyvestyn, 2009; Bennett et al, 2012). A viscometer is commonly used to determine the Bingham rheological parameters of fluids based on the shear stress (torque) and the shear rate (RPM). For oil field drilling, API (2010) suggests the Bingham rheological parameters are calculated based on the viscometer readings (shear stresses) at shear rates of 300 and 600 RPM; this method has been adopted in HDD industry. The Bingham model with a shear rate range of 300-600 RPM overestimates the shear stress for lower shear rates (Baroid, 1997, Growcock and Harvey, 2005), while HDD operates in a lower shear rate range, resulting in an overly conservative annular pressure prediction that promotes deeper and longer drill path designs and increases construction costs (Baumert et al., 2005). Baroid (1997) indicated that the over-prediction ranged from 40 to 90 percent when using a high shear rate range of 300-600 RPM for viscosity, and hence it is suggested the use of low shear rates of 3 and 6 RPM. Since the two-speed (300 and 600 RPM) viscometer is widely used in field by HDD industry in Canada, lower shear rates of fluid are not commonly measured in the field. Additionally, to date, the published annular pressure data during pilot boring of HDD in literature is limited.

Hence, in this study, a six-speed (3, 6, 100, 200, 300, and 600 RPM) Fann Model 35 (Fann Instrument Company) viscometer was used to determine the rheological parameters of annular fluid for two HDD cases. The Bingham model with rheological parameters calculated based on different shear rate ranges was used to predict the annular pressures during pilot boring.

The predicted pressures were then compared to the field measurements to determine appropriate shear rate range.

4-2- Methodology

To evaluate the annular fluid pressure during pilot boring in HDD, it is assumed that the drill pipe is placed in the centerline of the bore, the annulus radius is constant, and the bore is cleaned. The method from Baroid (1997), which characterized the fluid with the Bingham model, was used to calculate the frictional loss pressure in the concentric annuli. As shown in Figure 4-1, the Bingham model requires an initial shear stress to initiate the fluid to flow, called the yield point (*YP*); at greater stresses, the fluid exhibits Newtonian behaviour, where the plastic viscosity (*PV*) remains constant with increasing shear rate. The equation for Bingham model is as follow:

$$\tau = YP + PV * \gamma \quad (4-1)$$

where τ is the shear stress and γ is the shear rate.

In this study, a six-speed (3, 6, 100, 200, 300, and 600 RPM) viscometer was used to determine the Bingham rheological parameters.

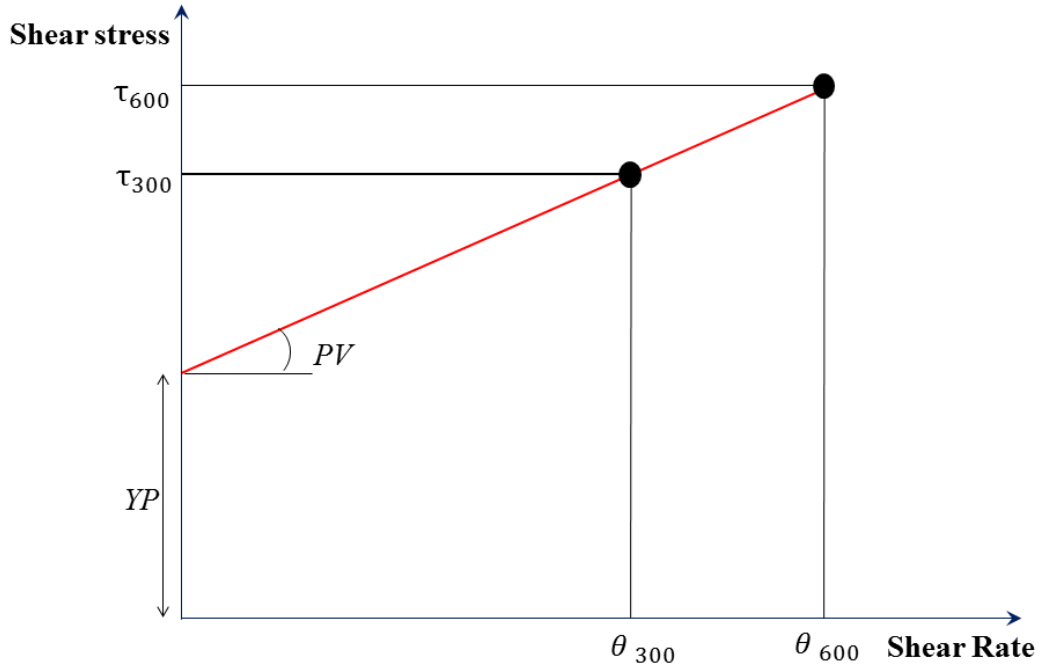


Figure 4-1 Illustration of Bingham plastic flow model (Drilling fluids processing handbook modified)

4-2-1- Justification of Viscometer Data

Using a viscometer to measure the Bingham rheological parameters is based on the assumption that the flow in the equipment is fully developed, which is generally valid for rotation speeds of 300 and 600 RPM, but might not for lower shear rates. To determine the acceptable shear rates, the following procedure can be employed (Bird et al. 2002):

1. Determine the shear stresses on the spindle (τ_{spindle}) and cup (τ_{cup}) of the viscometer; τ_{spindle} is the dial reading of viscometer, and τ_{cup} is calculated by Equation (4-2).

$$\tau_{\text{cup}} = \tau_{\text{spindle}} * (R_1/R_2)^2 \quad (4-2)$$

where R_1 is the radius of spindle and R_2 is the radius of cup. For the model 35 of Fann viscometer, R_1/R_2 is 0.935.

2. Determine the yield point (YP) from the linear regression line of the shear stress-shear rate curve based on dial readings; there are six readings for the first time.

3. Compare the obtained τ_{spindle} and τ_{cup} in Step 1 with the YP obtained from Step 2. If τ_{spindle} and τ_{cup} are both higher than YP , it is concluded that the fluid is fully developed. Otherwise, remove the points, which have lower τ_{spindle} and τ_{cup} than YP , from the regression line, and then proceed Steps 2 and 3 again.

4-2-2- Determination of Bingham Rheological Parameters

The Bingham rheological parameters can be determined from viscometer data with two different shear rates, e.g. 300 and 600 RPM as shown in Figure 4-1, where YP is the Y intercept of shear stress-shear rate curve and it is calculated by Equation (4-3), and PV is the slope and it is calculated by Equation (4-4).

$$YP = \frac{600 \times \theta_{300} - 300 \times \theta_{600}}{600 - 300} \times 0.51 \quad (4-3)$$

where θ_{300} and θ_{600} are the shear stresses at shear rates of 300 and 600 RPM from dial readings (Fann) of viscometer; 0.51 is the coefficient to convert the unit of Fann to Pa.

$$PV = \frac{\theta_{600} - \theta_{300}}{600 - 300} \times 0.3 \quad (4-4)$$

where 0.3 is the coefficient to convert the unit of Fann·s to Pa·s.

For other shear rate ranges, PV and YP also can be calculated using Equations (4-3) and (4-4) with the corresponding shear rates and stresses.

4-2-3- Calculation of Annular Pressure

Two components contribute to annular pressure in the bore: the hydrostatic fluid pressure acting on the bore, and the friction loss pressure that provides cuttings suspension and flow out of the bore. Hydrostatic pressure (P_h , unit: Pa) results from the weight of the vertical fluid column above the bottom of the bore, and it is calculated by Equation (4-5).

$$P_h = \rho * g * h \quad (4-5)$$

where ρ is the density (kg/m^3) of the fluid within the bore annulus, g is the gravitational constant (9.81 N/kg), and h is the elevation difference (m) between the drill rig entry point and the point of interest within the bore as far as the desired point is located below the entry point; otherwise the hydrostatic pressure is zero.

As introduced by Baroid (1997), the friction loss pressure (P_a , unit: Pa) can be calculated by Equation (4-6), where the units have been changed to SI:

$$P_a = \left(47.89 \times \frac{PV * v}{(D_B - D_{DP})^2} + 6 \times \frac{YP}{D_B - D_{DP}} \right) * L \quad (4-6)$$

where D_B is the diameter of the bore (m), D_{DP} is the outer diameter of the drill pipe (m), and L is the drill path length (m). v is the average fluid velocity (m/s) in the annulus, and it is derived from Equation (4-7).

$$v = 1.273 \times \frac{Q}{D_B^2 - D_{DP}^2} \quad (4-7)$$

where Q is the pump output (m^3/s). The circulating pressure (P) in the bore is the summation of the static and friction loss pressures, as shown in Equation (4-8).

$$P=P_h+P_a \quad (4-8)$$

4-3- Case Study

4-3-1- Project Overview and Measurements

Two HDD cases in northwestern Alberta, Canada, were used to examine the annular pressures predicted by the Bingham model using rheological parameters derived from different shear rate ranges compared with measured results in the field.

Case A was a 1,205 m long HDD installation with a pilot bit diameter (D_B) of 0.251 m and drill pipe diameter (D_{DP}) of 0.114 m. The average pump rate (Q) was 1700 L/min and the average fluid density (ρ) was 1100 kg/m³. The drill path entry point was located lower than exit point, as shown in Figure 4-2. The entry location was approximately 65 m below the exit location, resulting in the latter 221 m drill path length without a static column of fluid within the annulus. Case B is a 520 m long HDD installation (Figure 4-3) with a pilot bit diameter of 0.311 m and pipe diameter of 0.140 m. The average pump rate was 1350 L/min and the average fluid density was 1000 kg/m³. Additionally, Figure 4-2 and 4-3 demonstrate that the depth of the bores is relatively large, mainly for reducing the risk of hydraulic fracture caused by annular fluid pressure during construction.

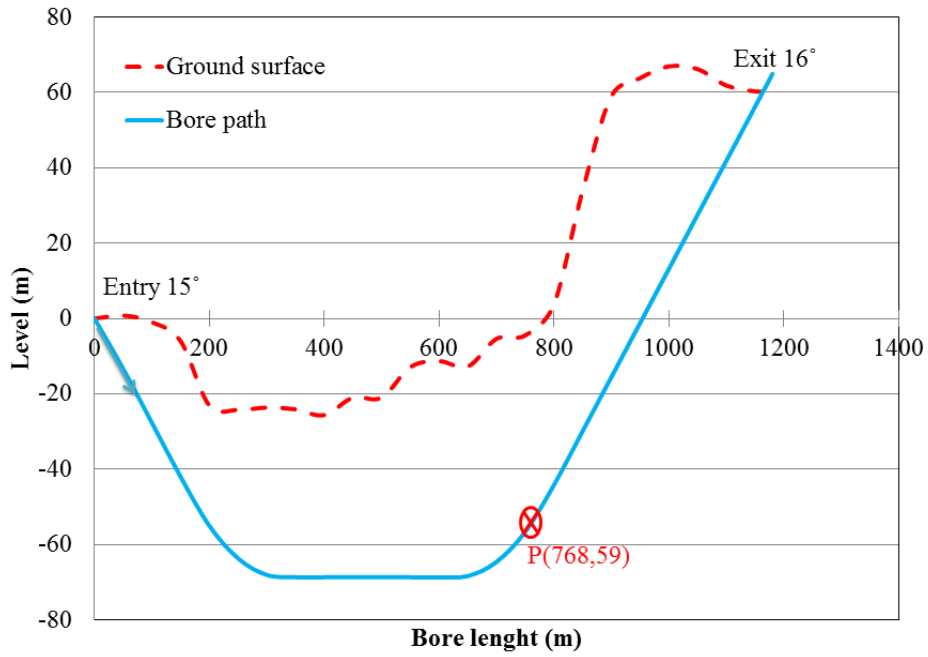


Figure 4-2 Drill path profile of Case A

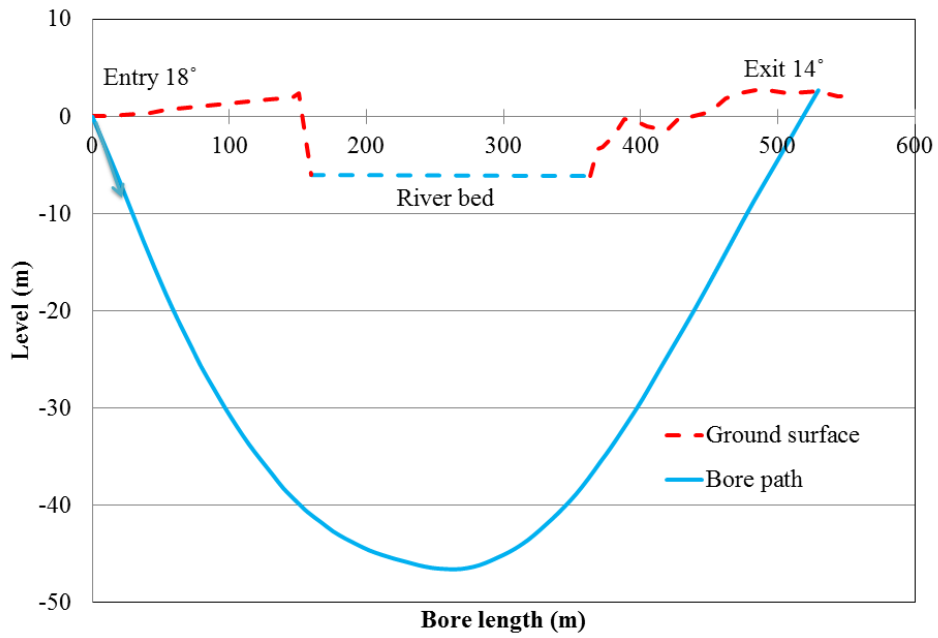


Figure 4-3 Drill path profile of Case B

The annular pressure was measured during pilot boring for the two cases. The measurement was taken via a wireline using a Paratrack pressure sensor located within the orienting sub behind the pilot drill bit while it was running into the pre-drilled cleaned bore annulus within the pilot bore. The sensor was calibrated before use, and it measured the total annular pressure inside the bore which is comprised of hydrostatic pressure and friction loss pressure. The annular measurements were transmitted to a data logger out of the bore every 10 seconds.

A six-speed (3, 6, 100, 200, 300, and 600 RPM) viscometer (Fann Model 35) was used to measure the rheological parameters of the fluids. The fluids were sampled from those came out to the entry pit when the drilling bit was at different locations throughout the bore after cleaning the bore to be assured that the rheological properties of the slurry is somehow similar to the drilling fluid. There were 30 and 6 samples tested for Cases A and B, respectively. The average and coefficient of variation of the viscometer data are presented in Table 4-1, and the shear stresses on the spindle and cup of viscometer are presented in Table 4-2.

Table 4-1 Viscometer data of the fluids

Shear rate (RPM)	Case A		Case B	
	Average (Fann)	Coefficient of variation	Average (Fann)	Coefficient of variation
θ_3	22	0.28	13	0.20
θ_6	23	0.28	14	0.24
θ_{100}	34	0.20	36	0.18
θ_{200}	38	0.21	49	0.14
θ_{300}	44	0.22	59	0.16
θ_{600}	48	0.28	83	0.17

Table 4-2 Shear stresses on the spindle and cup of viscometer

Shear rate (RPM)	Case A		Case B	
	Spindle (Pa)	Cup (Pa)	Spindle (Pa)	Cup (Pa)
θ_3	11.2	9.9	6.2	5.8
θ_6	11.8	10.3	7.2	6.3
θ_{100}	17.4	15.2	18.4	16.1
θ_{200}	19.4	17.0	25	21.9
θ_{300}	22.5	19.7	30.1	26.4
θ_{600}	24.5	21.5	42.4	37.2

Following the procedure in Section “Justification of Viscometer Data”, it is determined that the flow in the viscometer was not fully developed for shear rates of 3 and 6 RPM, which were not applicable to calculate Bingham rheological parameters (YP and PV). For the shear rates combination of 100-200, 200-300, and 300-600 RPM, the PV and YP were calculated using the method in Section “Determination of Bingham Rheological Parameters”. For example, the viscometer dial readings for fluids in Case A were 38 and 44 Fann at the shear rates of 200 and 300 RPM, respectively; using Equations (4-3) and (4-4), the YP and PV are calculated as follows.

$$YP = \frac{300 \times 38 - 200 \times 44}{300 - 200} \times 0.51 = 13.26 \text{ Pa} \quad (4-9)$$

$$PV = \frac{44 - 38}{300 - 200} \times 0.3 = 0.018 \text{ Pa} \cdot \text{s} \quad (4-10)$$

The YP and PV for other shear rate ranges can be calculated in the same way and the results are shown in Table 4-3, which illustrates that varying Bingham rheological parameters are determined from different shear rate ranges and hence can impact the annular pressure prediction.

Table 4-3 Bingham rheological parameters

Shear rate range (RPM)	Case A		Case B	
	<i>YP</i>	<i>PV</i>	<i>YP</i>	<i>PV</i>
	(Pa)	(Pa·s)	(Pa)	(Pa·s)
100-200	15.30	0.012	11.73	0.039
200-300	13.26	0.018	14.79	0.030
300-600	20.53	0.004	18.62	0.024

4-3-2- Comparison of Predicted and Field-Measured Annular Pressures

As introduced in the Section “Calculation of Annular Pressure”, the annular pressure during pilot boring can be calculated using Equations (4-5)-(4-8) providing the Bingham rheological parameters, annulus area, fluid column height, and pump rate. A sample of annular pressure calculation for Case A at a selected location P (shown in Figure 4-2) with Bingham rheological parameters derived from shear rate range of 200-300 RPM is presented as follows.

For Case A, $\rho=1100 \text{ kg/m}^3$, $D_B=0.251 \text{ m}$, $D_{DP}=0.114 \text{ m}$, $Q=1700 \text{ L/min}=0.0283 \text{ m}^3/\text{s}$; at location P, $L=768 \text{ m}$, $h=-59 \text{ m}$, it is noted that the location information was automatically collected and sent back to the data logger during construction; for the shear rate range of 200-300 RPM, $PV=0.018 \text{ Pa}\cdot\text{s}$, $YP=13.26 \text{ Pa}$ (Table 4-2). Substituting the above parameters to Equations (4-5)-(4-8), the calculations are conducted as the following processes (Equations (4-11)-(4-14)).

$$P_h=1100 \times 9.81 \times 59=636669 \text{ Pa} \quad (4-11)$$

$$v=1.273 \times \frac{0.0283}{0.251^2-0.114^2}=0.720 \text{ m/s} \quad (4-12)$$

$$P_a=\left(47.89 \times \frac{0.018 \times 0.72}{(0.251-0.114)^2} + 6 \times \frac{13.26}{0.251-0.114}\right) \times 768=471398 \text{ Pa} \quad (4-13)$$

$$P=636669+471398=1108067 \text{ Pa}=1108.067 \text{ kPa} \quad (4-14)$$

The annular pressures along the whole bore path were calculated in the same way, and the results were plotted in Figure 4-4 and 4-5, where the sensor-measured pressures were also plotted for comparison. Figure 4-4 indicates that the predicted annular pressure with the shear rate range of 300-600 RPM is considerably higher than the sensor-measured pressure, increasing in deviation from the measured pressure at a distance of up to 110 percent, averaging at a value of 30 percent along the drill path for Case A. Predicted pressure with shear rate range of 200-300 RPM is also higher than the measured result up to 90 percent, and had an average deviation of 17 percent. The low shear rate range of 100-200 RPM provided a closer approximation to the measured pressure.

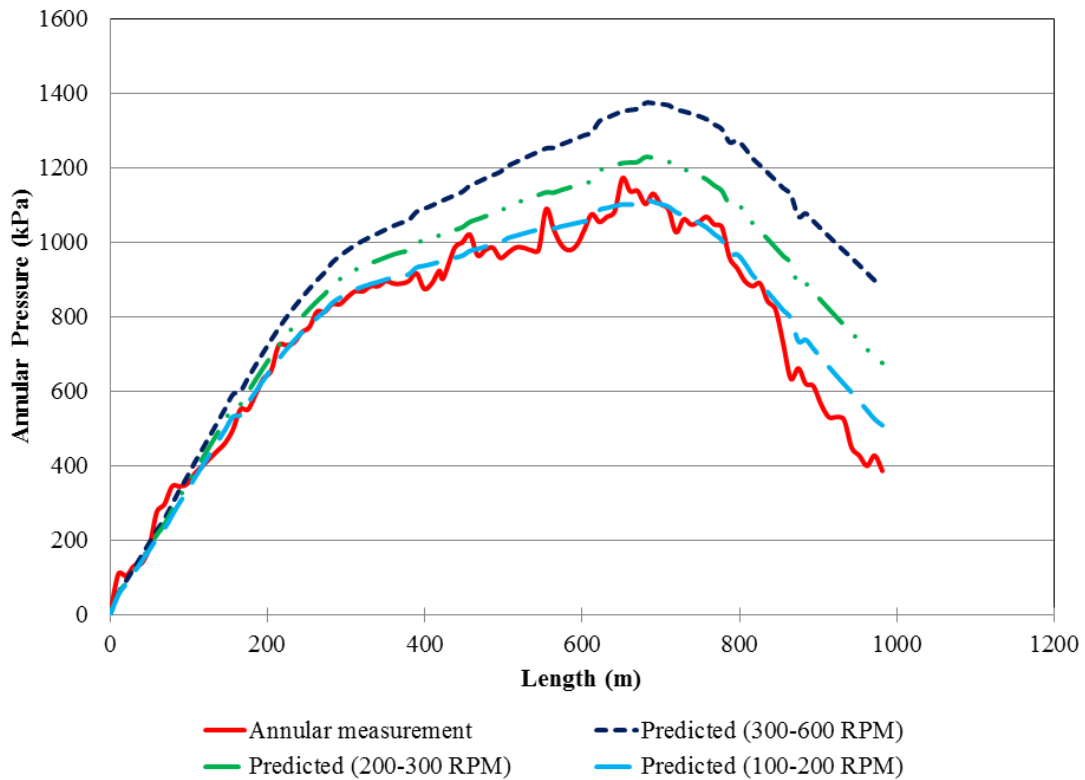


Figure 4-4 Comparison of predicted and measured annular pressure for Case A

For Case B, Figure 4-5 indicates that using the 300-600 RPM shear rate range also predicts higher annular pressure than the measurement. Deviation from the measured pressure increases with distance up to 75 percent and has an average value of 25 percent along the drill path for Case B. Similar to that in Case A, the shear rate range of 200-300 RPM overestimates measurements up to 65 percent, with an average value of 16 percent. The low shear rate range of 100-200 RPM provides a closer approximation to the measured pressure.

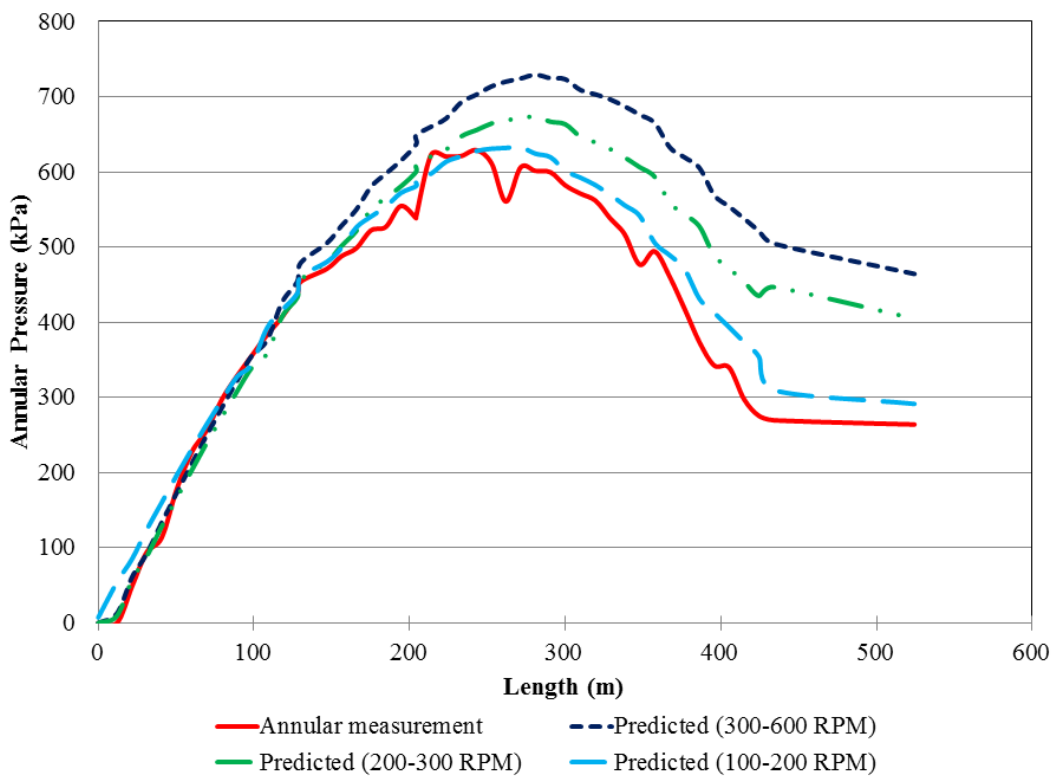


Figure 4-5 Comparison of predicted and measured annular pressure for Case B

4-4- Conclusion

In this study, the Bingham plastic flow model, with fluid rheological parameters determined from six-speed viscometer measurements at different shear rate ranges, was used to predict annular fluid pressure during pilot boring in HDD. The predicted pressures were then

compared to field measurements from two HDD cases, and the comparison indicated favourable results for the Bingham model at the low shear rate range of 100-200 RPM. Conversely, the results at high shear rate ranges of 200-300 and 300-600 RPM overestimated the measurement up to 30 percent on average along the drilling path and approximately 110 percent near the exit pit. Therefore, it is suggested that Bingham rheological parameters determined at low shear rate ranges, e.g. 100-200 RPM, be used for the prediction of annular pressure during pilot boring in HDD. However, it has to be justified that the flow is fully developed in the viscometer at these low shear rates, otherwise they are not applicable to calculate Bingham rheological parameters, e.g. 3 and 6 RPM in the two cases of this study; this is a limitation of using the Bingham model, therefore it is also suggested to investigate other fluid models (e.g. Power Law model) in future studies.

Reference

- American Petroleum Institute (API). 2010. Recommended practice on the rheology and hydraulics of oil-well drilling fluids API RP 13D, Washington, D.C., USA.
- Ariaratnam, S.T., Harbin, B.C., and Stauber, R.L. 2007. Modeling of annular fluid pressures in horizontal boring, *Tunnelling and Underground Space Technology*, 22, 610–619.
- Ariaratnam, S.T., Lueke, J.S., and Allouche, E.N. 1999. Utilization of trenchless construction methods by Canadian municipalities, *Journal of Construction Engineering and Management*, 125(2), 76-86.
- Ariaratnam, S.T., Stauber, R.M., Bell, J., Harbin, B., and Canon, F. 2003. Predicting and controlling hydraulic fracturing during horizontal directional drilling, Proceedings of the International Conference on Pipeline Engineering and Construction, Baltimore, Maryland, 1334-1345.

- Baroid. 1997. Fluids Handbook. Baroid Fluid Services, Chapter 9, Rheology and Hydraulics, Haliburton, Houston, TX.
- Baumert, M.E., Allouche, E.N., and Moore, I.D. 2005. Drilling fluid considerations in design of engineered horizontal directional drilling installations, *International Journal of Geomechanics*, 5(4), 339–349.
- Bennett, R.D., and Ariaratnam, S.T. 2008. Horizontal directional drilling good practices guidelines. Third Edition, HDD Consortium.
- Bennett, R.D., Osbak, M., and Wallin, M. (2012) ‘Improving the standard of mud management’, *In Proceedings of 2012 No-Dig Conference*, Nashville, Tennessee.
- Bird, R.B., Stewart, W.E., and Lightfoot, E.N. 2002. Transport phenomena, New York: John Wiley & Sons.
- Christopher, J.S., and Michael, M. 2003. Drilling fluid loss events in the Denver basin aquifers, *H2GEO: Geotechnical Engineering for Water Resources*, ASCE, 220-227.
- Conroy, P.J., Latorre, C.A., and Wakeley, L.D. 2002. Guidelines for installation of utilities beneath Corps of Engineers levees using horizontal directional drilling, *ERDC/GSL TR-02-9, Geotechnical Structures Laboratory*, Vicksburg, Mississippi.
- Duyvestyn, G. 2009. Comparison of predicted and observed HDD installation loads for various calculation methods, In Proceedings of 2009 International No-Dig Conference, Toronto, Ontario, Canada.
- Growcock, F., and Harvey, T. 2005. Drilling fluids. Drilling Fluids Processing Handbook, *UK: Elsevier Ink*, 15-66.
- Osbak, M. 2011. Theory and application of annular pressure management, In Proceedings of No-Dig 2011 Conference, Washington, D.C.

- Osbak, M., Akbarzadeh, H., Bayat, A., and Murray, C. 2012. Investigation of horizontal directional drilling construction risks, In Proceedings of No-Dig 2012 Conference, Nashville, Tennessee.
- Sarireh, M., Najafi, M., and Slavin, L. 2012. Usage and applications of horizontal directional drilling, In Proceedings of ICPTT 2012: Better pipeline infrastructure for a better life, Wuhan, China.
- Staheli, K., Bennett, R.D., O'Donnell, H.W., and Hurley, T.J. 1998. Installation of pipelines beneath levees using horizontal directional drilling, Technical Report CPARGL-98-1, U.S. Army Engineer Waterways Experiment Station, Vicksburg, Mississippi.
- Staheli, K., Christopher, G. P., and Wetter, L. 2010. Effectiveness of hydrofracture prediction for HDD design, In Proceedings of No-Dig 2012 Conference, Chicago, Illinois.
- Stauber, R.M., Bell, J., and Bennett, R.D. 2003. A rational method for evaluating the risk of hydraulic fracturing in soil during horizontal directional drilling (HDD), In Proceedings of 2003 No-Dig Conference, Las Vegas, Nevada.

5- Predicting the Plan Annular Pressure using the Power Law Flow Model in Horizontal Directional Drilling³

5-1- Introduction

Horizontal directional drilling (HDD) is a trenchless construction solution to the traditional open-cut method used for utility conduit installation. Over the past four decades, advancements in HDD have made it an effective and common method for installation, particularly in congested urban areas and environmentally sensitive ones such as beneath rivers and wetlands, as it provides minimal impact on the surrounding environment (Ariaratnam et al., 1999).

The HDD process includes pilot boring, reaming, and product pipe pullback (Allouche et al., 1998). The largest drilling concerns occur in the first stage (pilot boring), as it has the highest construction risk of hydraulic fracturing and loss of drilling fluid circulation (Baumert et al., 2005). In this stage, drilling fluid pressure should be maintained within an appropriate range to provide stability of the borehole and adequate circulating pressure to transport cuttings out of the borehole. Drilling fluid used in HDD generally comprises an admixture of water and bentonite. During HDD operations, the drilling fluid functions to: provide stability to the borehole, especially in collapsible soil and porous medium; decrease the frictional drag between the pipe and the borehole; cool the drill bit during excavation; and transport drill cuttings to the ground surface (Ariaratnam et al., 1999).

³ A version of this chapter was published in the Canadian Journal of Civil Engineering in 2015.

Excess drilling fluid pressure within the annular space of the borehole may result in shear or tensile failure of the surrounding soil or rock. This may cause the drilling fluid to migrate to the ground surface, decreasing circulating pressure within the borehole annulus and inducing negative environmental impacts. The inadvertent return of the drilling fluid to the surface is a critical risk encountered during HDD (Staheli et al., 2010; Christopher et al., 2003; Harris, 2004; Duyvestyn, 2006; Bennett et al., 2001; Osbak, 2011).

Annular pressure management is a technique employed to maintain drilling fluid pressure between the maximum allowable and plan pressures of the drilling fluid during HDD, which prevents mud loss failure through the borehole and also provides the borehole with stability. HDD contractors apply the annular pressure management system to achieve a targeted drilling fluid rheology and to predict the mechanical behaviour of drilling fluid as it interacts with soil in the borehole (Stauber et al., 2003; Osbak, 2011). Effective annular pressure management provides the necessary information to monitor and control risk events resulting from elevated annular pressures during HDD construction. To accomplish this, the circulating drilling fluid pressure must be predicted (plan pressure), and the boundary of allowable pressure thresholds must be established prior to project execution. The plan pressure can be estimated using the appropriate flow model and associated rheological parameters.

The Bingham plastic model is commonly used by HDD engineers to calculate the drilling fluid pressures within a borehole (Baroid, 1997). The Bingham plastic model accounts for the yield stress of laminar drilling fluids but overestimates the shear stress for lower shear rates (Hemphill et al., 1993; Baroid, 1997; Harris, 2004). As a result, the drilling fluid pressure derived from the Bingham plastic model is overly conservative, which can result in deeper and longer drill path design, thereby increasing overall construction costs (Baumert et al., 2005).

According to the American Petroleum Institute Recommended Practice (API 2009), the Power Law flow model is considered the standard model for calculating drilling fluid pressure within the borehole for petroleum industry. This model is more desirable than the Bingham plastic model in calculating drilling fluid pressures as it accounts for the nonlinear relationship between the shear stress and shear rate (shear thinning behaviour); however, its application in HDD industry has rarely reported.

5-2- Objective

This paper addresses the prediction of the plan annular pressure using the Power Law flow model with rheological parameters determined from a six-speed viscometer with varying shear rate ranged from 3 to 600 RPM. Real time data (updated rheological data and current pump rate) was considered as the input parameters of the Power Law model. The measured pressures from two HDD projects were used to compared with the predicted pressures using the Power Law model, and hence to validate its applicability in predicting annular pressure.

5-3- Methodology

5-3-1- Mechanical Behaviour of Drilling Fluid

Rheology is the study of characterizing fluid flow. The rheological relationship between shear stress and shear strain rate (shear rate) allows for the study of the deformation and movement of fluid (API, 2009; Harris, 2004). Shear stress is a force applied per unit area in the radial plane of the flow channel. Each adjacent layer of flow has a different velocity resulting from the frictional force acting upon the layers. As a result, the velocity profile increases gradually in the radial direction of flow channel, from zero on the boundary surface to the

maximum at the centerline of channel (free stream), as shown in Figure 5-1. The shear rate is the velocity gradient in the direction perpendicular to shear force.

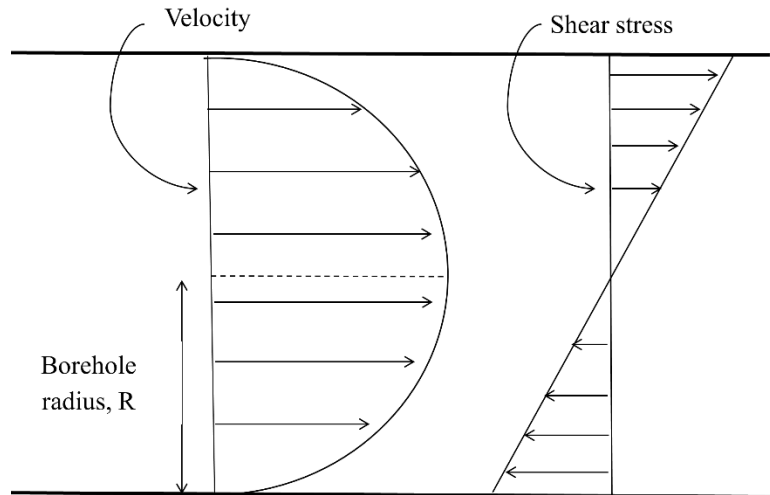


Figure 5-1 Distribution of velocity and shear stress in a flow channel

The behaviour of drilling fluid is determined by the flow regime, which can be laminar or turbulent depending on the fluid properties and annular geometry (Baroid, 1997). API (2009) assumes that the flow of drilling fluid in HDD is laminar; that is, parallel to the wall of the flow channel. Laminar flow occurs when the shear rate is low to moderate and flow layers pass each other in a consistent and parallel fashion. Figure 5-2 shows a scheme of the laminar flow layers of a viscous fluid between two plates; the bottom layer is fixed, while the top layer is free. As mentioned previously, due to the frictional interaction between the flow layers, each successive layer exerts a force attempting to drag the following layer causing a variation in velocity, ranging from v at the top to zero at the bottom.

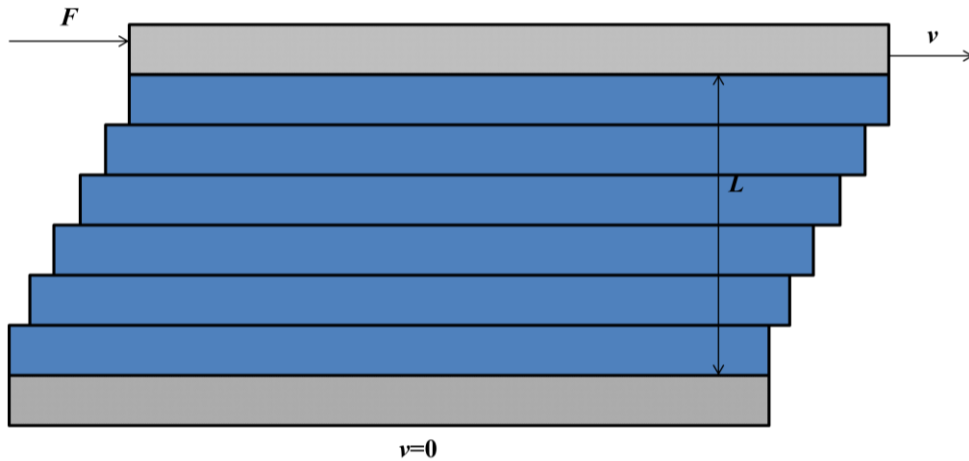


Figure 5-2 Schematic of laminar flow between two plates

Rheological models have been used to predict the flow behaviour of different types of fluids (Baroid, 1997). In the case of Newtonian fluid, there is a direct relationship between shear stress and shear rate, where the viscosity is constant at a given pressure and temperature. Freshwater, seawater, diesel oil, mineral oils, glycerin, clear brines, and synthetics are examples of Newtonian fluids (Baroid, 1997). The mathematical relationship of shear stress and shear rate is as follows:

$$\tau = \mu \dot{\gamma} \quad (5-1)$$

where τ is the shear stress, μ is the viscosity, and $\dot{\gamma}$ is the shear rate.

In non-Newtonian fluids, the viscosity is related to the shear rate and time at a given temperature and pressure. This type of fluid is subdivided into two categories according to time's impact on the fluids: time-dependent or time-independent fluid. Time-dependent fluids exhibit viscosity changes with time. Time-independent fluids have a constant viscosity at a constant shear rate over time (Harris, 2004). Most drilling fluids follow non-Newtonian fluid behaviour as

they are comprised of an admixture of solids and liquid. The electrochemical and physical interactions between the solid and liquid phases change, resulting in variations to the relationship between shear rate and shear stress (Osbaek, 2011).

In this study, it is assumed that the drilling fluid behaviour in HDD applications is non-Newtonian and time-dependent (updated rheological data) throughout the pilot bore drilling process. The time-dependency of drilling fluid means increased cutting soil particles in the fluid during HDD borehole excavation, altering drilling fluid properties.

5-3-2- Concentric Annular Flow

To evaluate the drilling fluid pressure through the borehole, it is assumed that the drill pipe passes along the centerline of the pilot hole. Considering the eccentricity of the drill pipe in the borehole through the variable mud density could decrease the mud loss pressure during HDD operations up to 50 percent (Haciislamoglu and Langlinais, 1990). To predict the friction loss pressure, the HDD industry has traditionally used the Bingham plastic model, which considers laminar concentric annular and non-Newtonian flows (Baroid, 1997). This research considers laminar concentric annular and non-Newtonian flow for the Power Law model.

5-3-3- Annular Pressure

Annular pressure is comprised of friction loss and hydrostatic pressure. During borehole excavation in HDD operations, the annular pressure is determined based on the total pump output rate, annular space within the borehole, and drilling fluid properties. When the pump is off and circulation stops, only the hydrostatic pressure remains within the borehole annulus. When pumping resumes, the fluid flows through the annulus. The flow regime for a concentric

drill pipe is represented in Figure 5-3. The lowest velocity in the streamline (zero) occurs along the drill pipe and wall of the borehole, while the highest velocity, at the midpoint of the streamline.

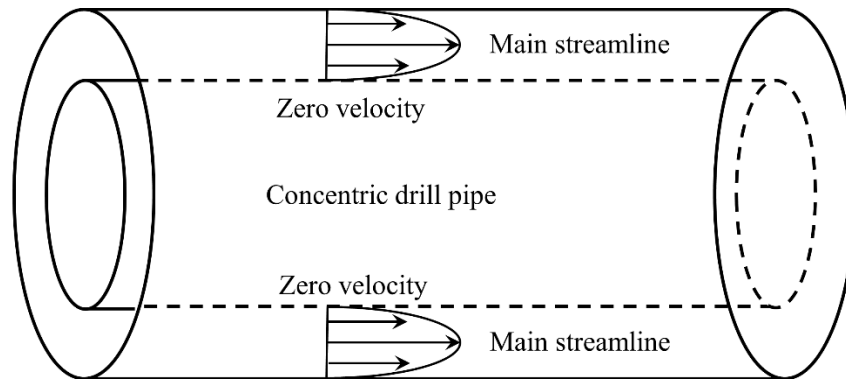


Figure 5-3 Concentric annular flow through the borehole

As a result of the differing velocities of the fluid layers, frictional interactions between the interfaces develop vertical strain in each layer and generate momentary force within all layers. In consequence, normal forces between the layers propagate to the wall of the borehole, causing radial outward pressure (Osbaek, 2011).

5-3-4- Predicting Annular Pressure

5-3-4-1- Power Law model

The Power Law model is a two-parameter and time-independent rheological model. In particular, the Power Law model addresses the shear thinning properties of drilling fluids and the prediction of flow within lower shear rates (Harris, 2004; Kassab et al, 2011). API (2009) has chosen it as a standard model to describe the rheological behaviour of drilling fluids, specifically

polymer-based fluids not exhibiting yield stress. Within the model, there is a non-linear power relationship between the shear stress and the shear rate; the constitutive equation is as follows:

$$\tau = k\dot{\gamma}^n \quad (5-2)$$

where k and n are Power Law constants; k is the consistency index related to the viscosity of the fluid, and n is the Power Law exponential index, which measures the degree of the fluid's non-Newtonian behaviour. To consider the shear thinning behaviour of drilling fluids, the n value should be assumed between zero and one (Baroid, 1997).

In order to calculate the two Power Law parameters, it is necessary to measure rheological properties of the drilling fluid using a viscometer. A viscometer is an instrument used in the field or lab to determine the rheological parameters of drilling fluids based on the shear stress (torque) and the shear rate (RPM). The Fann Model 35A (Fann Instrument Company) is a commonly used, six-speed (3, 6, 100, 200, 300, and 600 RPM) viscometer used to determine the rheological properties of the drilling fluids. According to the data measured by a viscometer, the Power Law parameters can be calculated by applying a logarithm on both sides of Power Law equation as shown below (Ariaratnam et al., 2003):

$$n = \frac{\log \frac{\tau_2}{\tau_1}}{\log \frac{\dot{\gamma}_2}{\dot{\gamma}_1}} \quad (5-3)$$

$$k = \frac{\tau_2}{\dot{\gamma}_2^n} \quad (5-4)$$

As seen in the Equations (5-3) and (5-4), it is possible to derive the Power Law indices by considering different shear rates and their corresponding shear stresses based on viscometer data. In order to use Equations (5-3) and (5-4) to predict annular pressure in oil industry units, shear

stress should be converted from degree of Fann to dyne/cm² by applying a factor of 5.11. Shear rate should also be converted from rpm to 1/sec by applying factor of 1.702. Therefore, the unit of consistency index (k) is $\frac{\text{dyne}\cdot\text{sec}^n}{\text{cm}^2}$.

5-3-4-2- Calculating frictional mud loss pressure

API (2009) calculates the Power Law indices using the shear rates corresponding to 3 and 100 RPM readings obtained from viscometer data (Ariaratnam et al., 2003). The linear velocity of the fluid in the concentric annulus is calculated as follows (API, 2009):

$$V_a = \frac{0.408Q}{D_2^2 - D_1^2} \quad (5-5)$$

where the Power Law parameters are expressed in imperial units, the velocity is expressed in ft/sec, Q is the pump output flow expressed in gallon per minute (gpm), and D_2 and D_1 are the drill bit and drill pipe diameter, respectively, expressed in inches. The effective viscosity defines fluid flowing through a specific geometry depending on the fluid velocity, annulus diameter, and Power Law indices. The effective viscosity is calculated as follows (API, 2009):

$$\mu_{ea} = 100K_a \left(\frac{144V_a}{D_2 - D_1} \right)^{n_a - 1} \left(\frac{2n_a + 1}{3n_a} \right)^{n_a} \quad (5-6)$$

The units applied in the Power Law model are related to the oil industry; the effective viscosity is defined in centipoise, and the consistency index (k) is defined in $\frac{\text{dyne}\cdot\text{sec}^n}{\text{cm}^2}$.

The Reynolds number in the annulus is calculated as follows (API, 2009):

$$N_{Re_a} = \frac{928(D_2 - D_1)V_a\rho}{\mu_{ea}} \quad (5-7)$$

The friction factor for the annulus considering laminar flow ($N_{Rea} < 2100$) is as follows (API, 2009):

$$f_a = \frac{24}{N_{Rea}} \quad (5-8)$$

By assuming the drilling fluid density (ρ) in pound per gallon (ppg), the gradient of the friction loss pressure in psi/ft can be calculated by using the following formula (API, 2009):

$$\frac{dP}{dL} = \frac{f_a V_a^2 \rho}{25.81(D_2 - D_1)} \quad (5-9)$$

To convert the unit of pressure drop to kPa, it should be multiplied by a factor of 6.87. Therefore, the frictional mud loss pressure can be calculated in each section of excavation multiplying Equation (5-9) by the length of the excavated borehole.

5-3-4-3- Annular shear rate of drilling fluid

The annular shear rate of viscometer in revolution per minute matches with the average velocity of the drilling fluid inside the annulus, which is expressed as follow (Moore, 1986; API, 2009):

$$RPM_a = \frac{1.418 V_a}{D_2 - D_1} * \left(\frac{2n+1}{3n} \right) \quad (5-10)$$

where V_a is the average velocity of the drilling fluid in ft/min, and the other parameters are the same as before.

This equation improves the assumption of determining the shear rates combination for predicting the annular pressure. To verify the properness of the selected two closest shear rates, first it is needed to compute the n parameter based on the defined shear rate range, thereafter the

obtained shear rates by using Equation (5-10) will be compared with the selected shear rates range. If the RPM_a is between the defined ranges, the selected ranges will be verified; otherwise a new range should be selected.

5-3-4-4- Assumptions in using Power Law model

To predict the annular pressure in the HDD bore hole using the Power Law model, some assumptions have been taken into account. This method of annular pressure calculation is applicable to cleaned and gauged boreholes without any cutting beds in a good condition. Any incidents during drilling, such as borehole collapse or hydraulic fracturing, can increase and decrease the drilling fluid pressure, respectively.

In this method, the effect of the soil medium surrounding the borehole on the drilling fluid pressure is ignored. Highly permeable soils can cause a loss of circulation during drilling. A portion of drilling fluid infiltrates the borehole to make an impermeable filter cake that seals the annulus and prevents pores from forming (Bennett and Ariaratnam, 2008). This thin layer of filter cake helps to reduce the loss of drilling fluid circulation and provides stability of the borehole in porous media (Kennedy et al., 2006; Wang and Sterling, 2007). Active soil mediums may also interact with water and bentonite and swell outward, causing a decrease in annulus size and an increase in the drilling fluid pressure. To overcome the defects caused by soil types (collapsible or expandable), additives are applied to the drilling fluid. Therefore, any divergence in annular pressure measurement from the plan pressure presumably indicates an incident (collapse, cutting bed developments, or hydraulic fracture) has occurred in the borehole during drilling.

5-4- Comparison of Prediction with Measurement

In this section, five combinations of shear rate ranges between the six shear rates (3-6, 6-100, 100-200, 200-300, and 300-600 RPM) are used in the Power Law model to predict the annular pressure. The shear rate range of 3-100 RPM recommended by API (2009) was also used for comparison. The Power Law parameters (k and n) can be calculated by selecting two different shear rates, as discussed in the Equations (5-4) and (5-5). To assess the validity of each shear rate range in the Power Law model, two HDD projects were used. To provide a better approximation of the annular pressure, time-dependent (updated data from daily sampling of the circulating drilling fluid) rheological parameters of drilling fluid during excavation were used in two case studies.

5-4-1- Case Study 1

Figure 5-4 shows the longitudinal cross section of the bore path for Case 1. The length of the HDD crossing was 600 m (1800 feet), which was introduced by measured depth, the borehole diameter was 311 mm (12 ¼ inches), and the drill pipe diameter was 140 mm (5 ½ inches). The average density of the drilling fluid was 1085 kg/m³ (9 ppg) and the average pump output rate was 1.35 m³/min (356 gpm). The pump rate was calculated based on the pump stroke rate using the following formula (Baroid, 1997):

$$\text{pump rate} \left(\frac{\text{m}^3}{\text{min}} \right) = (\text{liner size})^2 \times \text{stroke} \left(\frac{\text{mm}}{\text{min}} \right) \times \text{coefficient} \quad (5-11)$$

where the pump coefficient was derived based on the pump output rate (m³/min) for each liner size (mm).

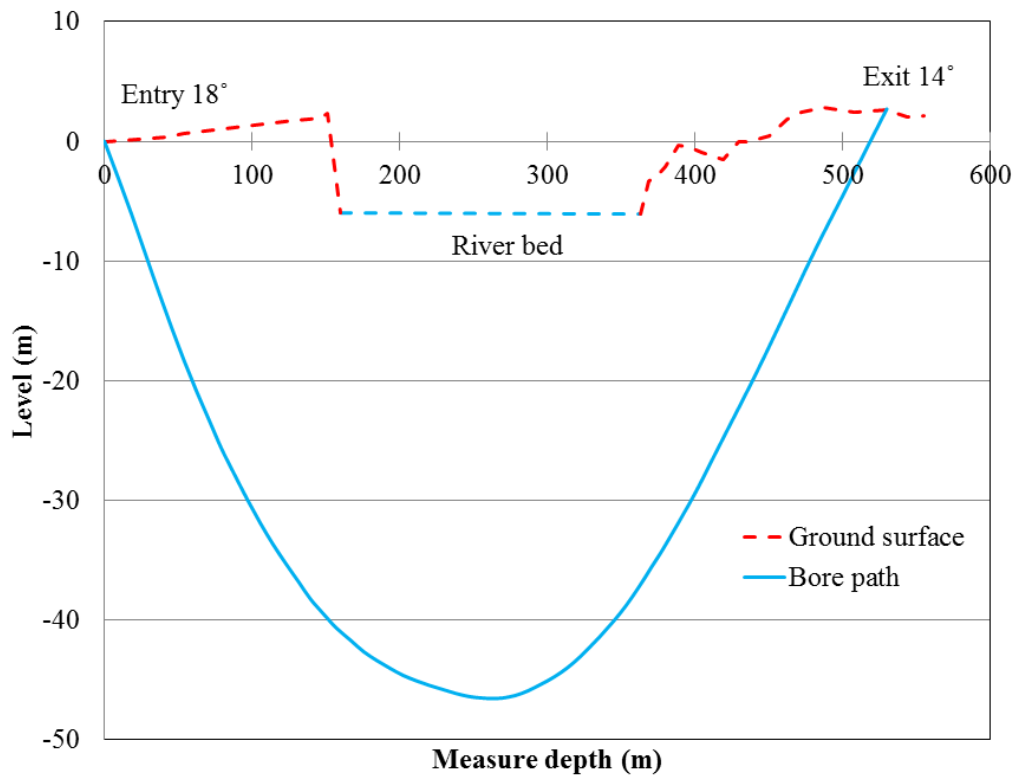


Figure 5-4 Longitudinal profile of HDD crossing of Case 1

It should be noted that HDD operations include a cleaning or hole-gauging pass to remove the buildup of cuttings from the borehole. When cleaning or gauging the borehole, the drill bit is moved backward to the entry pit and is then advanced toward the bottom of the borehole. These cleaning passes may expand the borehole diameter as a result of the bent mud motor assembly and the drilling tools' tendency to rest along the bottom of the hole. Therefore, gauging the borehole results in a reduction of annular pressure. To compare the annular pressure measurements with the predictions by the Power Law model, it is necessary to consider the down-hole measurements after the cleaning pass, as the actual borehole diameter must be as close as possible to the planned borehole diameter. The pilot hole annular pressure was measured

via wire-line using an annular pressure tool sensor located within the orienting sub behind the mud motor.

In order to predict the drilling fluid pressure, the contractor sampled and tested the circulating fluid at the entry pit multiple times per day. Table 5-1 shows the average values for the rheological parameters of the drilling fluids based on the daily sampling. The rheological parameters of the drilling fluid were extracted using a six-speed viscometer (Fann Model 35A). The Power Law constant parameters were then calculated for different ranges of shear rates based on the measured shear stress/shear rate data. Table 5-2 provides the slope and Y intercept of each shear rate combination which corresponds to the n and k parameters of the Power Law model (Equations (5-3) and (5-4)), and also the corresponding annular shear rate calculated based on the average pump rate, annulus diameters, and the n value (Equation (5-10)).

Table 5-1 Rheological properties: six-speed viscometer data of Case 1

Rheological property	
Drilling fluid density, ρ (kg/m ³)	1000
Funnel viscosity (s)	91
Viscometer readings (degree of Fann):	
θ_{600}	83
θ_{300}	59
θ_{200}	49
θ_{100}	36
θ_6	14
θ_3	13

Table 5-2 Power law parameters of Case 1

Shear rates (RPM)	k (dyne.sec ⁿ /cm ²)	n	RPM_a
300-600	14.00	0.49	20.2
200-300	17.33	0.45	21.1
100-200	18.72	0.44	21.4
6-100	32.79	0.33	25.7
3-100	41.30	0.29	27.3
3-6	55.80	0.10	60.2

By applying the constitutive parameters of the Power Law model, the frictional mud loss pressure through the borehole was calculated (Equations (5-3) to (5-11)), while the hydrostatic pressure was calculated according to the mud column density and height. The total annular pressure was calculated by summing the frictional mud loss pressure and hydrostatic pressure. Figure 5-5 depicts the measured and predicted annular pressure along the borehole path (measured depth). The predicted pressures calculated with the five shear rate ranges from 3 to 600 RPM generally show a good agreement with the annular pressure measurements, and the best prediction is achieved by the range of 6-100 RPM. This range is very close to the recommendation (3-100 RPM) by API (2009), which also provides a satisfactory prediction as shown in Figure 5-5.

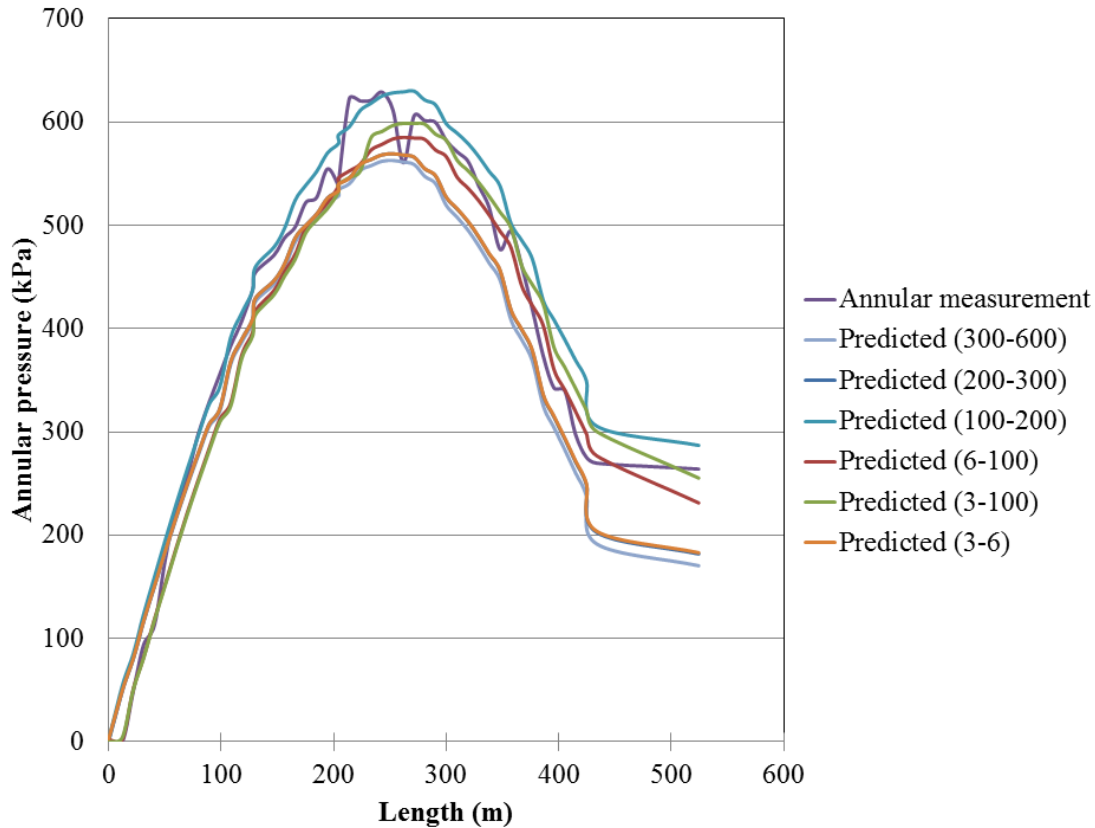


Figure 5-5 Comparison of the predicted and measured annular pressures of Case 1

As discussed earlier, by using Equation (5-10) the proper shear rate range can be determined. The obtained viscometer shear rate (RPM_a) in this case for shear rates of 3-100 and 6-100 RPM is about 27 and 26 RPM, respectively, which verifies the properness of selected shear rate ranges. Therefore, these ranges, which dominate the annulus shear rate, improve the prediction of circulating pressure.

5-4-2- Case Study 2

The HDD crossing in Case 2 was deeper compared to Case 1, the length of the crossing (measure depth) was around 1200 m (3940 ft). The longitudinal cross section of the bore path is shown in Figure 5-6. The borehole diameter was 251 mm (9.88 inches) and the drill pipe

diameter was 114 mm (4.5 inches), the average pump rate of the drilling fluid according to the Equation (5-11) was around 1.7 m³/min (449 gpm).

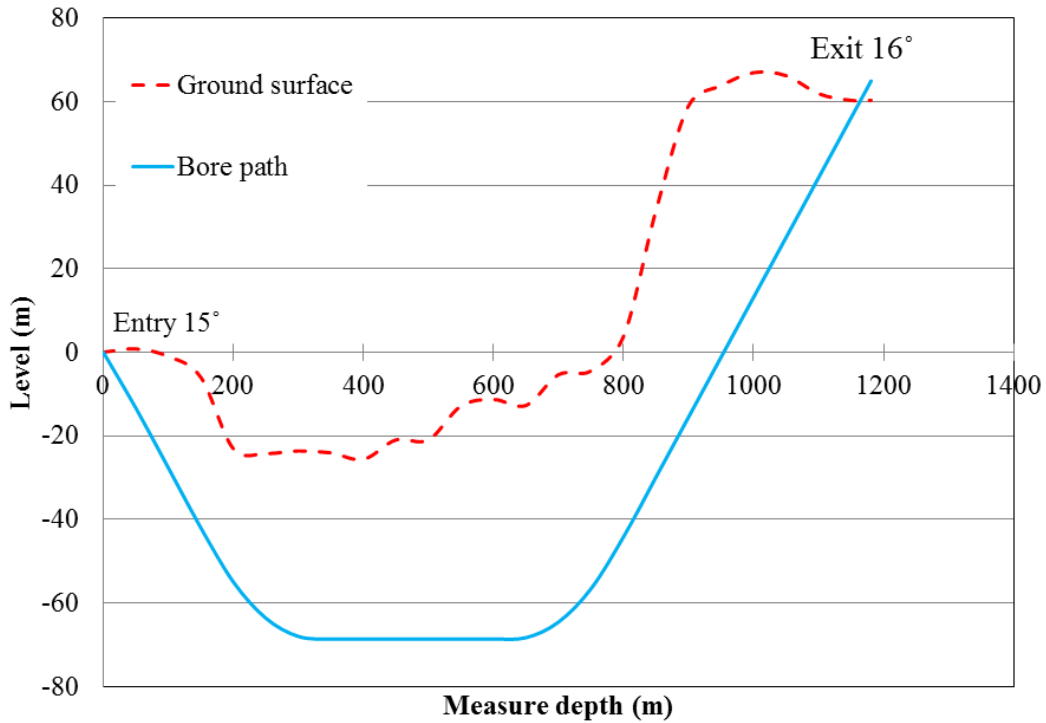


Figure 5-6 Longitudinal cross-section of HDD crossing of Case 2

The average value of the rheological parameters of the drilling fluid was also measured with a viscometer (Fann model 35A) based on the daily sampling of the circulated drilling fluid. Table 5-3 shows the rheological parameters of the drilling fluid. Table 5-4 provides the Power Law parameters and the corresponding annular shear rate for each combination.

Table 5-3 Rheological properties: six speed viscometer data of Case 2

Rheological property	
Drilling fluid density, ρ (kg/m ³)	1100
Funnel viscosity (s)	72
Viscometer readings (degree of Fann):	
θ_{600}	48
θ_{300}	44
θ_{200}	38
θ_{100}	34
θ_6	23
θ_3	22

Table 5-4 Power Law parameters of Case 2

Shear rates (RPM)	k (dyne.sec ⁿ /cm ²)	n	$RPMa$
300-600	102.78	0.125	116.7
200-300	23.59	0.56	46.7
100-200	86.38	0.16	96.3
6-100	85.10	0.14	86.8
3-100	91.80	0.12	98.1
3-6	101.26	0.06	217.9

Similar to the Case 1, the total annular pressure was calculated by applying the Power Law model. The comparison of the annular pressure measurements with the Power Law model predictions for different shear rate combinations is shown in Figure 5-7. In Figure 5-7, the results for the shear rate ranges of 100-200, 200-300, and 300-600 RPM are overlapped and for the shear rate ranges of 3-100 and 6-100 RPM are coincident too. The results indicate that the predicted model with the shear rates of 3 to 600 RPM show a good agreement with the measurement. Shear rate ranges of 3-100 and 6-100 RPM provide the best prediction. The shear rates of the drilling fluid in this case by using the shear rates of 3-100 and 6-100 RPM were

about 98 and 87 RPM respectively, which were placed in appropriate selected ranges. Again, this implies that if the shear rate combinations are closer to the real shear rates in the annulus, the prediction would be more precise.

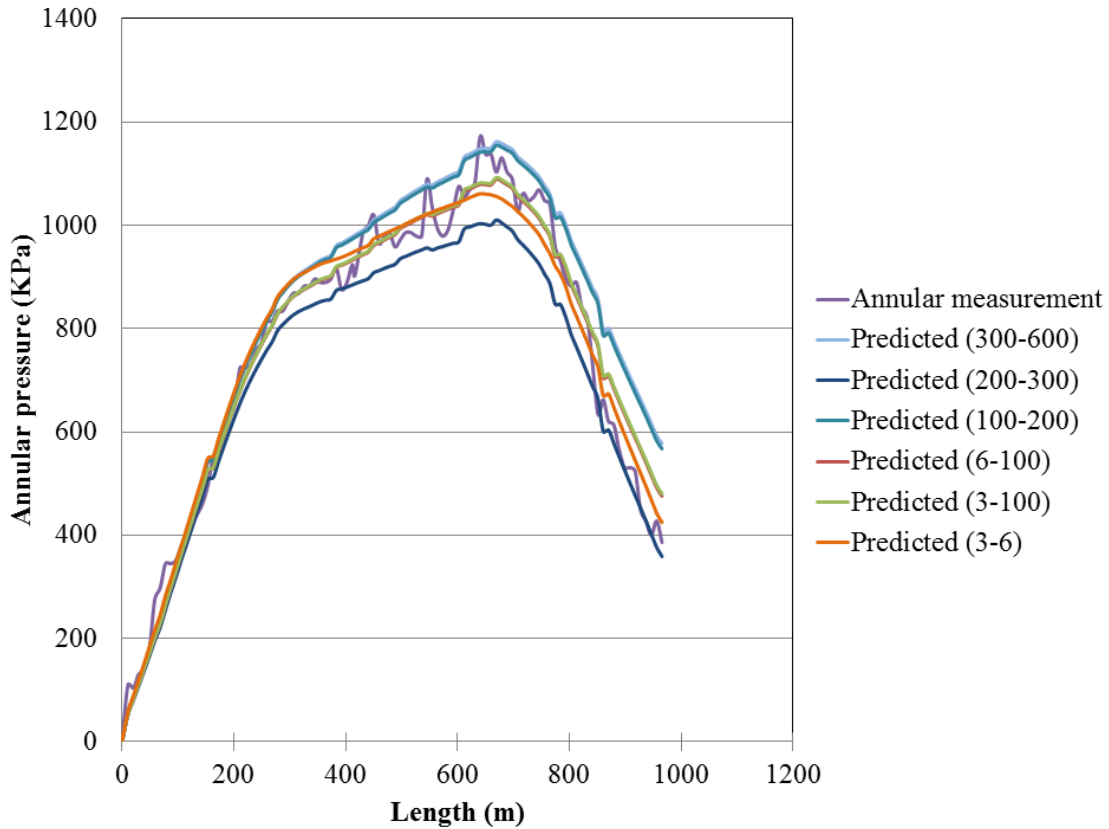


Figure 5-7 Comparison of the predicted and measured annular pressures of Case 2

5-4-3- Discussion

As presented earlier, deviations of the measured annular pressures from the calculated plan pressures indicate abnormal downhole conditions during drilling. Higher measured annular pressure than the plan pressure can arise from cutting bed development at the borehole bottom or bit balling during drilling. Lower measured annular pressure than the plan pressure may be caused by frac-out around the borehole. The annular pressure measurements of the two cases

mentioned above indicate that there were no incidents occurred during drilling; hence the annular pressures predicted by the Power Law model agree well with the measurements.

The example shown in Figure 5-8 illustrates how to use the plan pressure and measured annular pressure to reveal upcoming incidents during pilot boring. The continuous line depicted in Figure 5-8 corresponds to the measured annular pressure taken during running into the hole (RIH) operations before moving the drilling assembly backward to clean the borehole. The dashed line depicted in Figure 5-8 corresponds to the plan pressure calculated using the Power Law model with shear rate range suggested by API (2009), i.e. 3-100 RPM. If there was collapse or expansion occurred in the borehole wall, the annular pressure measurement would not match the plan pressure. As shown in Figure 5-8, the measured annular pressure started to diverge from the plan pressure at around 60 m, indicating buildup of cutting bed at the borehole bottom. In order to reduce the annular pressure, the drill bit was pulled back to the entry pit, and the borehole was cleaned and gauged five times at 192, 204, 291, 330, and 360 meters (Figure 5-8). Each time after the borehole was cleaned, the measured annular pressure dropped to the plan pressure (Figure 5-8). It should be noted that the measured annular pressure dropped below the plan pressure due to that the borehole was oversized by the bent assembly of mud motor during trip back at around 270 m. The example (Figure 5-8) demonstrates that the annular pressure management can be used to reveal upcoming incidents during drilling, and it can be vital in cost-effective design of the borehole in HDD projects.

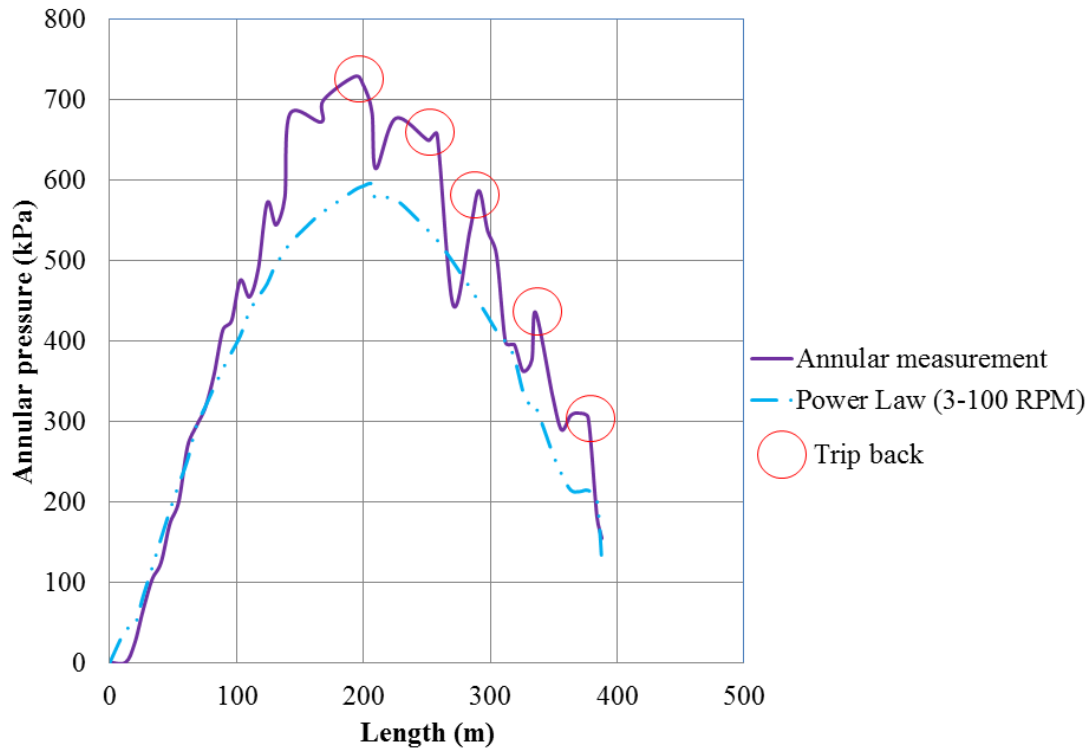


Figure 5-8 Annular pressure measurement during drilling and after cleaning the borehole

5-5- Conclusion

Updating the rheological parameters, which exhibit time-dependent behaviour, can provide a realistic assessment of the drilling fluid during HDD operations; these rheological parameters can be used to predict the plan annular pressure of drilling fluid using the Power Law model. The comparison of measured and predicted annular pressures in the two field cases indicated that the Power Law model using the rheological parameters determined from the six-speed viscometer with shear rate ranged from 3 to 600 RPM could properly predict the annular pressure. The best prediction was achieved by the shear rate range of 6-100 RPM due to embracing the real shear rate of drilling fluid inside the annulus; this shear rate range is close to

the recommendation (3-100 RPM) by API (2009). Hence, it is suggested that the Power Law model be used to predict the annular pressure during pilot boring of HDD; the predicted pressure can be used as the plan pressure for annular pressure management to reveal upcoming incidents during construction. Nevertheless, more validation using field measurements is needed before this method can be confidently applied to the industry.

Reference

- Allouche, E.N., Ariaratnam, S.T., and Biggar, K.W. 1998. Environmental remediation using horizontal directional drilling: applications and modeling, *Practice Periodical of Hazardous, Toxic, and Radioactive Waste Management*, 2(3), 93-99.
- American Petroleum Institute (API). 2009. Recommended practice on the rheology and hydraulics of oil-well drilling fluids, API RP 13D. Washington, D.C.
- Ariaratnam, S.T., Lueke, J.S., and Allouche, E.N. 1999. Utilization of trenchless construction methods by Canadian municipalities, *Journal of Construction Engineering and Management*, 125(2), 76-86.
- Ariaratnam, S.T., Stauber, R.M., Bell, J., and Canon, F. 2003. Evaluation of rheologic properties of fluids returns from horizontal directional drilling, No Dig Conference, North American Society for Trenchless Technology NASTT, Arlington, Va.
- Baroid. 1997. Fluids Handbook. Baroid Fluid Services, Chapter 9, Rheology and Hydraulics, Haliburton, Houston, TX.
- Baumert, M.E., Allouche, E.N., and Moore, I.D. 2005. Drilling fluid considerations in design of engineered horizontal directional drilling installations, *International Journal of Geomechanics*, 5(4), 339-349.
- Bennett, D., Ariaratnam, S. and Como, C. 2001. Horizontal directional drilling good practice guidelines, HDD Consortium, Washington.

- Bennett, R.D., and Ariaratnam, S.T. 2008. Horizontal directional drilling good practices guidelines. Third Edition, HDD Consortium.
- Christopher, J.S., and Michael, M. 2003. Drilling fluid loss events in the Denver basin aquifers, *H2GEO: Geotechnical Engineering for Water Resources*, ASCE, 220-227.
- Duyvestyn, G. M. 2006. Challenging ground conditions and site constraints, not a problem for HDD, In Proceedings of 2006 North American No-Dig Conference, Nashville, Tennessee.
- Haciislamoglu, M., and Langlinais, J. 1990, Non-Newtonian flow in eccentric annuli. *Journal of Energy Resources Technology*, 112(3): 163–169.
- Harris, O. 2004. Evaluation of equivalent circulating density of drilling fluids under high pressure-high temperature conditions. M.Sc. thesis, University of Oklahoma, Norman, OK.
- Hemphill, T., Campos, W., and Pilehvari, A. 1993. Yield-power law model more accurately predicts drilling fluid rheology, *Oil and Gas Journal*, 91(34): 45-50.
- Kassab, S.Z., Ashraf, S.I., and Elessawi, M.M. 2011. Drilling fluid rheology and hydraulics for oil fields. *European Journal of Scientific Research*, 57(1): 68-86.
- Kennedy, M.J., Moore, I.D., and Skinner, G.D. 2006. Development of tensile hoop stress during horizontal directional drilling through sand, *International Journal of Geomechanic*, 6(5), 367-373.
- Moore, P.L. 1986. *Drilling Practices Manual*, PennWell Publishing Company, 2nd Edition.
- Osbak, M. 2011. Theory and application of annular pressure management, In Proceedings of No-Dig 2011 Conference, Washington, D.C.
- Staheli, K., Christopher, G. P., and Wetter, L. 2010. Effectiveness of hydrofracture prediction for HDD design, In Proceedings of No-Dig 2012 Conference, Chicago, Illinois.

Stauber, R.M., Bell, J., and Bennett, R.D. 2003. A rational method for evaluating the risk of hydraulic fracturing in soil during horizontal directional drilling (HDD), In Proceedings of 2003 No-Dig Conference, Las Vegas, Nevada.

Wang, X., and Sterling, R.L. 2007. Stability analysis of a borehole wall during horizontal directional drilling, *Tunneling and Underground Space Technology*, 22, 620–632.

6- Estimation of Maximum Annular Pressure during HDD in Non-Cohesive Soils⁴

6-1- Introduction

Horizontal directional drilling (HDD) is a popular trenchless construction technique for pipeline and underground utility conduit installation. As it provides minimal surface disruption, HDD has been widely used particularly in congested urban zones and environmentally sensitive areas, such as beneath rivers, wetlands, and wildlife habitats (Ariartanam et al., 1999). Drilling fluid, which generally comprises fresh water mixed with bentonite or/and polymers, is a circulating fluid that emerges from the bottom hole assembly into the borehole during HDD operations. Its major functions are (1) to carry the cutting soils out of the bore, (2) to stabilize the bore by developing a circular pressure inside it, and (3) to form a filter cake around the cavity in granular material such as sand and gravel (Bennett and Ariaratnam, 2008). Drilling fluid pressure should be kept below the allowable pressure; otherwise, surpassing the hydrofracture limit of surrounding soil causes migration of drilling fluid to the ground surface, which may lead to negative social and environmental impacts (Sanchez and McHugh, 2004; Harris et al., 2005; Duyvestyn, 2006; Bennett and Wallin, 2008; Staheli et al., 2010; Osbak, 2011). Hence, the estimation of the maximum allowable pressure of drilling fluid is important to minimize the construction and environmental impacts associated with annular pressure during HDD.

According to numerical and experimental studies, two common mechanisms of failure can occur around the cavity during HDD: (1) shear failure, which is common in frictional material during shallow excavation, and (2) tensile failure, which may occur in cohesive material

⁴ A version of this chapter was published in the International Journal of Geomechanics in 2016.

during deep excavation (Xia and Moore 2006; Kennedy et al. 2006). Several closed-forms and numerical methods assume that shear failure is the dominant mode around the bore during cavity expansion (Lugar and Hergarden, 1988; Yanagisawa and Panah, 1994; Van Brussel and Hergarden, 1997; Keulen, 2001; Arends, 2003; Wang and Sterling, 2007; Xia and Moore, 2006, 2007). In general, cavity expansion methods are based on the elastic-perfectly plastic model, mainly assuming the soil behaves as a Mohr-Coulomb material (Carter et al., 1986; Lugar and Hergarden, 1988; Yu and Houlsby, 1991) and considering failure criterion using undrained or drained modified Cam-Clay hardening/softening critical state model (Chen and Abousleiman, 2012, 2013).

The common applied cavity expansion method to predict the maximum allowable pressure during HDD is the Delft's method. It was proposed by Lugar and Hergarden (1988) as an extension of a solution derived by Vesic (1972) based on the Mohr-Coulomb elastic-perfectly plastic constitutive model. Van Brussel and Hergarden (1997) suggested that the maximum annular pressure during HDD was limited to an extension of the plastic radius halfway to the ground surface in purely cohesive soil ($R_{p,max} = 1/2 H$ [where H is the depth of the borehole from the crown to the ground surface]) and to two thirds of the way in non-cohesive soils ($R_{p,max} = 2/3H$). This maximum plastic radius-based method is widely used for determining the maximum annular pressure in HDD (Delft Geotechnics, 1997; Staheli et al., 1998; Carlos et al., 2002; Stauber et al., 2003). Another approach of using cavity expansion methods to capture the maximum annular pressure is based on maximum allowable hoop strain around the bore. Verruijt (1993) proposed a strain failure criterion employing maximum tangential strain (hoop strain) in an elastic-plastic medium with a consideration of the dilative behaviour of soil; this criterion can predict the maximum annular pressure in a pressurized bore. In this case, based on a full-scale

field test, Keulen (2001) suggested 2% hoop strain for calculating the maximum annular for HDD.

The objective of this study is to investigate the effectiveness of estimating the maximum allowable pressure during HDD in non-cohesive soils by using two theoretical cavity expansion methods, including the Delft's method and the Yu and Houlsby's (1991) method; the laboratory and field tests conducted by Elwood (2008), Xia (2009), and Kuelen (2001) were used for validation. First, the method based on the maximum plastic radius (i.e. two thirds of overburden depth) suggested by Van Brussel and Hergarden (1997) was examined. Second, the Verruijt (1993) hoop strain failure method considering a 2% hoop strain suggested by Keulen (2001) was also examined. Last, this study also investigated the correlation between the calculated limit pressures and the measured failure pressures; this led to a new method for estimating the maximum allowable pressure.

6-2- Methodology

In this study, it is assumed that the borehole is cylindrical and the medium is infinite; the effect of boundary walls in the test cells and ground surface are neglected in order to adopt the introduced cavity expansion assumptions.

6-2-1- Delft's method

The Delft's method adopts a small-strain analysis in the plastic zone, uses tension positive, and neglects soil dilatancy. The main assumptions are as follows:

- The borehole is axially symmetric and the soil medium is isotropic and homogenous with an unbounded boundary.

- The geostatic stress in the soil medium is independent of the gravity, and the stress gradient is neglected.
- The state of stress obeys Hook's law until the onset of yield, which is defined by the Mohr-Coulomb failure criterion. Also, elastic strain is neglected in the plastic zone and plastic volume change is neglected in the plastic zone.

As depicted in Figure 6-1, a bore with the radius of R_0 is perforated and the annular pressure is exerted on the bore wall. The annular pressure increases gradually until it reaches the Mohr-Coulomb shear yield stress of surrounding soil. The bore diameter (R_g) expands elastically with an increase in annular pressure until the onset of yield, which expands plastically (R_p) following the Mohr-Coulomb yield criterion. The pressure required to expand the plastic radius to a safe radius ($R_{p,max}$) is the maximum allowable pressure P_{max} .

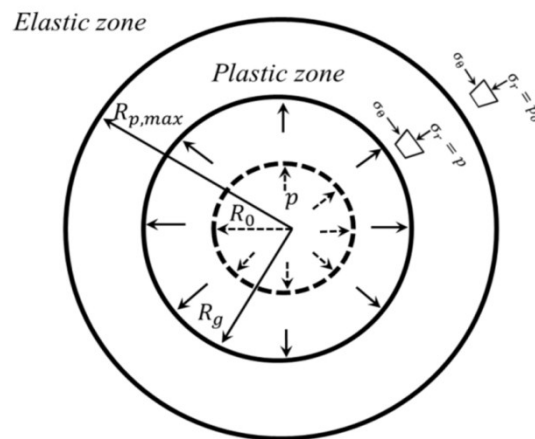


Figure 6-1 Schematic of pressure-expansion relation in a borehole

This pressure is calculated as follows:

$$P_{max} = P'_{max} + u \quad (6-1)$$

$$P'_{max} = (\sigma'_0(1 + \sin\varphi) + c\cos\varphi + ccot\varphi) \times \left\{ \left(\frac{R_0}{R_{p,max}} \right) + \frac{(\sigma'_0\sin\varphi + c\cos\varphi)}{G} \right\}^{\frac{-\sin\varphi}{1+\sin\varphi}} - ccot\varphi \quad (6-2)$$

where P_{max} is the maximum allowable drilling fluid pressure; u is the pore water pressure within the medium; P'_{max} is the maximum allowable effective pressure; P'_0 is the initial effective stress, equal to the effective overburden pressure (i.e. H multiplied by soil unit weight); φ is the internal friction angle; c is the cohesion of the soil; R_0 is the initial borehole radius; G is the shear modulus of the surrounding soil; and $R_{p,max}$ is the defined maximum plastic radius around the borehole. As suggested by Van Brussel and Hergarden (1997), P'_{max} is calculated assuming the plastic radius R_p reached $2/3 H$ in non-cohesive soil.

According to Verruijt (1993), to predict the maximum allowable pressure using the maximum hoop strain around the bore, the pressure is calculated as follows:

$$P_{max} = \left\{ \left[\varepsilon_{\theta,max} \cdot \frac{2G}{P_0 + c\cot\varphi} \cdot \frac{1+m}{1-m} \right]^{\frac{1-m}{k+1}} \cdot \frac{2}{1+m} (P_0 + c\cot\varphi) \right\} - c\cot\varphi \quad (6-3)$$

$$m = \frac{1 - \sin\varphi}{1 + \sin\varphi} \quad (6-4)$$

$$k = \frac{1 - \sin\psi}{1 + \sin\psi} \quad (6-5)$$

where $\varepsilon_{\theta,max}$ is the maximum hoop strain and ψ is the dilation angle. Keulen (2001) proved that the Verruijt (1993) model is identical to the Delft's method when dilation angle is neglected ($k = 1$).

The effective limit pressure will be obtained using Equation 6-2 if the final radius of the borehole or the plastic radius tends to infinite ($\frac{R_0}{R_{p,max}}=0$), therefore:

$$P'_{\text{limit}} = (p'_0(1 + \sin \varphi) + c \cos \varphi + c \cot \varphi) \left\{ \frac{(p'_0 \sin \varphi + c \cos \varphi)}{G} \right\}^{\frac{-\sin \varphi}{1 + \sin \varphi}} - c \cos \varphi \quad (6-6)$$

A complete derivation description of the Delft's method is presented in Equations 6-2 and 6-3, which are published by Lugar and Hergarden (1988) and Keulen (2001), respectively.

6-2-2- Yu and Houlsby's (1991) method

This closed-form method is formulated as a large-strain analysis in the plastic zone in consideration to the non-associated flow rule to formulate dilative behaviour of soil material. Small-strain theory is adopted in the elastic zone, and to accommodate large deformation within the plastic zone, increments of logarithmic strain are defined. All other assumptions are the same as those in the Delft's method.

The state of stress-strain for large-strain analysis within the plastic zone can be drawn by solving logarithmic strain and stress components. A solution for the pressure-expansion relation can be determined by integrating the large-strain expression in the plastic zone, and the result is presented as a ratio of final (R_g) to initial borehole radius (R_0).

$$\frac{R_g}{R_0} = \left(\frac{R^{\gamma}}{(1-\delta)^{\frac{\beta+m}{\beta}} \frac{\gamma}{\chi} A_1(R, \xi)} \right)^{\frac{\beta}{\beta+m}} \quad (6-7a)$$

$$A_1(R, \xi) = \sum_{n=0}^{\infty} A_n^1 \quad (6-7b)$$

$$A_n^1 = \begin{cases} \frac{\xi^n}{n!} \ln(R) & \text{if } n=\gamma \\ \frac{\xi^n}{n!(n-\xi)} [R^{n-\gamma}-1] & \text{otherwise} \end{cases} \quad (6-7c)$$

where

$$R = \frac{(m+\alpha)[Y+(\alpha-1)p]}{\alpha(1+m)[Y+(\alpha-1)p_0]} \quad (6-7d)$$

$$\frac{R_p}{R_g} = R^{\alpha/[m(\alpha-1)]} \quad (6-7e)$$

$$\chi = \exp\left\{ \frac{(\beta+m)(1-2\nu)[Y+(\alpha-1)p_0][1+(2-m)\nu]}{E(\alpha-1)\beta} \right\} \quad (6-7f)$$

$$\xi = \frac{[1-\nu^2(2-m)](1+m)\delta}{(1+\nu)(\alpha-1)\beta} \left[\alpha\beta + m(1-2\nu) + 2\nu \frac{m\nu(\alpha+\beta)}{1-\nu(2-m)} \right] \quad (6-7g)$$

$$\alpha = \frac{1 + \sin \phi}{1 - \sin \phi} \quad (6-7h)$$

$$\beta = \frac{1 + \sin \psi}{1 - \sin \psi} \quad (6-7i)$$

$$Y = \frac{\alpha(\beta+m)}{m(\alpha-1)\beta} \quad (6-7j)$$

$$\delta = \frac{Y+(\alpha-1)p_0}{2(m+\alpha)G} \quad (6-7k)$$

$$Y = \frac{2c \cos \phi}{1 - \sin \phi} \quad (6-7l)$$

where p is the internal pressure; p_0 is the initial hydrostatic pressure; m is a factor to differentiate between cylindrical ($m = 1$) and spherical ($m = 2$) analyses, which in this study is equal to one; G is the shear modulus of material; ν is Poisson's ratio; r is the radius to the point of interest

greater than R_g ; R_g is the current borehole radius; R is the cavity expansion ratio; R_p is the plastic radius around the bore; A_1 is the infinite power series; and $\chi, \xi, \alpha, \beta, \gamma, \delta$ and Y are functions of material properties. The cavity expansion ratio (R) can be calculated using Equation 6-7c based on the applied internal pressure (P). Then, the final radius (R_g) can be derived using Equation 6-7. Finally, the plastic radius can be obtained using Equation 6-7d.

Following the Verruijt (1993) model, the hoop strain around the bore is calculated by using the definition of tangential strain in a plastic zone under large-strain analysis as shown below (Yu, 2000):

$$\varepsilon_{\theta} = \ln \frac{r}{r_0} \quad (6-8)$$

where r is the typical material point which moves from initial position r_0 . Therefore, the hoop strain on the cavity wall is:

$$\varepsilon_{\theta} = \ln \frac{R_g}{R_0} \quad (6-9)$$

where final radius R_g is obtained from Equation 6-7.

Limit pressure is defined as a pressure that expands the current borehole radius to infinite, while the cavity pressure reaches a finite value; therefore, R_{lim} can be obtained using the following equation:

$$A_1(R_{lim}, \xi) = \frac{\chi}{\gamma} (1 - \delta)^{\frac{\beta+m}{\beta}} \quad (6-10)$$

where A_1 is related to R_{lim} by Equation 6-7b.

Then the limit cavity pressure (P_{lim}) can be derived by the following equation:

$$R_{lim} = \frac{(m+\alpha)[Y+(\alpha-1)p_{lim}]}{\alpha(1+m)[Y+(\alpha-1)p_0]} \quad (6-11)$$

6-2-3- Experimental Tests Used for Calculation

6-2-3-1- Small-scale laboratory test (Elwood, 2008)

Seven small-scale laboratory tests were carried out at Queen's University, Canada (Elwood, 2008). The tests were conducted in four stages. In the first stage, the uniform sandy soil was dumped in a box with dimensions of 0.32×0.78×0.8 m from a height of 1.5 m and compacted in a layer of 20 cm by a hand tamper to an average bulk unit weight of 19 kN/m³. The soil parameters are shown in Table 6-1. Different overburden pressures were applied by using an actuator located on a metal plate over the top of a sand box to simulate different overburden depth (Table 6-2). Then, the 60 cm-long clean bore was excavated manually by Shelby tube (outer diameter of 45 mm) while the first 20 cm was sealed by a packer.

Table 6-1 Soil properties for laboratory and field tests

Reference	Friction angle ϕ (°)	Cohesion (kPa)	Poisson's ratio ν	Dilation angle ψ (°)	Young's modulus (MPa)
Small-scale test (Elwood 2008)	31	5.0	0.33	20	20
Large-scale test (Xia 2009)	33	1.6	0.33	15	25
Field test (BTL47-2) (Keulen 2001)	30	0	0.33	0	10
Field test (BTL47-3) (Keulen 2001)	25	5.0	0.37	0	5

Table 6-2 Failure pressure measurements for laboratory and field tests

Reference	Test number	Borehole diameter (mm)	Overburden pressure (kPa)	Failure pressure (kPa)
Small-scale test (Elwood 2008)	SS1	45	8.7	127.2
	SS2	45	12.7	133.7
	SS3	45	16.7	162.4
	SS4	45	20.7	190.2
	SS5	45	24.7	204.7
	SS6	45	33.7	215.3
	SS7	45	45.7	285.9
Large-scale test (Xia 2009)	LS1	55	13.6	87.5
	LS2	55	19.9	112.7
	LS3	55	21.0	121.5
Field test (Keulen 2001)	BTL47-3	75	42.7	65.0
	BTL47-2	75	63.4	200.0

6-2-3-2- Large-scale laboratory test (Xia, 2009)

Three large-scale laboratory tests were also carried out at Queen’s University (Xia, 2009). The tests were performed in a pit with dimensions of 1.5×2×2 m, and the sandy soil was compacted by a vibratory plate to an average bulk unit weight of 17 kN/m³. The soil parameters are shown in Table 6-1. A 55 mm-diameter bore was formed in a length of 1.5 m with cover depth of 0.78 m, and the first 0.5 m was sealed by packer.

For both the small- and large-scale laboratory tests, pressurized fluid was pumped into the bore constantly until it was exposed at the surface. The annular pressure was measured using a pressure transducer. The internal mud pressure accumulated until it reached the peak pressure and decreased afterwards, causing a loss of circulation; the peak pressure was considered as the

failure pressure, as listed in Table 6-2. More details of the small- and large-scale laboratory tests can be found in Elwood (2008) and Xia (2009), respectively.

6-2-3-3- Full-scale field test (Keulen, 2001)

Keulen (2001) reported a series of full-scale field tests performed at Delft University of Technology, Netherlands, to investigate the pressure-induced fracture during HDD. Two tests (BTL47-2 and BTL47-3) in a sand medium were used in this study with the soil properties shown in Table 6-1. The bore was excavated to the specific depth and a drill bit was pushed further without pumping to block the return flow. The drill bit was pushed to the depth of 9.4 m in BTL47-2 and 3.35 m in BTL47-3. The failure pressure (Table 6-2) was measured when the fluid was blocked before pushing the soil aside while the peak pressure occurred. More details on the field tests can be found in Keulen (2001).

6-3- Estimation of Maximum Allowable Pressure

6-3-1- Maximum Plastic Radius-Based Method

The maximum allowable pressure calculated by the Delft's method is limited to the plastic radius propagated to two thirds of overburden depth in non-cohesive soil (Van Brussel and Hergarden, 1997); the same allowable plastic radius was used for the Yu and Houlsby's (1991) method in this study. The calculated maximum allowable pressure versus failure measurements are depicted in Figure 6-2. The slopes of the linear regression lines indicate that both methods overestimate the failure measurements, i.e. both methods are unsafe for estimating the failure pressures of these tests when considering $R_{p,max}=2/3H$. This result is consistent with the findings in Elwood (2008) and Xia (2009). Nevertheless, more data is needed to further

validate this finding. Additionally, the R^2 of the linear regressions indicates that the Yu and Houlsby's (1991) method correlates with the failure measurements better than the Delft's method because Yu and Houlsby (1991) consider a more complex geotechnical behaviour of the soil.

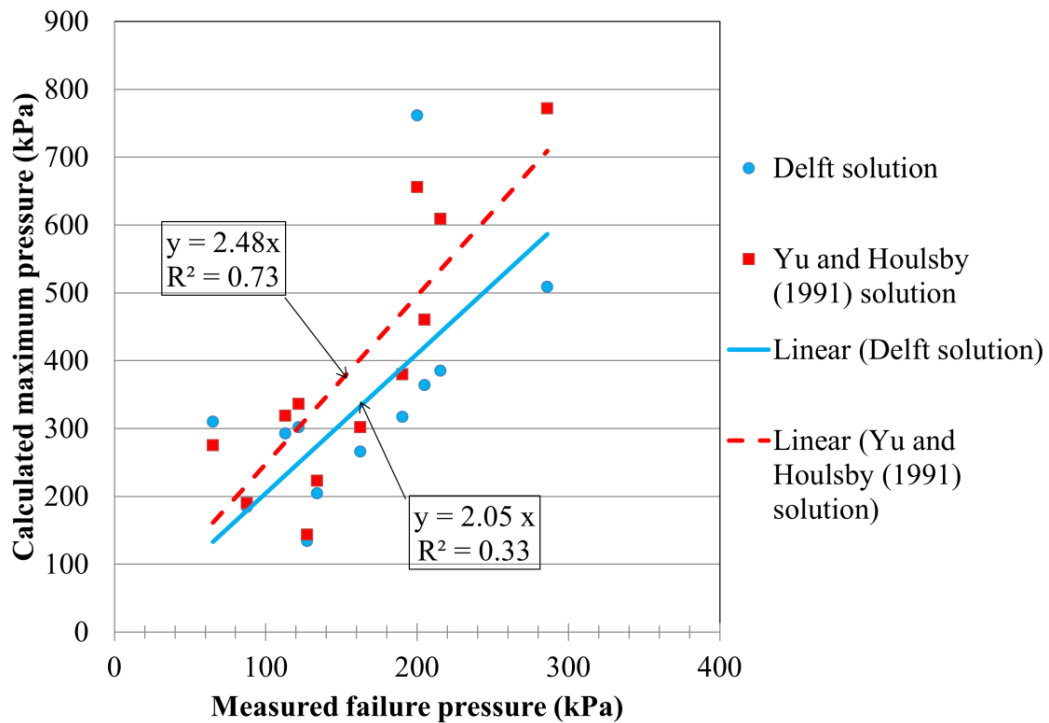


Figure 6-2 Comparison of calculated maximum allowable pressure ($R_{p,max}=2/3H$) with measured failure pressure

Table 6-3 demonstrates the back-calculated normalized plastic radius with respect to the overburden depth ($R_{p,max}/H$). The plastic radius was back-calculated by substituting the failure measurements with the failure pressures in cavity expansion methods. Table 6-3 implies that increase in the overburden pressure leads to reduction in normalized plastic radius when failure occurred for both methods. The back-calculated $R_{p,max}/H$ for both methods are identical, which implies that the Delft's method and the Yu and Houlsby's (1991) method predict the maximum

allowable pressure similarly for a smaller plastic radius, but for $R_{p,max}/H=2/3$, the Delft's method predicts lower pressures compared to the Yu and Houlsby's (1991) method (Figure 6-2). The coefficient of variation in Table 6-3 indicates that no correlation exists between the plastic radius and failure pressure. On the other hand, the normalized $R_{p,max}/H$ for all the overburden pressure for each method is lower than the coefficient of 2/3. Therefore, limiting the plastic radius by employing a reduction factor of two thirds of overburden depth is not a suitable approach. Some field and experimental results also confirm the unsafe estimation of failure pressure using the Delft's method (Duyvestyn, 2006; Moore, 2005).

Table 6-3 Back-calculated normalized plastic radius with respect to the overburden depth

Reference	Test number	Overburden pressure (kPa)	$R_{p,max}/H$ (Delft)	$R_{p,max}/H$ (Yu and Houlsby 1991)
Small scale test (Elwood 2008)	SS1	8.7	0.59	0.58
	SS2	12.7	0.31	0.31
	SS3	16.7	0.24	0.24
	SS4	20.7	0.20	0.20
	SS5	24.7	0.15	0.15
	SS6	33.7	0.08	0.08
	SS7	45.7	0.06	0.06
Large scale test (Xia 2009)	LS1	13.6	0.21	0.22
	LS2	19.9	0.13	0.13
	LS3	21.0	0.13	0.13
BTL research (Keulen 2001)	BTL47-3	42.7	0	0
	BTL47-2	63.4	0	0
Average	-	-	0.16	0.16
Coefficient of variation	-	-	0.99	0.98

6-3-2- Maximum Hoop Strain-Based Method

Figure 6-3 depicts the calculated maximum allowable pressures, based on 2% of hoop strain (Verruijt, 1993; Keulen, 2001), versus the corresponding measured failure pressures. The slopes of the linear regression lines for both methods are less than one, which imply that the measurements are underestimated, agreeing with Keulen (2001). Also, the low values of R^2 for the two methods indicate that no high correlation exists between the calculations and measurements.

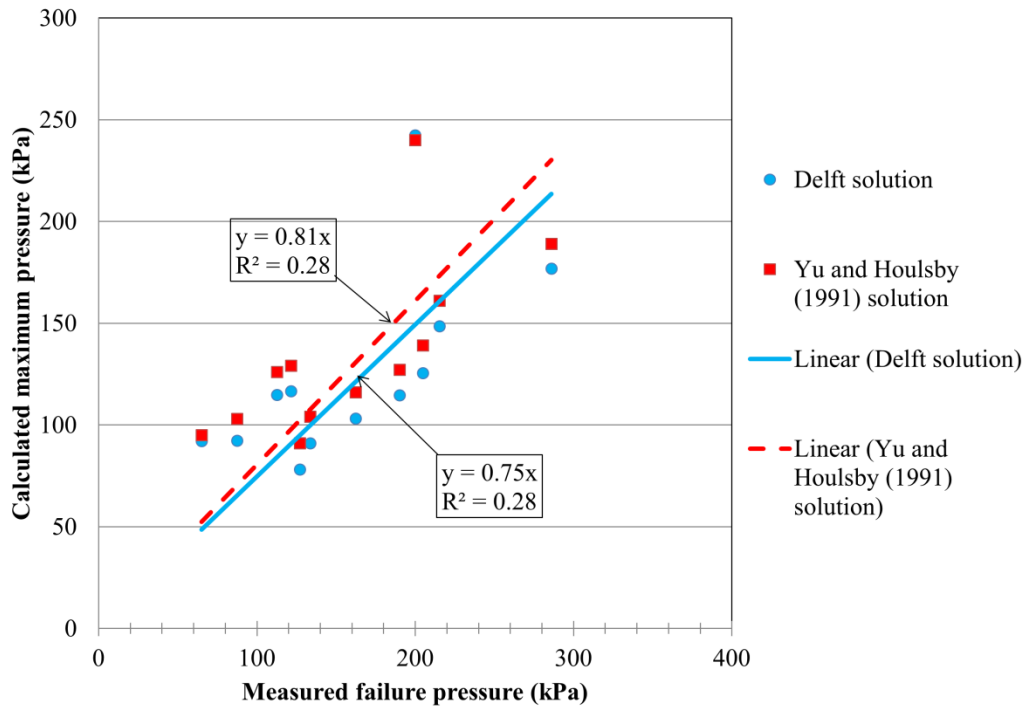


Figure 6-3 Comparison of predicted maximum allowable pressure ($\epsilon_{\theta, \max}=2\%$) with measured failure pressure

Table 6-4 lists the back-calculated maximum hoop strains for both cavity expansion methods, showing that the hoop strain increases slightly with an increase in the overburden pressure for each test. The calculated maximum hoop strain for the Yu and Houslby's (1991)

method is lower than the Delft's method due to considering the non-associated flow rule. However, the maximum hoop strain is sensitive to the soil parameters as well as the overburden pressure. The average value for the back-calculated maximum hoop strain is about 5% in the Delft's method, which is higher than the 2% suggested by Keulen (2001). The coefficient of variation indicates that there is no high correlation between the hoop strain and the failure pressure. Hence, it is not a proper way to define specific ranges for hoop strain to estimate the failure pressure.

Table 6-4 Back-calculated hoop strain for cavity expansion methods

Reference	Test number	Overburden pressure (kPa)	$\varepsilon_{\theta, \max}$ (Delft)	$\varepsilon_{\theta, \max}$ (Yu and Houslby 1991)
Small-scale laboratory test (Elwood 2008)	SS1	8.7	0.074	0.044
	SS2	12.7	0.057	0.039
	SS3	16.7	0.069	0.044
	SS4	20.7	0.081	0.053
	SS5	24.7	0.078	0.052
	SS6	33.7	0.056	0.042
	SS7	45.7	0.077	0.057
Large-scale laboratory test (Xia 2009)	LS1	13.6	0.017	0.014
	LS2	19.9	0.019	0.016
	LS3	21.0	0.022	0.018
Field test (Keulen 2001)	BTL47-3	42.7	0.006	0.006
	BTL47-2	63.4	0.011	0.011
Average	-	-	0.047	0.033
Coefficient of variation	-	-	0.628	0.562

6-3-3- Limit Pressure-Based Method

Figure 6-4 shows the calculated limit pressures versus experimental failure pressures; the limit pressures were calculated using Equation 6-6 for the Delft's method and Equations 6-10 and 11 for the Yu and Houlsby's (1991) method. The slope of the linear regression line for the Delft's method (2.11) is lower than Yu and Houlsby's (1991) method (3.28) due to disregarding the dilation angle; however, they are both higher than one, i.e. the calculated limit pressures are higher than the measured failure pressures. The discrepancy may be due to the assumption of uniform expansion to infinity; in reality, cylindrical cavities in geomaterials may break down at much lower pressures, which can be explained by bifurcation models (Vardoulakis and Papanastasiou, 1988; Papanastasiou and Vardoulakis, 1989; Papanastasiou and Zervos, 2004; Papanastasiou and Thiercelin, 2011).

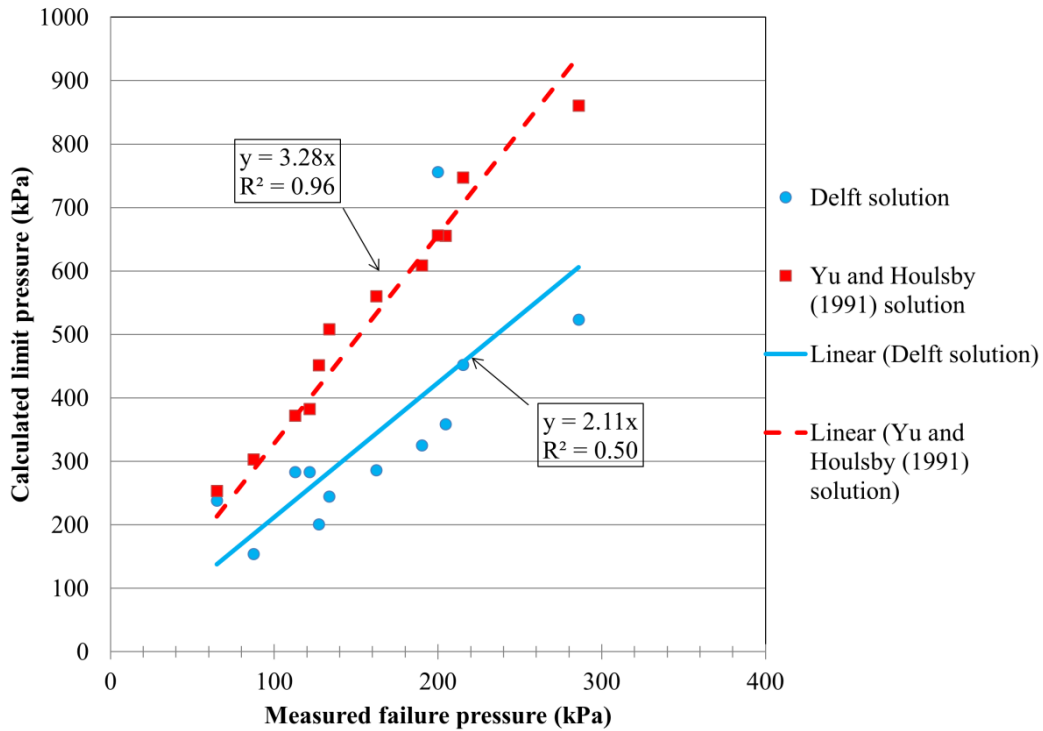


Figure 6-4 Comparison of calculated limit pressure with measured failure pressure

Nevertheless, Figure 6-4 shows that the R^2 (0.96) for the Yu and Houlsby’s (1991) method is much higher compared to that for the Delft’s method (0.50). This result indicates that a high correlation exists between the measured failure pressures and the calculated limit pressure based on the Yu and Houlsby’s (1991) method, which can be used for the maximum allowable annular pressure estimation.

6-4- Conclusion

This study investigated the effectiveness of estimating the maximum allowable annular pressure during HDD in non-cohesive soils by using two theoretical cavity expansion methods;

12 experimental results from a small-scale laboratory, large-scale laboratory, and full-scale field tests were used for verification. The back-calculation results indicated that an increase in overburden pressure led to a decrease in plastic radius onset of failure; no reliable correlation could be found between the hoop strain and failure pressure, explaining that the previous maximum plastic radius-based and hoop strain methods could not estimate the maximum allowable pressure properly. The limit pressures calculated using the two cavity expansion methods were higher than the measured failure pressures due to the assumption of uniform expansion to infinity; in reality, cylindrical cavities in geomaterials may break down at much lower pressures, which can be explained by bifurcation models. However, a high correlation ($R^2 = 0.96$) was observed between the measurements and the calculations based on the Yu and Housby's (1991) method ($P_{\max} \approx P_{\lim}/3.3$). This correlation may be used as a limit pressure-based method for the estimation of maximum allowable annular pressure during HDD in non-cohesive soils; nevertheless, more experimental data, especially field data, is still needed for validation.

Reference

- Arends, G. 2003. Need and possibilities for a quality push within the technique of horizontal directional drilling (HDD), In Proceedings of 2003 No-Dig Conference, Las Vegas.
- Ariaratnam, S.T., Lueke, J.S., and Allouche, E.N. 1999. Utilization of trenchless construction methods by Canadian municipalities, *Journal of Construction Engineering and Management*, 125(2), 76-86.
- Bennett, D., and Wallin, K. 2008. Step-by-step evaluation of hydrofracture risks for HDD projects, In Proceeding of No-Dig Conference, North American Society for Trenchless Technology (NASTT), Cleveland.

- Bennett, R.D., and Ariaratnam, S.T. 2008. Horizontal directional drilling good practices guidelines. Third Edition, HDD Consortium.
- Carlos, A.L., Lillian, D.W., and Patrick, J.C. 2002. Guidelines for installation of utilities beneath Corps of Engineers levees using horizontal directional drilling. *US Army Corps of Engineers Research and Development Center*, ERDC/GSL TR-02-9.
- Carter, J.P., Booker, J.R., and Yeung, S.K. 1986. Cavity expansion in cohesive frictional soils, *Geotechnique*, 36(3), 349-358.
- Chen, S.L., and Abousleiman, N.Y. 2012. Exact undrained elastoplastic solution for cylindrical cavity expansion in modified Cam Clay soil, *Geotechnique*, 62(5), 447–456.
- Chen, S.L., and Abousleiman, N.Y. 2013. Exact drained solution for cylindrical cavity expansion in modified Cam Clay soil, *Geotechnique*, 63(6), 510–517.
- Delft Geotechnics. 1997. A report by Department of Foundations and Underground Engineering prepared for O'Donnell Associates, Inc., Sugarland, Texas.
- Duyvestyn, G. M. 2006. Challenging ground conditions and site constraints, not a problem for HDD, In Proceedings of 2006 North American No-Dig Conference, Nashville, Tennessee.
- Elwood, D. 2008. Hydraulic fracture experiments in a frictional material and approximations for maximum allowable mud pressure, Master thesis, Queen's University, Kingston, Ontario, Canada.
- Harris, T., Drexel, H., and Rahman, S. 2005. Horizontal directional drilling application of fusible C-950 TM PVC pressure pipe, Proceedings of 2005 No-Dig Conference, New Orleans, Florida.
- Kennedy, M.J., Moore, I.D., and Skinner, G.D. 2006. Development of tensile hoop stress during horizontal directional drilling through sand, *International Journal of Geomechanic*, 6(5), 367-373.

- Keulen, B. 2001. Maximum allowable pressures during horizontal directional drillings focused on sand, PhD thesis, Delft University of Technology, Delft, Netherlands.
- Luger, H.J., and Hergarden, H.J.A.M. 1988. Directional drilling in soft soil: influence of mud pressures, In Proceedings of No-Dig Conference on Trenchless Technology, Washington, D.C.
- Moore, I.D. 2005. Analysis of ground fracture due to excessive mud pressure, Proceedings of 2005 No-Dig Conference, Orlando, Florida.
- Osbak, M. 2011. Theory and application of annular pressure management, In Proceedings of No-Dig 2011 Conference, Washington, D.C.
- Papanastasiou, P., and Thiercelin, M. 2011. Modeling borehole and perforation collapse with the capability of predicting the scale effect, *International Journal of Geomechanics*, 11(4), 286–293.
- Papanastasiou, P., and Vardoulakis, I. 1989. Bifurcation analysis of deep boreholes: II. Scale effect.” *International Journal of Numerical and Analytical Methods in Geomechanics*, 13, 183–198.
- Papanastasiou, P.C, and Zervos, A. 2004. Wellbore stability analysis: From linear elasticity to post-bifurcation modeling, *International Journal of Geomechanics*, 4(1), 2–12.
- Sanchez, C., and McHugh, M. 2004. Drilling fluid loss events in the denver basin aquifers, *H2GEO: Geotechnical Engineering for Water Resources*, ASCE, 220–227.
- Staheli, K., Bennett, R.D., O'Donnell, H.W., and Hurley, T.J. 1998. Installation of pipelines beneath levees using horizontal directional drilling, Technical Report CPARGL-98-1, U.S. Army Engineer Waterways Experiment Station, Vicksburg, Mississippi.
- Staheli, K., Christopher, G. P., and Wetter, L. 2010. Effectiveness of hydrofracture prediction for HDD design, In Proceedings of No-Dig 2012 Conference, Chicago, Illinois.

- Stauber, R.M., Bell, J., and Bennett, R.D. 2003. A rational method for evaluating the risk of hydraulic fracturing in soil during horizontal directional drilling (HDD), In Proceedings of 2003 No-Dig Conference, Las Vegas, Nevada.
- Van Brussel, G.G., and Hergarden, H.J.A.M. 1997. Research (CPAR) program: Installation of pipeline beneath levees using horizontal directional drilling, Department of Foundation and Underground Engineering, Delft Geotechnics, 1-16.
- Vardoulakis, I., and Papanastasiou, P. 1988. Bifurcation analysis of deep boreholes: I. surface instabilities, *International Journal of Numerical and Analytical Methods in Geomechanics*, 12(4), 379–399.
- Verruijt, A. 1993. *Grondmechanica*, Delftse Uitgevers Maatschappij, Delft, Netherlands.
- Vesic, A.C. 1972. Expansion of cavities in infinite soil mass, *Journal of Soil Mechanic and Foundation Division*, 98, No. SM3, 265–290.
- Wang, X., and Sterling, R.L. 2007. Stability analysis of a borehole wall during horizontal directional drilling, *Tunneling and Underground Space Technology*, 22, 620–632.
- Xia, A. 2009. Investigation of maximum mud pressure within sand and clay during horizontal directional drilling, PhD thesis, Queen’s University, Kingston, Ontario.
- Xia, H. and Moore, I.D. 2006. Estimation of maximum mud pressure in purely cohesive material during Directional Drilling, *International Journal Geomechanics and Geoengineering*, 1(1), 3-11.
- Xia, H. and Moore, I.D. 2007. Discussion of limiting mud pressure during directional drilling in clays, Geo2007, Ottawa, Canada.
- Yanagisawa, E. and Panah, A. K. 1994. Two dimensional study of hydraulic fracturing criteria in cohesive clays, *Soils and Foundations*, 34(1), 1-9.
- Yu, H.S. 2000. *Cavity expansion methods in geomechanics*, Kluwer Academic Publishers, Norwell, Massachusetts.

Yu, H.S., and Houlsby, G.T. 1991. Finite cavity expansion in dilatant soil: loading analysis, *Geotechnique*, 41(2), 173-183.

7- Numerical Modeling of the Failure Pressure during Horizontal Directional Drilling in Non-Cohesive Soil⁵

7-1- Introduction

Horizontal directional drilling (HDD) has been widely used for four decades as an alternative method to the traditional cut and cover (open-cut) technique used to install and replace underground conduits and buried pipe infrastructure (Ariaratnam et al., 1999). HDD procedure includes three steps: pilot boring, reaming the borehole, and pipe pull back (Allouche et al., 1998). Drilling fluid, which is comprised of bentonite and additives, is used in all three steps to facilitate operational processes (Ariaratnam et al., 1999). As the drilling fluid circulates inside the borehole during HDD, annular pressure should be maintained below the maximum allowable pressure to mitigate the risk of hydraulic fracturing.

Due to the existence of drilling fluid inside the borehole, there are two types of annular pressure that affect the borehole wall: one is mud column weight, and the other one is the annular pressure that arises from the circulation of drilling fluid (Ariaratnam et al., 2007). If annular pressure exceeds the tensile or shear strength of the surrounding soil, hydraulic fracture (frac-out) occurs around the borehole (Kennedy et al., 2006; Xia and Moore, 2005). Hydraulic fracturing around the borehole is a major risk for HDD as it has the potential to affect the entire project and cause serious environmental and operational impacts; when hydraulic fracture occurs, it disturbs the stability of the borehole, the efficiency of the drilling process, and the surrounding infrastructure and environment (Bennett and Wallin, 2008; Christopher and

⁵ A version of this chapter was submitted to *Geomechanics and Geoengineering: An International Journal* in 2016.

Michael, 2003; Duyvestyn, 2006; Harris et al., 2005; Osbak, 2011; Sanchez and McHugh, 2004; Staheli et al., 2010).

Two common mechanisms of failure (shear or tensile) may occur around the cavity according to the geotechnical parameters of soil and the initial geostatic stresses in the soil medium. Tensile failure may occur prior to the shear failure and is common in stiff clay, heavily over-consolidated clay at shallow depths, and rocks formations (Kennedy et al., 2006; Xia and Moore, 2006). Shear failure, on the other hand, is a common mode of failure in frictional mediums and cohesive frictional materials in shallow depths in which the overburden pressure is low and, consequently, the shear strength of the soil is low.

Several cavity expansion methods can predict the maximum allowable pressure based on the assumption of shear failure mode (Arends, 2003; Keulen, 2001; Luger and Hergarden, 1988; Van Brussel and Hergarden, 1997; Wang and Sterling, 2007; Xia and Moore, 2006, 2007; Yanagisawa and Panah, 1994). Luger and Hergarden (1988) proposed the first method to predict the maximum allowable pressure due to the shear failure of the soil, advancing the work of Vesic (1972). The introduced model is generated from small-strain cavity expansion theory and formulated based on the Mohr-Coulomb constitutive model without considering the soil dilatancy. According to this model, the expansion pressure required to expand the borehole in which the plastic zone reaches a specific radial distance was estimated. This model is known as Delft's method, and it is generally accepted for determining frac-out pressure in HDD industry practice (Baumert et al., 2005; Conroy et al., 2002; Delft Geotechnics, 1997; Elwood et al., 2007; Kennedy et al., 2004; Staheli et al., 1998; Staheli et al., 2010; Stauber et al., 2003; Xia and Moore, 2007; Yanagisawa and Panah, 1994). Some analytical solutions have also been created to predict the yielding shear stresses around the borehole according to the mechanical

characteristics of the soil, such as large-strain cavity expansion theory by Yu and Houlsby (1991) and small-strain cavity expansion by Carter et al. (1986). These methods overcome the shortcoming of Delft's method by considering sophisticated behaviour of the soil, such as adopting non-associate flow rule behaviour of soil and solving the equilibrium equations and boundary value problem in terms of radial and tangential stress. All of the abovementioned analytical and close-form methods to calculate the maximum allowable or failure pressure are formulated based on the assumption of cavity expansion in an infinite isotropic medium, neglecting the stress gradient of overburden stress (Arends, 2003; Keulen, 2001; Lugar and Hergarden, 1988; Moore, 2005; Van Brussel and Hergarden, 1997; Wang and Sterling, 2007; Xia and Moore, 2007).

Xia (2009) conducted a series of large- and small-scale laboratory tests and finite element modeling on sand to verify and evaluate the effectiveness of Delft's method and quantify the maximum allowable pressure of drilling fluid during HDD. Results showed that Delft's method overestimated the maximum allowable pressure by more than 150 percent compared to numerical modeling and experimental results. Elwood (2008) investigated the maximum allowable pressure of drilling fluid in cohesionless soil by conducting an experimental test and numerical modeling. Elwood's research also indicated that cavity expansion theories overestimated the maximum allowable pressure compared to the experimental results. Rostami et al. (2016) used the failure pressure results of tests conducted by Xia (2009), Elwood (2008), and Keulen (2001) to clarify if any correlation exists between the failure pressure of the soil and the plastic radius or plastic strain around the borehole. They concluded that Delft's method, based on maximum plastic radius, and Keulen's (2001) method, based on maximum hoop strain, are not reliable to estimate the plastic strain around the borehole or the failure pressure when there is no

correlation between failure pressure and plastic radius. Also, they observed a high correlation ($R^2=0.96$) between limit pressure (in which the plastic strain or displacement reaches to infinite) of the soil based on Yu and Houlsby's (1991) method and the failure pressure ($P_{\max} \approx P_{\lim}/3.3$). However, the suggested limit pressure coefficient (3.3) was based on some limited tests in shallow depths and may result in non-conservative estimation of failure pressure in deep depths.

As discussed in the literature, close-form methods such as Delft's and Yu and Houlsby's (1991) methods overestimate the maximum allowable pressure of the drilling fluid following maximum allowable plastic radius or plastic strain. The objectives of this study were to extend the limit pressure approach suggested by Rostami et al. (2016) and find a coefficient of limit pressure that can appropriately estimate the failure pressure during HDD in non-cohesive soil in different overburden depths using Yu and Houlsby's (1991) large-strain cavity expansion method and ABAQUS numerical modeling. To achieve these objectives, this study first validated the capability of ABAQUS numerical modeling to estimate failure pressure following the limit pressure approach based on several case studies. Then, to take advantage of the limit pressure approach to predict the failure pressure, the significant constitutive parameters of the host soil and physical properties of the borehole were investigated. To identify the significant parameters in estimating the limit pressure following ABAQUS numerical modeling, a parametric study on the constitutive parameters was conducted. Accordingly, the comparison of the limit pressure calculated using Yu and Houlsby's (1991) method with ABAQUS numerical modeling provided a coefficient of limit pressure for the rational ranges of the identified significant parameters, which may be used for estimating the failure pressure during HDD in non-cohesive soils.

7-2- Numerical Model Development

This study employed a plane large-strain finite element numerical model using ABAQUS software (version 6.13) to simulate the cavity expansion process and calculate the limit pressure at which the plastic strain or displacement at the borehole wall reaches to infinite. The mesh discretization for the geometrical model was generated as a four node bilinear plane strain quadrilateral (Dassault Systèmes Simulia Corp., 2013), and the sides of the soil medium were fixed horizontally with free vertical movement while the bottom was fully fixed (Figure 7-1). During the cavity expansion process, the host soil was assumed to be linearly elastic until the onset of yield (following Hooke's law considering small-strain theory) and perfectly plastic after yielding (following the Mohr Coulomb yield criterion considering large-strain theory and non-associated flow rule, which was adopted similar to the assumptions considered by Yu and Houslyby (1991). A linear elastic model was applicable for small elastic strains and in isotropic conditions; the stress-strain relation for small-strain theory is formulated as follows (Dassault Systèmes Simulia Corp., 2013):

$$\sigma = D^{el} \varepsilon^{el} \quad (7-1)$$

where σ is the total stress (Cauchy strain in finite strain problem), D^{el} is the fourth-order elasticity tensor, and ε^{el} is the total elastic strain. The total strain (ε) comprises of elastic (ε^{el}) and plastic strain (ε^{pl}) which is calculated as follows:

$$\varepsilon = \varepsilon^{el} + \varepsilon^{pl} \quad (7-2)$$

The plastic behaviour is formulated based on yield criterion, which was Mohr-Coulomb in this study, and consists of two yield surfaces; a shear criterion based on Mohr-Coulomb, and

tension cut-off based on the Rankine surface which was ignored in this study. According to the plasticity model in ABAQUS, the yield behaviour is generalized as $f=0$ where f is the yield function. The yield function (f) is defined as follows:

$$f=(\sigma_1-\sigma_3)+(\sigma_1+\sigma_3)\sin\varphi+2C\cos\varphi \quad (7-3)$$

where σ_1 and σ_2 are the major and minor principal stresses, C is the cohesion of the soil and φ is the friction angle of the soil. Conventional plastic theory explains the evolution of plastic strain using the flow rule equations. Accordingly, in the case of non-associated flow rule which was used to describe the positive dilatancy of soils such as sand, the potential function (g) is not equal to the yield function (f). The potential function (g) is formulated as follows:

$$g=(\sigma_1-\sigma_3)+(\sigma_1+\sigma_3)\sin\psi+2C\cos\psi \quad (7-4)$$

where ψ is the dilation angle of the soil. Thus, when the material is flowing plastically, the increment of plastic strain is defined as follows:

$$d\varepsilon_i^p=\lambda\frac{\partial g}{\partial\sigma_i} \quad (7-5)$$

where λ is a multiplier that defines the magnitude of plastic strain, $\frac{\partial g}{\partial\sigma_i}$ determines the direction of plastic strain, and subscript i denotes the direction of principal strains.

During the cavity expansion process to reach the limit pressure, soil properties may undergo changes; however, constant initial soil properties were used due to the complexity of considering property changes.

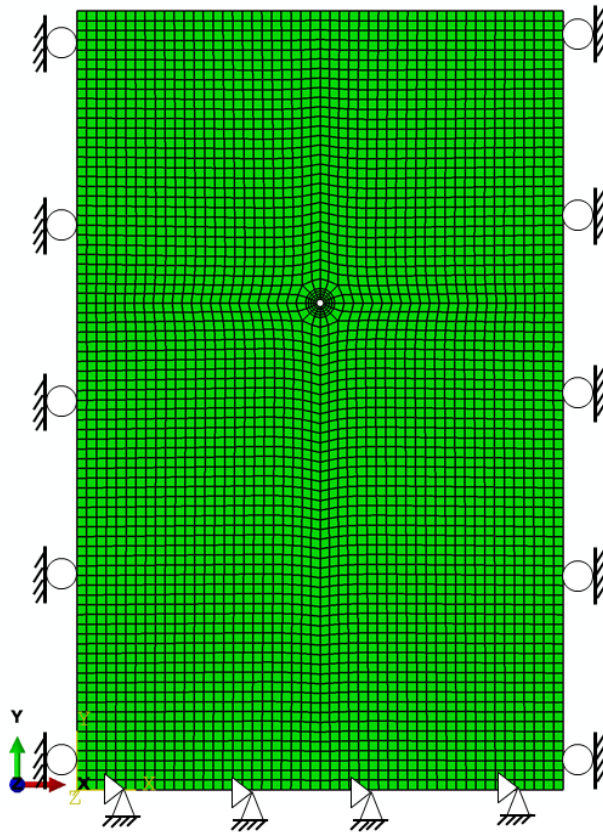


Figure 7-1 The mesh discretization and boundary condition in ABAQUS numerical modeling

The first step of numerical modeling was creating the equilibrium condition by applying geostatic stress gradient corresponding to the soil weight to the entire host soil medium. The first step was created in step module by considering full Newton running techniques and unsymmetrical matrix functions due to adopting a non-associate flow rule function. Also, to consider the large-strain calculation due to the assumption of limit pressure, the non-linear geometry (NLgeom) was employed. The equilibrium condition was generated when the borehole was perforated in the soil medium. Afterwards, a uniform radial internal pressure was established inside the borehole in small increments beginning at 0 kPa up to a specific large magnitude in which the plastic strain or displacement at the borehole wall reaches to infinite. It should be

noted that the actual radial expansion pressure during HDD is not uniform, but the uniform pressure assumption was adopted in this study for simplicity so that the soil expansion pressure was applied in the same way as in the analytical cavity expansions methods (e.g. Yu and Houlsby, 1991). Also, the seepage of the drilling fluid into the borehole wall during HDD was neglected due to the assumption of filter cake formation (Rostami et al., 2017). Thus, the single phase model was generated. The annular pressure as a positive load inside the bore and the gravitational acceleration (9.81 m/s^2) in negative Y direction, which affected the soil mass, were entered into the ABAQUS load manager, while geostatic stress as a negative value and coefficient of lateral earth pressure were defined into the ABAQUS predefined field manager in the load module. Jaky's (1944) equation was used to estimate the coefficient of lateral earth pressure at rest for frictional soils as shown in Equation (7-6).

$$K_0 = 1 - \sin \phi' \quad (7-6)$$

where K_0 is the coefficient of earth pressure at rest, and ϕ' is the drained friction angle.

The annular pressure in the load module was activated in the second step of running step after generation of geostatic stress. To obtain the limit pressure value, a large value for the annular pressure was applied through the fictitious time increment. The numerical result for determining the limit pressure with respect to displacement was obtained from the mesh node at the crown of the borehole. Figure 7-2 shows a typical deformation contour around the borehole after running a pressure expansion model. According to the definition of the limit pressure, due to applying high annular pressure, the pressures reached the limit cavity expansion pressures; the mesh displacements increased significantly, and the ABAQUS runs aborted. The ABAQUS runs typically aborted for one of two reasons: either the integral equation was not converged, or mesh

distortion was created, both resulting in numerical termination. However, the output results for displacement are reliable while the abortion corresponds to the significant increase in the borehole wall displacement. The output results for the limit pressure were discussed in the following sections.

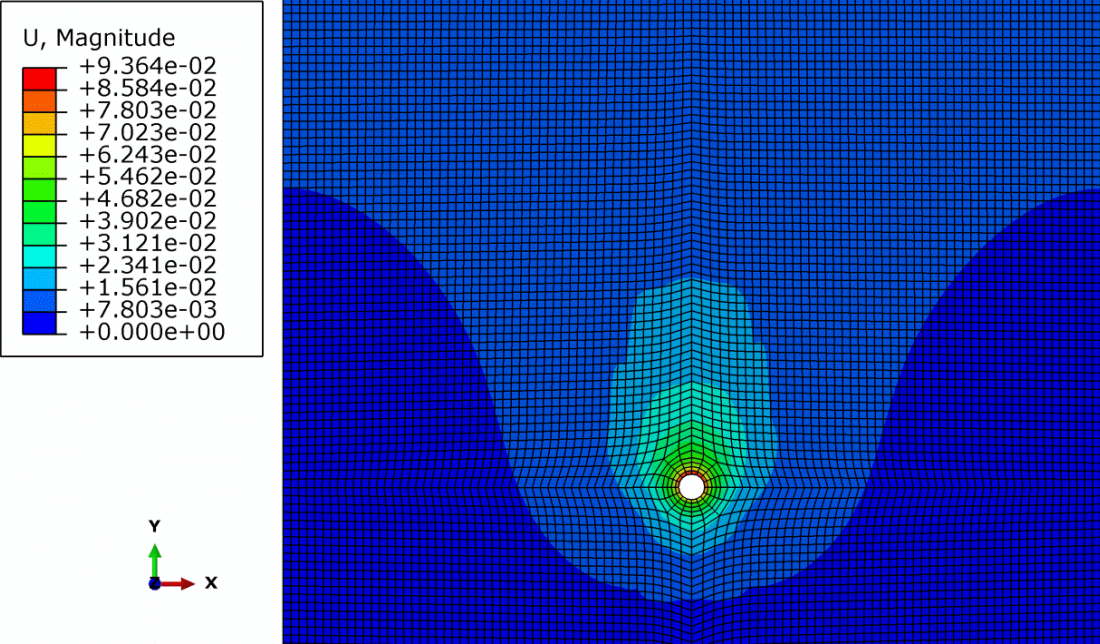


Figure 7-2 Typical deformation contour in ABAQUS numerical modeling

Yu and Houlsby’s (1991) cavity expansion method is another numerical solution that Rostami et al. (2016) used to estimate the failure pressure following the suggested limit pressure approach. In this case, the limit pressure can be calculated using the limit pressure equation or using the pressure-expansion equations derived by Yu and Houlsby (1991) in which the annular pressure should be increased until the displacement at the borehole wall tends to infinite; Rostami et al. (2016) also described the method of calculating limit pressure.

It should be noted that the limit pressure was independent of the initial borehole radius, while the limit pressure was defined when the ratio of the final borehole to initial borehole radius reaches to infinite and the borehole radius factor was canceled out. Thereafter, the estimated limit pressure based on the cavity expansion method can be compared with the ABAQUS numerical modeling. The calculated limit pressure based on the analytical method was expected to be higher than the ABAQUS numerical modeling with a similar expansion pressure trend due to some of the simplified numerical assumptions. Both numerical and analytical methods were formulated following Hooke's law during elastic expansion and Mohr-Coulomb failure criterion during plastic expansion; non-associated flow rule was used when considering large-plain strain analysis. While in the analytical method the soil medium was considered infinite, the stress gradient in different depths was neglected, and the K_0 was assumed to be one. In the parametric study section, the significant constitutive parameters that impact the limit pressure were determined based on ABAQUS numerical modeling, and the coefficient of the limit pressure was obtained for the Yu and Houlsby's (1991) method for different geotechnical conditions accordingly.

7-3- Validation of Limit Pressure Method

To validate the limit pressure approach suggested by Rostami et al. (2016), several case studies based on laboratory and field tests were used. In this case, ABAQUS FEM software was used to simulate the pressure expansion process during HDD and calculate the limit pressure. The numerical model was developed according to the defined boundary conditions, borehole diameter, and soil properties in case studies. Elwood (2008) performed several small-scale laboratory tests to simulate the hydraulic fracture during HDD in poorly graded sand. In this test, overburden depth or surcharge pressure was treated as a variable. During the hydraulic fracture

test, the measured failure pressure was the pressure in which the drilling fluid was exposed at the surface or the annular pressure dropped significantly. Further information on the test procedure can be found in Rostami et al. (2016) and Elwood (2008).

Staheli et al. (2010) introduced the other case study according to a real HDD project that had a diameter of 30 cm constructed into an alluvial deposit, mainly comprised of dense sand, gravel and silt. The inadvertent return of drilling fluid occurred at a depth of 9 m when the ground water level was at the surface. The geotechnical investigation of the soil medium was performed based on vertical boring and split spoon sampling. The bulk density of the sand medium is about 2,080 kg/m³. Table 7-1 shows the estimated geotechnical parameters for the numerical modeling for case studies. Table 7-2 illustrates the measured failure pressure for different overburden depths and the calculated failure pressure based on ABAQUS numerical modeling.

Table 7-1 Geotechnical properties of the soil for laboratory and field tests

Reference	Friction angle ϕ (°)	Cohesion c (kPa)	Poisson's ratio ν	Dilation angle ψ (°)	Young's modulus E (MPa)
Small-scale test (Elwood, 2008)	31.5	5	0.33	20	20.00
Field test (Staheli, 2010)	28.0	1	0.30	0	11.97

Table 7-2 Measured and calculated failure pressure for laboratory and field tests

Reference	Test number	Borehole diameter (m)	Overburden pressure (kPa)	Measured failure pressure (kPa)	Measured/Calculated (ABAQUS)
Small-scale test (Elwood, 2008)	SS1	0.045	8.7	127.2	0.96
	SS2	0.045	12.7	133.7	1.15
	SS3	0.045	16.7	162.4	1.17

	SS4	0.045	20.7	190.2	1.11
	SS5	0.045	24.7	204.7	1.05
	SS6	0.045	33.7	215.3	1.02
	SS7	0.045	45.7	285.9	1.26
Field test (Staheli, 2010)	Loc-2	0.300	96.7	379	1.04

Table 7-2 illustrates that by increasing the overburden pressure, the failure pressure increases. According to the ratio of measured to calculated limit pressure, the ABAQUS numerical modeling can properly estimate the failure pressure. However, more field case studies are required to validate the limit pressure approach for estimating the failure pressure in non-cohesive soils in deep depths. This study conducted a parametric study by relying on the sufficient estimation ABAQUS numerical modeling made regarding failure pressure.

7-4- Parametric Study

A parametric study was conducted using ABAQUS numerical modeling to investigate the effect of geotechnical parameters of the soil medium, such as elastic modulus, friction angle, Poisson's ratio, and coefficient of lateral earth pressure, as well as the physical properties of the borehole, such as overburden depth and borehole diameter on the limit pressure. The geotechnical parameters of sand medium were determined based on USCS soil type through a typical range (Obrzud and Truty 2012; Peck et al., 1974). The rational ranges for the borehole diameter according to the bit diameter of the HDD machine and different safe overburden depths were selected (Guidelines and Specifications for Trenchless Technology Projects reported by Hashash et al. (2011)). It should be noted that the geotechnical parameters of the soil correlate to each other; for instance, elastic modulus correlates with friction angle and the relative density in

the frictional material, while shear strength correlates with cohesion, friction correlates with dilation angle, and so on. To proceed with the parametric study, it is assumed that each variable changes independently while other variables remain constant at their mean value. Table 7-3 shows the rational ranges of the parameters for the parametric study. The density of sandy soil was assumed to be $1,900 \text{ kg/m}^3$, and the dilation angle of the soil based on the non-associated flow rule assumption was considered 12 degree as a constant value. The cohesion of the soil was neglected for the defined frictional soil.

Table 7-3 Variation of independent parameters for parametric study

Parameters	Min				Max	Average
Friction angle (°)	25	30	35	40	45	35
Overburden depth (m)	2	4	6	8	10	6
Borehole diameter (m)	0.100	0.125	0.150	0.175	0.200	0.150
Coefficient of lateral earth pressure	0.2	0.3	0.4	0.5	0.6	0.4
Elastic modulus (MPa)	20	30	40	50	60	40
Poisson's ratio	0.2	0.25	0.3	0.35	0.4	0.3

While the friction angle varied, the coefficient of lateral earth pressure changed following Equation (7-1). The effect of variation of each independent parameter on the limit pressure based on the percentage value was plotted in Figure 7-3. Using the Yu and Houlsby's method (1991) is expected to yield similar limit pressure trends for parameter variation due to the similar assumptions between numerical and analytical methods, while higher limit pressure variation due to considering some simplified assumptions as discussed before.

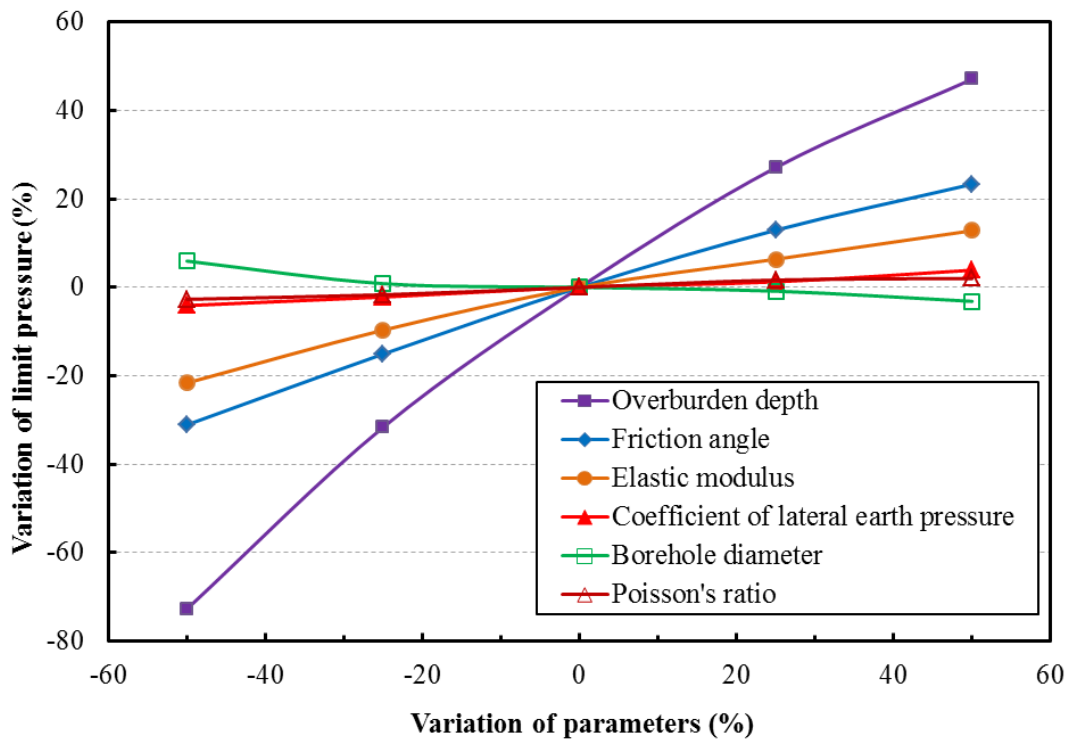


Figure 7-3 Effect of variation of each parameter on the limit pressure based on ABAQUS numerical modeling

Figure 7-3 shows that all the parameters except borehole diameter have a positive correlation with the limit pressure, which means that an increase in the value of each parameter increases the limit pressure. An increase in the borehole diameter, however, decreases the limit pressure around 3 percent. Overburden depth has the highest effect on the limit pressure with a maximum impact of 72 percent, which is positively correlated with the limit pressure due to increasing the overburden stress and, inconsequently, the shear strength of the soil. Friction angle is the next most influential parameter with a maximum impact of 31 percent, which is positively correlated with the limit pressure due to increasing the shear strength of the soil according to the failure criterion of the Mohr-Coulomb model. The next most significant parameter is the elastic modulus of the soil with a maximum impact of 20 percent, which is positively correlated with

the limit pressure due to increasing the annular pressure required to change the stress state of the soil from elastic to plastic criteria to reach to the infinite wall displacement or plastic strain.

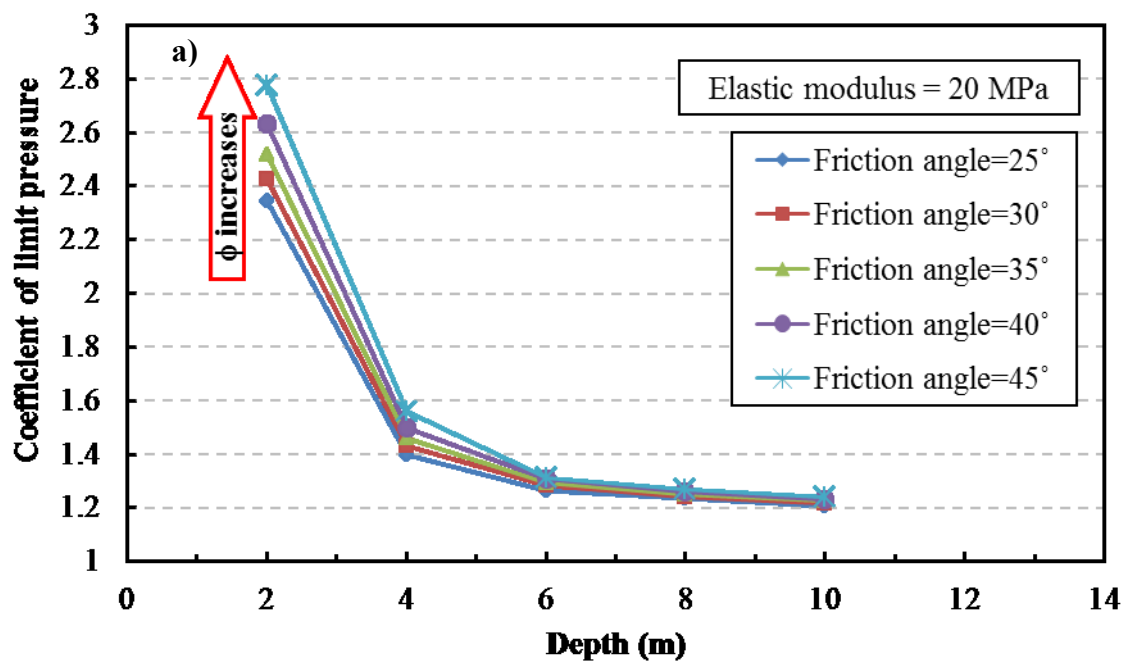
The other parameters have negligible effects on the limit pressure, which impacted the limit pressure less than 10 percent. An increase in the coefficient of lateral earth pressure increases the limit pressure slightly due to applying more confining stress on the borehole wall. An increase in the Poisson's ratio decreases the plastic strain or displacement of the wall; thus, higher pressure is required to extend the plastic strain or displacement to infinite. An increase in the borehole diameter decreases the limit pressure because the larger borehole diameter is more unstable.

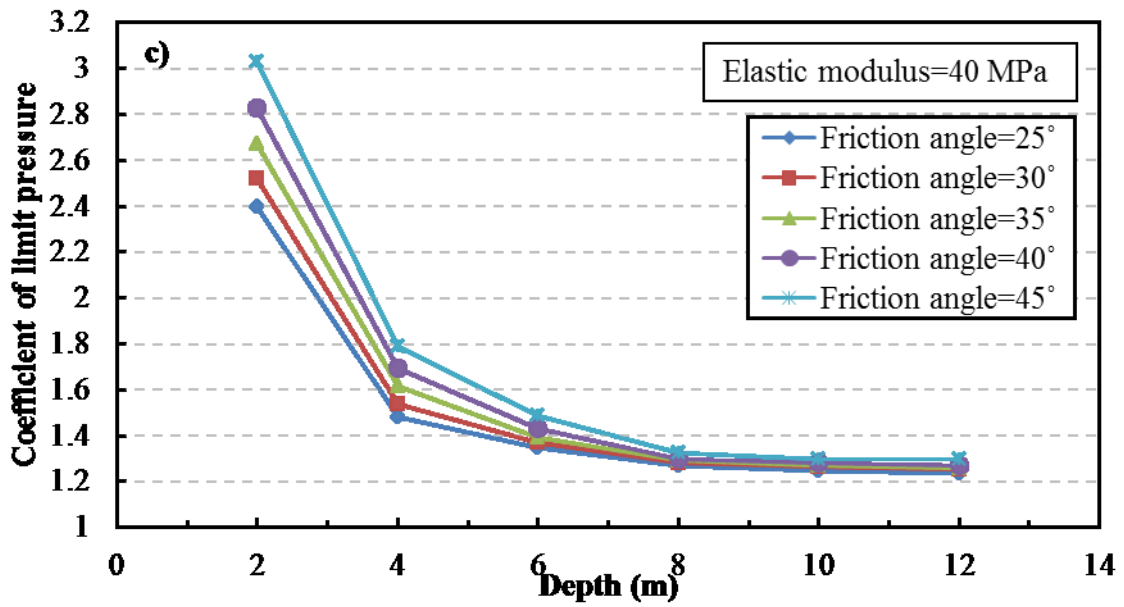
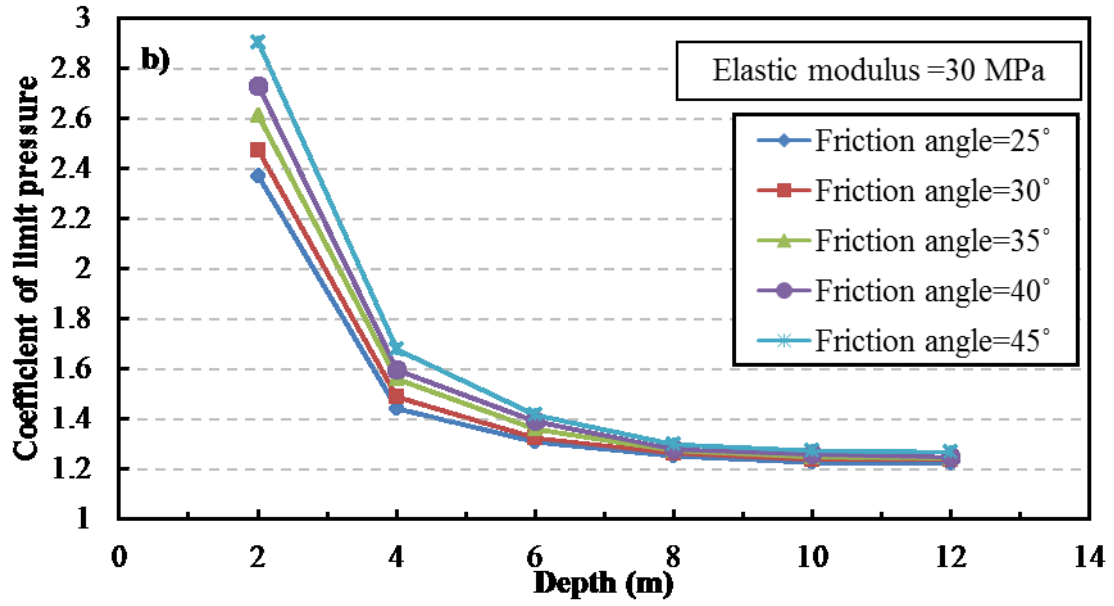
Hence, three identified parameters (overburden depth, friction angle, and elastic modulus of the soil medium) have a significant impact on the limit pressure or failure pressure, which are essential for designing the borehole in a HDD project. The only parameter that HDD engineers can directly define when designing the bore path is the overburden depth, while deeper excavations mitigate the risk of hydraulic fracture related to the shear failure. However, passing through the soil medium with a higher friction angle and elastic modulus provides higher thresholds for hydraulic fracture pressure and safe conditions for drilling. On the other hand, sometimes passing through good soil conditions by reaching and deviating from the bore path is not practical or economical for a HDD project. According to the parametric study conducted, the derived significant parameters were considered to be essential variables to calculate the coefficient of limit pressure following Yu and Houlsby's (1991) analytical method.

7-5- Coefficient of Limit Pressure

As discussed in the previous section, three significant parameters (overburden depth, friction angle, and elastic modulus) were selected for calculating the coefficient of limit pressure by

correlating the Yu and Houlsby's (1991) large-strain analytical method with ABAQUS numerical modeling in a proposed rational range (Table 7-3). The coefficient of limit pressure is denoted as the ratio of the limit pressure calculated based on the analytical method and the ABAQUS numerical modeling. Figure 7-4 illustrates the coefficient of limit pressure for different overburden depths from 2 meters to 12 meters while considering different friction angles and elastic moduli.





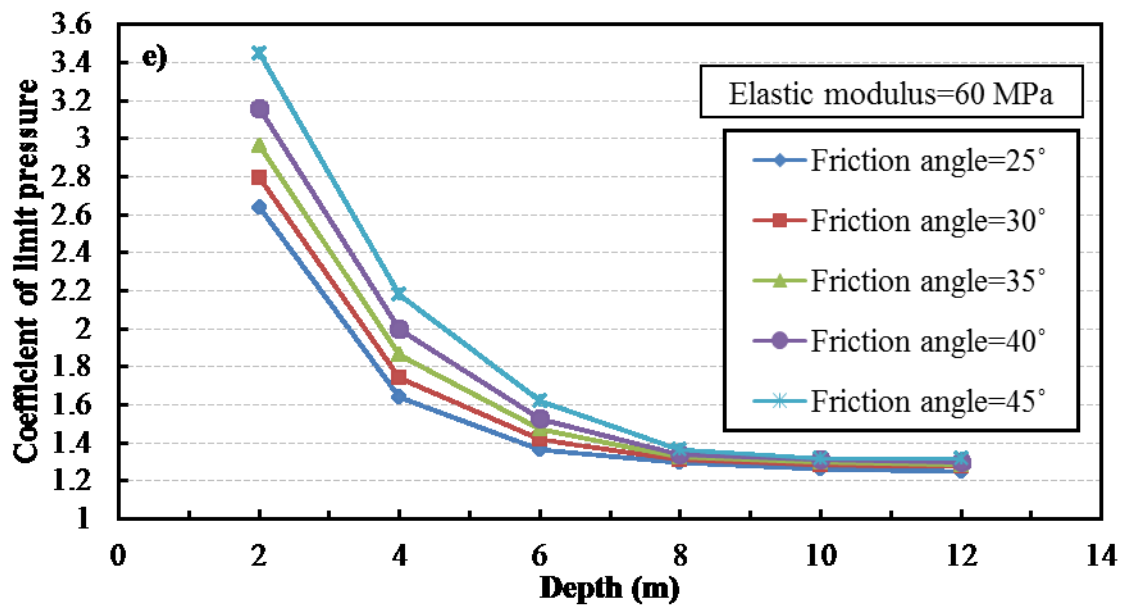
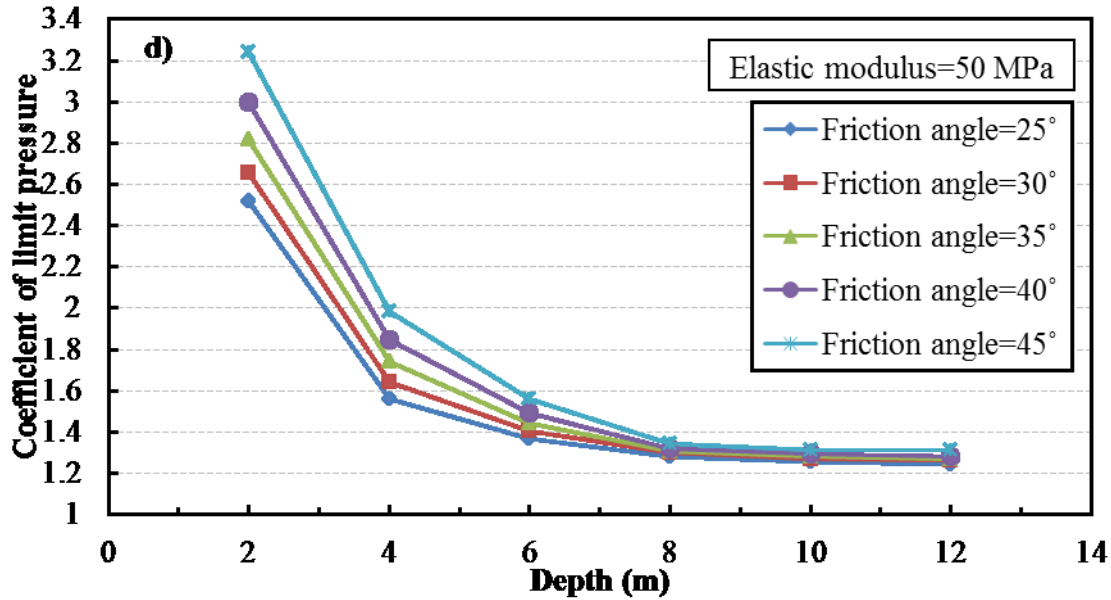


Figure 7-4 The coefficient of limit pressure used for Yu and Houlsby's (1991) method: a) Elastic modulus of 20 MPa, b) Elastic modulus of 30 MPa, c) Elastic modulus of 40 MPa, d) Elastic modulus of 50 MPa, e) Elastic modulus of 60 MPa

As it was explained, the analytical method overestimates the limit pressure due to the simplified assumptions, but the discrepancy between the two methods decreases by increasing

the overburden depth due to tending the soil medium to the infinite medium. According to Figure 7-4, the coefficient of limit pressure decreases to a constant value around 1.3 in all geotechnical conditions by increasing the overburden depth to more than 10 meters. However, neglecting the coefficient of lateral earth pressure, stress gradient, and boundary effect leads to a difference in limit pressure estimation even when overburden depth is high enough. If the same assumptions of Yu and Houlsby's (1991) method are adopted by ABAQUS numerical modeling, the radial and tangential stresses around the cavity are similar to the cavity expansion method results (Xia, 2009). Thus, the strain and displacement around the cavity for both methods are identical. Similar to the results obtained in the parametric study, the overburden depth affects the coefficient of limit pressure more than the friction angle and the elastic modulus. Figure 7-4 confirms that by increasing the friction angle and elastic modulus, the discrepancy between the analytical method and ABAQUS numerical modeling increases. It implies that the simplified assumption of Yu and Houlsby's (1991) analytical method, such as an infinite medium and neglecting stress gradient, provide a medium with higher shear strength compared to ABAQUS numerical modeling, which leads to an increase in the limit pressure.

Since the Yu and Houlsby's (1991) analytical method is more simplistic compared to numerical modeling, it is more suitable for the HDD industry. Additionally, it provides better approximation of the failure pressure compared to the common methods in the HDD industry, which overestimate the hydraulic fracture pressure significantly and disturb the safe completion of HDD projects. Nevertheless, since the numerical and analytical methods are only validated through small-scale laboratory tests with low overburden depths and one real field case study, more case studies with different overburden depths are required to validate the suggested coefficient of limit pressure.

7-6- Conclusion

This study shows that the approach suggested by Rostami et al. (2016), based on limit pressure using ABAQUS numerical modeling, can estimate the failure pressure during HDD sufficiently. However, the analytical method cannot reflect the effects of overburden depth, initial borehole radius, coefficient of lateral earth pressure, and boundary conditions (ground surface impact) on the calculated limit pressure. Thus, the limit pressure calculated based on Yu and Houlsby's (1991) method is higher than the numerical modeling results.

The parametric study results confirm that the parameters of overburden depth, friction angle, and elastic modulus of the soil medium have the highest impact on the limit pressure or failure pressure. During borehole design of HDD projects in sandy soil, determining these three parameters properly is essential to mitigating the risk of hydraulic fracture. According to the generated graphs for the coefficient of limit pressure, although the soil limit pressure obtained from the analytical method is higher than that from numerical modeling, the difference decreases when the overburden depth increases with a maximum discrepancy of ~30% for typical sandy soil medium. The discrepancy between the calculated limit pressure based on analytical method and ABAQUS numerical modeling increases by increasing the friction angle and the elastic modulus. The overburden depth has the highest impact in determining the coefficient of limit pressure. Since the analytical method suggested by Yu and Houlsby (1991) following the limit pressure approach suggested by Rostami et al. (2016) is more simplistic compared to the numerical modeling, it is more suitable for the HDD industry to estimate the failure pressure.

Nevertheless, since the numerical modeling was only validated through small-scale laboratory tests with low overburden depths and one field case study, it is suggested that the limit pressure approach and the generated graphs for the coefficient of limit pressure be validated

through more case studies with different overburden depths. Also, further research studies are required to extend the suggested limit pressure approach for estimating the failure pressure in cohesive frictional materials while considering shear mode of failure.

Reference

- Allouche, E.N., Ariaratnam, S.T., and Biggar, K.W. 1998. Environmental remediation using horizontal directional drilling: applications and modeling, *Practice Periodical of Hazardous, Toxic, and Radioactive Waste Management*, 2(3), 93-99.
- Arends, G. 2003. Need and possibilities for a quality push within the technique of horizontal directional drilling (HDD), In Proceedings of 2003 No-Dig Conference, Las Vegas.
- Ariaratnam, S.T., Harbin, B.C., and Stauber, R.L. 2007. Modeling of annular fluid pressures in horizontal boring, *Tunnelling and Underground Space Technology*, 22, 610–619.
- Ariaratnam, S.T., Lueke, J.S., and Allouche, E.N. 1999. Utilization of trenchless construction methods by Canadian municipalities, *Journal of Construction Engineering and Management*, 125(2), 76-86.
- Baumert, M.E., Allouche, E.N., and Moore, I.D. 2005. Drilling fluid considerations in design of engineered horizontal directional drilling installations, *International Journal of Geomechanics*, 5(4), 339–349.
- Bennett, D., and Wallin, K. 2008. Step-by-step evaluation of hydrofracture risks for HDD projects, In Proceeding of No-Dig Conference, North American Society for Trenchless Technology (NASTT), Cleveland.
- Carter, J.P., Booker, J.R., and Yeung, S.K. 1986. Cavity expansion in cohesive frictional soils, *Geotechnique*, 36(3), 349-358.
- Christopher, J.S., and Michael, M. 2003. Drilling fluid loss events in the Denver basin aquifers, *H2GEO: Geotechnical Engineering for Water Resources*, ASCE, 220-227.

- Conroy, P.J., Latorre, C.A., and Wakeley, L.D. 2002. Guidelines for installation of utilities beneath Corps of Engineers levees using horizontal directional drilling, *ERDC/GSL TR-02-9, Geotechnical Structures Laboratory*, Vicksburg, Mississippi.
- Dassault Systèmes Simulia Corp. 2013. Abaqus Analysis User's Manual, version 6.13, Dassault Systèmes Simulia Corp., Providence, Rhode Island.
- Delft Geotechnics. 1997. A report by Department of Foundations and Underground Engineering prepared for O'Donnell Associates, Inc., Sugarland, Texas.
- Duyvestyn, G. M. 2006. Challenging ground conditions and site constraints, not a problem for HDD, In Proceedings of 2006 North American No-Dig Conference, Nashville, Tennessee.
- Elwood, D, Xia, H., and Moore, I.D. 2007. Hydraulic fracture experiments in a frictional material and approximations for maximum allowable mud pressure, In Proceedings of 60th Canadian Geotechnical Society Annual Conference, Ottawa, Ontario, Canada, 1681-1688.
- Elwood, D. 2008. Hydraulic fracture experiments in a frictional material and approximations for maximum allowable mud pressure, Master thesis, Queen's University, Kingston, Ontario, Canada.
- Harris, T., Drexel, H., and Rahman, S. 2005. Horizontal directional drilling application of fusible C-950 TM PVC pressure pipe, Proceedings of 2005 No-Dig Conference, New Orleans, Florida.
- Hashash, Y., Javier, J., Petersen, T., and Osborne, E. 2011. Evaluation of horizontal directional drilling (HDD), *FHWA-ICT-11-095*.
- Jaky, J. 1944. The coefficient of earth pressure at rest, *Journal of the Society of Hungarian Architects and Engineers*, 7, 355-358.

- Kennedy, M.J., Moore, I.D., and Skinner, G.D. 2006. Development of tensile hoop stress during horizontal directional drilling through sand, *International Journal of Geomechanic*, 6(5), 367-373.
- Kennedy, M.J., Skinner, G.D., and Moore, I.D. 2004. Elastic calculations of limiting mud pressures to control hydro fracturing during HDD, In Proceedings of No-Dig Conference 2004, New Orleans, Louisiana.
- Keulen, B., 2001. Maximum allowable pressures during directional drillings focused on sand, Thesis Paper: pp. 25-32, Appendices pp. 39-74.
- Luger, H.J., and Hergarden, H.J.A.M. 1988. Directional drilling in soft soil: influence of mud pressures, In Proceedings of No-Dig Conference on Trenchless Technology, Washington, D.C.
- Moore, I.D. 2005. Analysis of ground fracture due to excessive mud pressure, Proceedings of 2005 No-Dig Conference, Orlando, Florida.
- Obrzud, R., and Truty, A. 2012. The hardening soil model-a practical guidebook z soil.
- Osbaek, M. 2011. Theory and application of annular pressure management, In Proceedings of No-Dig 2011 Conference, Washington, D.C.
- Peck, R.B., Hanson, W.E., and Thornburn, T.H. 1974. Foundation engineering, Vol. 10, New York: Wiley.
- Rostami, A., Deng, S., Yi, Y., and Bayat, A. 2017. Initial experimental study on formation of filter cake in sand during horizontal directional drilling, NASTT No-Dig Show Conference, Washington, D.C.
- Rostami, A., Yi, Y., and Bayat, A. 2016. Estimation of maximum annular pressure during hdd in noncohesive soils, *International Journal of Geomechanics*, 06016029.
- Sanchez, C., and McHugh, M. 2004. Drilling fluid loss events in the denver basin aquifers, *H2GEO: Geotechnical Engineering for Water Resources*, ASCE, 220–227.

- Staheli, K., Bennett, R.D., O'Donnell, H.W., and Hurley, T.J. 1998. Installation of pipelines beneath levees using horizontal directional drilling, Technical Report CPARGL-98-1, U.S. Army Engineer Waterways Experiment Station, Vicksburg, Mississippi.
- Staheli, K., Christopher, G. P., and Wetter, L. 2010. Effectiveness of hydrofracture prediction for HDD design, In Proceedings of No-Dig 2012 Conference, Chicago, Illinois.
- Stauber, R.M., Bell, J., and Bennett, R.D. 2003. A rational method for evaluating the risk of hydraulic fracturing in soil during horizontal directional drilling (HDD), In Proceedings of 2003 No-Dig Conference, Las Vegas, Nevada.
- Van Brussel, G.G., and Hergarden, H.J.A.M. 1997. Research (CPAR) program: Installation of pipeline beneath levees using horizontal directional drilling, Department of Foundation and Underground Engineering, Delft Geotechnics, 1-16.
- Vesic, A.C. 1972. Expansion of cavities in infinite soil mass, *Journal of Soil Mechanics and Foundation Division*, 98, No. SM3, 265–290.
- Wang, X., and Sterling, R.L. 2007. Stability analysis of a borehole wall during horizontal directional drilling, *Tunneling and Underground Space Technology*, 22, 620–632.
- Xia, A. 2009. Investigation of maximum mud pressure within sand and clay during horizontal directional drilling, PhD thesis, Queen's University, Kingston, Ontario.
- Xia, H. and Moore, I.D. 2006. Estimation of maximum mud pressure in purely cohesive material during Directional Drilling, *International Journal Geomechanics and Geoengineering*, 1(1), 3-11.
- Xia, H. and Moore, I.D. 2007. Discussion of limiting mud pressure during directional drilling in clays, Geo2007, Ottawa, Canada.
- Yanagisawa, E. and Panah, A. K. 1994. Two dimensional study of hydraulic fracturing criteria in cohesive clays, *Soils and Foundations*, 34(1), 1-9.

Yu, H.S., and Houlsby, G.T. 1991. Finite cavity expansion in dilatant soil: loading analysis, *Geotechnique*, 41(2), 173-183.

8- Conclusion and Recommendation

8-1- Conclusion

The behaviour of the borehole annulus pressure in HDD is complex and requires analysis when planning and executing pilot boring. The annular pressure prediction in HDD is a critical design element. The excessive annular pressures are the result of a restricted borehole annulus or excessive drilling fluid pressures, which can significantly risk the project schedule and the environment when hydraulic fracturing or shear failure occurs. In this study, a proper annular pressure management technique is introduced; accordingly, the following conclusions are drawn:

1- To simulate the formation of filter cake at the borehole wall during HDD, an initial experimental study on a sandy soil sample is conducted; the results show that drilling fluids with concentrations of 2%, 3%, and 4% bentonite decrease the permeability of the soil sample significantly and prevent further seepage of drilling fluid into the soil sample. Also, the triaxial shear test on the sandy soil sample after drilling fluid injection does not show change in the shear strength of the soil sample. However, the seepage of the drilling fluid into the soil sample may increase the plastic behaviour and decrease the friction angle of the soil; as a result, the shear strength of the soil decreases. Thus, during HDD in a sandy soil medium, it can be assumed that if a proper concentration of bentonite has been used in the drilling fluid and if the formation of the filter cake at the borehole wall can be guaranteed, the borehole meets one of the major conditions of an ideal borehole in which the loss of circulation declines due to the negligible seepage of drilling fluid into the borehole wall.

2- The Bingham plastic flow model was generally recommended to predict annular pressure at shear rates of 300–600 RPM during HDD operation. This model provides a

conservative estimate and would promote deeper and longer drill paths at the design phase, requiring a greater installation expense than necessary. For the HDD industry to modify the suggested rheological model (Bingham plastic model) to estimate the annular pressure during pilot boring, new shear rate ranges are introduced as 100–200 RPM, which can provide the most favorable agreement with the annular measurements. The predicted pressure can be used as the plan pressure for annular pressure management to reveal upcoming incidents during construction.

3- To estimate the annular pressure in an ideal borehole during pilot boring in HDD projects, the Power Law model considering shear rates of 6–100 RPM is introduced. The Power Law's rheological parameters can be identified by using a six-speed viscometer. The estimated annular pressure compared to the measured annular pressure in different case studies shows that the Power Law model can provide a good estimation of annular pressure and can be recommended to the HDD industry for annular pressure estimation. The predicted pressure can be used as the plan pressure for annular pressure management to reveal upcoming incidents during construction.

4- Two cavity expansion methods (Delft's and Yu and Houlsby's [1991] methods) are used to estimate the maximum allowable pressure during HDD considering the allowable limit plastic radius, plastic strain, and pressure. The results show that failure pressure is not correlated with the limit plastic radius and strain following both theoretical methods while it correlates strongly with the limit pressure following Yu and Houlsby's (1991) method. According to this correlation, the coefficient of limit pressure is 3.3 which is divided by the limit pressure ($P_{\max} \approx P_{\lim}/3.3$) using Yu and Houlsby's (1991) method. This correlation may be used as a limit

pressure-based method for the estimation of maximum allowable annular pressure during HDD in non-cohesive soils in shallow depth.

5- To extend the limit pressure approach to estimating the maximum allowable pressure during HDD in different geotechnical conditions, the commercial finite element program, known as ABAQUS numerical modeling, is used. The results show that the numerical modeling can estimate the failure pressure properly as they are compared to several case studies. However, the limit pressure calculated based on Yu and Houlsby's method overestimates the failure pressure significantly. Thus, to correlate the limit pressure from the numerical method with that from the analytical method, a coefficient of limit pressure is required. In this case, the essential parameters that impact the limit pressure are identified using a parametric study. The results show that overburden depth and the friction angle and elastic modulus of soils have the highest impact on the limit pressure; accordingly, the coefficients of limit pressure are obtained for rational ranges of the identified essential physical and geotechnical parameters. These coefficients of limit pressure are provided in several plots for different geotechnical conditions and can be recommended to the HDD industry for the better estimation of failure pressure in non-cohesive soils.

8-2- Recommendation

As the HDD industry responds to the demands for trenchless infrastructure comprising greater drill path lengths and increasing borehole diameters, annular pressure management is now recognized as a vital component of success. The proposed plan pressure and maximum allowable pressure estimations in this study can be extended to capture more sophisticated behaviour of annular pressure during HDD, and the future works are suggested as follows:

1- The study of drilling fluid management by conducting experiments of drilling fluids is required with a view to investigating the rheological (yield point, plastic viscosity, density, etc.) and hydraulic (velocity profile, shear stress profile, and pressure loss) parameters of drilling fluids in light of the impact of temperature on rheological properties of the drilling fluid (as the temperature rises during drilling). However, there is limited research that assesses the rheological properties and hydraulic parameters of shear thinner and filtration control drilling fluid using different concentrations of additives. This can assist the HDD contractors in better understanding the rheological behaviour of drilling fluids and selecting a proper drilling fluid with desirable functions, such as cleaning performance and carrying capacity; it results in the mitigation of the risks associated with unsuitable drilling fluids.

2- The study of the interaction of common drilling fluids (bentonite-based drilling fluids with additives) used in the HDD industry with collapsible soils (sand and low cohesive soils), is needed. This can be achieved by conducting drilling fluid injection tests on soil samples and employing triaxial or direct shear tests on them. The goal is to improve the formation of cake at the soil surface to prevent further seepage and improve the geotechnical parameters of soil.

3- The analytical method suggested by Yu and Houlsby (1991) should be expanded to encompass the impact of coefficient of lateral earth pressure (anisotropic condition) and

boundary effects in shallow depths. The common cavity expansion methods are simplified and formulated based on an isotropic stress and an infinite medium.

4- The suggested approach by Rostami et al. (2016) as a limit pressure to estimate the maximum allowable pressure should be verified by more case studies in different overburden depths. Also, further investigation is required to verify this approach for cohesive frictional soils when shear failure is the dominant type of failure.

5- Due to the lack of field case studies that demonstrate the hydraulic fracture in specific types of soils, it is suggested to conduct an experimental research study to simulate the hydraulic fracturing phenomenon in a small-scale test. Also, the numerical and analytical methods should be used to interpret the hydraulic fracturing in experimental tests.

6- The introduction of a mud weight window in HDD industry can provide a precious and safe plan for annular pressure management before starting the HDD operation.

Reference

- Allouche, E.N., Ariaratnam, S.T., and Biggar, K.W. 1998. Environmental remediation using horizontal directional drilling: applications and modeling, *Practice Periodical of Hazardous, Toxic, and Radioactive Waste Management*, 2(3), 93-99.
- American Petroleum Institute (API). 2009. Recommended practice on the rheology and hydraulics of oil-well drilling fluids, API RP 13D. Washington, D.C.
- Arends, G. 2003. Need and possibilities for a quality push within the technique of horizontal directional drilling (HDD), In Proceedings of 2003 No-Dig Conference, Las Vegas.
- Ariaratnam, S.T., Harbin, B.C., and Stauber, R.L. 2007. Modeling of annular fluid pressures in horizontal boring, *Tunnelling and Underground Space Technology*, 22, 610–619.
- Ariaratnam, S.T., Lueke, J.S., and Allouche, E.N. 1999. Utilization of trenchless construction methods by Canadian municipalities, *Journal of Construction Engineering and Management*, 125(2), 76-86.
- Ariaratnam, S.T., Stauber, R.M., Bell, J., and Canon, F. 2003. Evaluation of rheologic properties of fluids returns from horizontal directional drilling, No Dig Conference, North American Society for Trenchless Technology NASTT, Arlington, Va.
- Ariaratnam, S.T., Stauber, R.M., Bell, J., Harbin, B., and Canon, F. 2003. Predicting and controlling hydraulic fracturing during horizontal directional drilling, Proceedings of the International Conference on Pipeline Engineering and Construction, Baltimore, Maryland, 1334-1345.
- ASTM D2850-15. 2015. Standard test method for unconsolidated-undrained triaxial compression test on cohesive soils, ASTM International, West Conshohocken, PA, USA.
- ASTM D5084. 2003. Standard test methods for measurement of hydraulic conductivity of saturated porous materials using a flexible wall permeameter, American Society for Testing and Materials, Philadelphia, PA, USA.

- ASTM D698. 2012. Test Methods for Moisture-Density Relations of Soils and Soil-Aggregate Mixtures. Method A (Standard Proctor).
- Baroid. 1997. Fluids Handbook. Baroid Fluid Services, Chapter 9, Rheology and Hydraulics, Haliburton, Houston, TX.
- Baumert, M.E., Allouche, E.N., and Moore, I.D. 2005. Drilling fluid considerations in design of engineered horizontal directional drilling installations, *International Journal of Geomechanics*, 5(4), 339–349.
- Bennett, D., and Wallin, K. 2008. Step-by-step evaluation of hydrofracture risks for HDD projects, In Proceeding of No-Dig Conference, North American Society for Trenchless Technology (NASTT), Cleveland.
- Bennett, D., Ariaratnam, S. and Como, C. 2001. Horizontal directional drilling good practice guidelines, HDD Consortium, Washington.
- Bennett, R.D., and Ariaratnam, S.T. 2008. Horizontal directional drilling good practices guidelines. Third Edition, HDD Consortium.
- Bennett, R.D., Osbak, M., and Wallin, M. 2012. Improving the standard of mud management, In Proceedings of 2012 No-Dig Conference, Nashville, Tennessee.
- Bird, R.B., Stewart, W.E., and Lightfoot, E.N. 2002. Transport phenomena, New York: John Wiley & Sons.
- Canadian Association of Petroleum Producers, 2004. Planning for Horizontal Directional Drilling for pipeline construction, CAPP publication 2004-0022
- Carlos, A.L., Lillian, D.W., and Patrick, J.C. 2002. Guidelines for installation of utilities beneath Corps of Engineers levees using horizontal directional drilling. *US Army Corps of Engineers Research and Development Center*, ERDC/GSL TR-02-9.
- Carter, J.P., Booker, J.R., and Yeung, S.K. 1986. Cavity expansion in cohesive frictional soils, *Geotechnique*, 36(3), 349-358.

- Chen, S.L., and Abousleiman, N.Y. 2012. Exact undrained elastoplastic solution for cylindrical cavity expansion in modified Cam Clay soil, *Geotechnique*, 62(5), 447–456.
- Chen, S.L., and Abousleiman, N.Y. 2013. Exact drained solution for cylindrical cavity expansion in modified Cam Clay soil, *Geotechnique*, 63(6), 510–517.
- Christopher, J.S., and Michael, M. 2003. Drilling fluid loss events in the Denver basin aquifers, *H2GEO: Geotechnical Engineering for Water Resources*, ASCE, 220-227.
- Conroy, P.J., Latorre, C.A., and Wakeley, L.D. 2002. Guidelines for installation of utilities beneath Corps of Engineers levees using horizontal directional drilling, *ERDC/GSL TR-02-9, Geotechnical Structures Laboratory*, Vicksburg, Mississippi.
- Das, B. M. 2013. *Advanced soil mechanics*. CRC Press.
- Dassault Systèmes Simulia Corp. 2013. *Abaqus Analysis User's Manual*, version 6.13, Dassault Systèmes Simulia Corp., Providence, Rhode Island.
- Delft Geotechnics. 1997. A report by Department of Foundations and Underground Engineering prepared for O'Donnell Associates, Inc., Sugarland, Texas.
- Duyvestyn, G. 2009. Comparison of predicted and observed HDD installation loads for various calculation methods, In *Proceedings of 2009 International No-Dig Conference*, Toronto, Ontario, Canada.
- Duyvestyn, G. M. 2006. Challenging ground conditions and site constraints, not a problem for HDD, In *Proceedings of 2006 North American No-Dig Conference*, Nashville, Tennessee.
- Elwood, D, Xia, H., and Moore, I.D. 2007. Hydraulic fracture experiments in a frictional material and approximations for maximum allowable mud pressure, In *Proceedings of 60th Canadian Geotechnical Society Annual Conference*, Ottawa, Ontario, Canada, 1681-1688.

- Elwood, D. 2008. Hydraulic fracture experiments in a frictional material and approximations for maximum allowable mud pressure, Master thesis, Queen's University, Kingston, Ontario, Canada.
- Gleason, M.H., Daniel, D.E., and Eykholt, G.R. 1997. Calcium and Sodium Bentonite for Hydraulic Containment Applications, *Journal of Geotechnical and Geoenvironmental Engineering*, ASCE, 123(5), 438-445.
- Grim, R., and Guven, N. 1978. Bentonite: Geology, Mineralogy, Properties, and Uses, Elsevier Science Publishing, New York.
- Growcock, F., and Harvey, T. 2005. Drilling fluids. *Drilling Fluids Processing Handbook*, UK: Elsevier Ink, 15-66.
- Haciislamoglu, M., and Langlinais, J. 1990. Non-Newtonian flow in eccentric annuli. *Journal of Energy Resources Technology*, 112(3): 163–169.
- Harris, O. 2004. Evaluation of equivalent circulating density of drilling fluids under high pressure-high temperature conditions. M.Sc. thesis, University of Oklahoma, Norman, OK.
- Harris, T., Drexel, H., and Rahman, S. 2005. Horizontal directional drilling application of fusible C-950 TM PVC pressure pipe, Proceedings of 2005 No-Dig Conference, New Orleans, Florida.
- Harris, T., Drexel, H., and Rahman, S. 2005. Horizontal directional drilling application of fusible C-950 TM PVC pressure pipe, Proceedings of 2005 No-Dig Conference, New Orleans, Florida.
- Hashash, Y., Javier, J., Petersen, T., and Osborne, E. 2011. Evaluation of horizontal directional drilling (HDD), *FHWA-ICT-11-095*.
- Hemphill, T., Campos, W., and Pilehvari, A. 1993. Yield-power law model more accurately predicts drilling fluid rheology, *Oil and Gas Journal*, 91(34): 45-50.

- Jaky, J. 1944. The coefficient of earth pressure at rest, *Journal of the Society of Hungarian Architects and Engineers*, 7, 355-358.
- Kassab, S.Z., Ashraf, S.I., and Elessawi, M.M. 2011. Drilling fluid rheology and hydraulics for oil fields. *European Journal of Scientific Research*, 57(1): 68-86.
- Kennedy, M.J., Moore, I.D., and Skinner, G.D. 2006. Development of tensile hoop stress during horizontal directional drilling through sand, *International Journal of Geomechanic*, 6(5), 367-373.
- Kennedy, M.J., Skinner, G.D., and Moore, I.D. 2004. Elastic calculations of limiting mud pressures to control hydro fracturing during HDD, In Proceedings of No-Dig Conference 2004, New Orleans, Louisiana.
- Keulen, B. 2001. Maximum allowable pressures during horizontal directional drillings focused on sand, PhD thesis, Delft University of Technology, Delft, Netherlands.
- Keulen, B., 2001. Maximum allowable pressures during directional drillings focused on sand, Thesis Paper: pp. 25-32, Appendices pp. 39-74.
- Kim, S.H., and Tonon, F. 2010, Face stability and required support pressure for TBM driven tunnels with ideal face membrane drained case, *Tunneling and Underground Space Technology*, 25(5), 526–542.
- Luger, H.J., and Hergarden, H.J.A.M. 1988. Directional drilling in soft soil: influence of mud pressures, In Proceedings of No-Dig Conference on Trenchless Technology, Washington, D.C.
- Min, F., Zhu, W., and Han, X. 2013. Filter cake formation for slurry shield tunneling in highly permeable sand. *Tunnelling and Underground Space Technology*, 38, 423–430.
- Min, F.L., Zhu, W., Han, X.R., and Zhong, X.C. 2010. The effect of clay content on filter cake formation in highly permeable gravel, *Geotechnical Special Publication*, 204 GSP, 210–215.

- Moore, I.D. 2005. Analysis of ground fracture due to excessive mud pressure, Proceedings of 2005 No-Dig Conference, Orlando, Florida.
- Moore, P.L. 1986. Drilling Practices Manual, PennWell Publishing Company, 2nd Edition.
- Najafi, M. 2005. Trenchless technology: pipeline and utility design, construction, and renewal, McGraw-Hill, New York.
- Obert, L., and Duvall, W. I. 2013. Rock Mechanics and the Design of Structures in Rock.
- Obrzud, R., and Truty, A. 2012. The hardening soil model-a practical guidebook z soil.
- Osbak, M. 2011. Theory and application of annular pressure management, In Proceedings of No-Dig 2011 Conference, Washington, D.C.
- Papanastasiou, P., and Thiercelin, M. 2011. Modeling borehole and perforation collapse with the capability of predicting the scale effect, *International Journal of Geomechanic*, 11(4), 286–293.
- Papanastasiou, P., and Vardoulakis, I. 1989. Bifurcation analysis of deep boreholes: II. Scale effect.” *International Journal of Numerical and Analytical Methods in Geomechanics*, 13, 183–198.
- Papanastasiou, P.C, and Zervos, A. 2004. Wellbore stability analysis: From linear elasticity to post-bifurcation modeling, *International Journal of Geomechanic*, 4(1), 2–12.
- Peck, R.B., Hanson, W.E., and Thornburn, T.H. 1974. Foundation engineering, Vol. 10, New York: Wiley.
- Rostami, A., Deng, S., Yi, Y., and Bayat, A. 2017. Initial experimental study on formation of filter cake in sand during horizontal directional drilling, NASTT No-Dig Show Conference, Washington, D.C.
- Rostami, A., Yi, Y., and Bayat, A. 2016. Estimation of maximum annular pressure during hdd in noncohesive soils, *International Journal of Geomechanics*, 06016029.

- Rostami, A., Yi, Y., and Bayat, A. 2016. Investigating filter-cake formation on borehole stability during horizontal directional drilling in non-cohesive soil, NASTT No-Dig Show Conference, Dallas, Texas
- Sanchez, C., and McHugh, M. 2004. Drilling fluid loss events in the denver basin aquifers, *H2GEO: Geotechnical Engineering for Water Resources*, ASCE, 220–227.
- Sarireh, M., Najafi, M., and Slavin, L. 2012. Usage and applications of horizontal directional drilling, In Proceedings of ICPTT 2012: Better pipeline infrastructure for a better life, Wuhan, China.
- Staheli, K., Bennett, R.D., O'Donnell, H.W., and Hurley, T.J. 1998. Installation of pipelines beneath levees using horizontal directional drilling, Technical Report CPARGL-98-1, U.S. Army Engineer Waterways Experiment Station, Vicksburg, Mississippi.
- Staheli, K., Christopher, G. P. and Wetter, L. 2010. Effectiveness of hydrofracture prediction for HDD design, In Proceedings of No-Dig 2012 Conference, Chicago, Illinois.
- Stauber, R.M., Bell, J., and Bennett, R.D. 2003. A rational method for evaluating the risk of hydraulic fracturing in soil during horizontal directional drilling (HDD), In Proceedings of 2003 No-Dig Conference, Las Vegas, Nevada.
- Van Brussel, G.G., and Hergarden, H.J.A.M. 1997. Research (CPAR) program: Installation of pipeline beneath levees using horizontal directional drilling, Department of Foundation and Underground Engineering, Delft Geotechnics, 1-16.
- Vardoulakis, I., and Papanastasiou, P. 1988. Bifurcation analysis of deep boreholes: I. surface instabilities, *International Journal of Numerical and Analytical Methods in Geomechanics*, 12(4), 379–399.
- Verruijt, A. 1993. *Grondmechanica*, Delftse Uitgevers Maatschappij, Delft, Netherlands.
- Vesic, A.C. 1972. Expansion of cavities in infinite soil mass, *Journal of Soil Mechanic and Foundation Division*, 98, No. SM3, 265–290.

- Wang, X., and Sterling, R.L. 2007. Stability analysis of a borehole wall during horizontal directional drilling, *Tunneling and Underground Space Technology*, 22, 620–632.
- Xia, A. 2009. Investigation of maximum mud pressure within sand and clay during horizontal directional drilling, PhD thesis, Queen's University, Kingston, Ontario.
- Xia, H. and Moore, I.D. 2006. Estimation of maximum mud pressure in purely cohesive material during Directional Drilling, *International Journal Geomechanics and Geoengineering*, 1(1), 3-11.
- Xia, H. and Moore, I.D. 2007. Discussion of limiting mud pressure during directional drilling in clays, Geo2007, Ottawa, Canada.
- Yanagisawa, E. and Panah, A. K. 1994. Two dimensional study of hydraulic fracturing criteria in cohesive clays, *Soils and Foundations*, 34(1), 1-9.
- Yu, H.S. 2000. *Cavity expansion methods in geomechanics*, Kluwer Academic Publishers, Norwell, Massachusetts.
- Yu, H.S., and Houlsby, G.T. 1991. Finite cavity expansion in dilatant soil: loading analysis, *Geotechnique*, 41(2), 173-183.